

POLITECNICO DI TORINO

Corso di Laurea in Mechanical Engineering

Master Degree Thesis

**Cooling system model validation
of a CNG engine for Off-Road
applications**



Relatore

Prof. Mirko BARATTA

Candidato

Antonio SIRAGUSA

A.Y 2017 - 2018

Summary

The project target is to design and validate the cooling system model of a CNG engine for Off Road applications, and to perform fluid dynamic and thermal simulations for predicting the system performances at different engine operating conditions.

The model, created using a unidimensional approach, is designed in order to be used either in the prototyping phase, to test new technical solutions and design proposals, or to predict the cooling system behavior within the customer vehicle. An experimental activity at the engine test bench has been carried out to provide the target data for the model calibration and to compare the simulations results with the target measured quantities.

The validation criteria have been set in order to reproduce the cooling system performances with a maximum error tolerance of 10 %.

The aim of the thesis is to offer a fast and valid support for the engine cooling system design and validation activities, and to create a flexible tool able to be applied to different engines configurations and at different design phases.

The objective is to promote the cost savings reducing the need of experimental activities at the test bench.

Contents

List of Figures	VII
1 Introduction	1
1.1 NEF67 CNG engine	3
2 The engine cooling system	7
2.1 Description and main functions	7
2.2 Cooling circuit components	9
2.2.1 Cooling fluid	9
2.2.2 Centrifugal pump	9
2.2.3 Thermostat	11
2.2.4 Expansion Tank	12
2.2.5 Oil cooler	14
2.2.6 Radiator	16
2.2.7 Fan	18
2.2.8 EGR cooler	20
2.2.9 Intercooler	21
2.3 Heat balance equations	22
3 Cooling circuit unidimensional modeling	27
3.1 Software	28
3.2 Engine water jacket 1D model	29
3.2.1 External connections opening	30
3.2.2 Geometry discretization	31
3.2.3 Equivalent flow split elements	32
3.2.4 GT model	33
3.3 Engine water jacket 1D model calibration	35
3.3.1 Standard procedure	36
3.3.2 New procedure	37
3.4 Cooling circuit components integration	48
3.5 Steady state thermal modeling	61
3.6 Vehicle and test bench model configurations	63
4 Test bench model calibration	69
4.1 Engine test bench	70
4.2 Experimental measurements campaign	71
4.2.1 Instrumentation	72
4.2.2 Sensors location	79
4.2.3 Engine setup and data acquisition	80

4.2.4	Simulation results	84
4.2.5	Heat rejection	89
5	Project results and model applications	95
5.1	Model applications	97
5.2	Conclusions	100
	References	XI

List of Figures

1.1	NEF67 CNG	4
1.2	Torque-Power characteristics	4
1.3	Tactor equipped with NEF67 CNG engine	5
2.1	Centrifugal water pump technical drawing	10
2.2	Water pump characteristic	10
2.3	Thermostat lift characteristic	11
2.4	Expansion tank location (Top view)	12
2.5	Pressurization cap operating modes	13
2.6	Oil cooler (oil and water plates)	14
2.7	Oil cooler (oil plates immersed in water)	14
2.8	Oil cooler heat release performance	15
2.9	Radiator	16
2.10	Radiator heat release performance	17
2.11	Electromagnetic clutch	18
2.12	Fan location with respect to the radiator	19
2.13	Fan characteristic	19
2.14	EGR cooler	20
2.15	Intercooler characteristic	21
3.1	GT-SUITE engine cooling system simulations	28
3.2	Water jacket views	29
3.3	Water jacket ports	30
3.4	Water jacket discretized volumes	31
3.5	H6 and C6 flow split components	32
3.6	3D CFD simulation boundary data	33
3.7	Water jacket GT model	34
3.8	3D CFD simulation target flow rates	35
3.9	Excel table used for manual calibration	36
3.10	PID Controller settings (Main)	39
3.11	PID Controller settings (Limits)	40
3.12	PID Controller settings (Initialization)	41
3.13	PID Controller settings (Convergence)	42
3.14	PID controller	42
3.15	Head/gasket calibrated orifices diameters	43
3.16	PID controllers converged solutions	44
3.19	Comparison between standard and new calibration procedures	45
3.17	Average pressure distribution	46
3.18	Coolant mass flow rate distribution	47

3.20	NEF67 CNG cooling circuit layout	48
3.21	Pump map	49
3.22	Thermostat temperature-lift characteristic	50
3.23	By-pass temperature-lift characteristics	51
3.24	Oil cooler permeability	52
3.25	Radiator geometriacal details	53
3.26	Radiator permeability	54
3.27	Radiator heat rejection	54
3.28	Cabin heater permeability	55
3.29	Cabin heater heat request (at costant coolant flow rate 500 l/h)	55
3.30	Water cooled turbocharger	56
3.31	Gas pressure regulator tested permeability	57
3.32	Pressurized cap discharge coefficient characteristic	58
3.33	Equivalent pipe element	59
3.34	Discretized pipe: 3D-1D conversion	59
3.35	Junction equivalent flow split element	60
3.36	Water jacket heat addition components specifications	62
3.37	Complete water jacket model	65
3.38	Cooling circuit unidimensional model(test bench configuration)	66
3.39	Cooling circuit unidimensional model(vehicle configuration)	67
4.1	Engine test bench	70
4.2	PT100 temperature sensor	73
4.3	PT100 temperature sensor specifications	74
4.4	UNIK PTX 5072 pressure transducer	75
4.5	UNIK PTX 5072 pressure transducer specifications	76
4.6	MUT2200EL magnetic sensor	78
4.7	MC608A converter	78
4.8	MUT2200EL magnetic sensor specifications	78
4.9	Sensors location at the engine test bench	79
4.10	Pump inlet flow split	90
4.11	Radiator and turbocharger heat rejection	93
5.1	Example of extreme environmental conditions	97
5.2	Air speed and ambient temperature variation effects on radiator inlet temperature	98

Chapter 1

Introduction

The thesis is the result of a collaboration with FPT Industrial Spa, the Brand of CNH Industrial dedicated to the development, production, sale and assistance of powertrains for On Road, Off Road, Marine and Power Generation applications. The project, carried out during a six months internship in the Engine Virtual Validation department, has as main target, the design and validation of a cooling system unidimensional virtual model able to support the development of a NEF 67 CNG engine, for off road applications.

The main reason to perform a virtual validation activity is to reduce the need of bench tests, promoting the cost savings and improving the design efficiency, both in terms of results quality and validation time.

The selected software for the project is GT-Suite by Gamma Technologies.

The choice of using a unidimensional approach for the modeling activity is related to the possibility of reproducing the cooling system fluid dynamic and thermal phenomena with good precision, comparable with that of 3D simulations and, most importantly, of reducing the computational time.

A preliminary study on the engine cooling theory and thermal management, and a training period with the software, have been fundamental to create the basic skills for supporting the cooling system engineer on its validation activity and familiarize with the unidimensional modeling and simulations. In particular, working with already existing models, gave the practical opportunity to learn the modeling methodology, the required input data, and the theory behind the computational fluid dynamics, essential for the simulations setup.

Moreover, the participation in technical meetings has been the further step for understanding the possible criticalities in the design process and the responsibilities related to the validation activity.

From this background, stems the idea of applying the acquired skills during the internship in a real project, in order to support the team in the engine development with a predictive tool and to improve the used modeling methodology with new solutions able to enhance the results precision and to reduce the simulation time. Has been necessary a strong collaboration with the design engineers to gather all the geometrical, fluid dynamic and thermal characteristics of the cooling system components, and with the CFD team, for the 3D simulations results to be used in the preliminary phase of the model calibration.

In that regard, to comply with the request of improvement of the modeling methodology, has been proposed a new procedure for the engine water jacket model calibration, based on PID controllers, able to obtain the same results of the 3D CFD simulations with a reduced computational time. The proposed method, due to its flexibility and quickness, has been easily implemented to already existing cooling system models and will be used as reference method for the following ones. The project is enhanced by the experimental activity performed at the engine test bench, for measuring the target data for the model calibration.

The experimental campaign, has been carried out after a practical insight on the engine disassembling, to study the engine architecture and the particular cooling system layout.

The activity turned out to be the most interesting of the project, and fundamental for linking the virtual model simulations with the real engine behavior.

Working on the prototype on the definition of the sensor locations, attending the test and collecting the data for the post processing, made the physical phenomena understanding easier and contributed to enhance the knowledge on the internal combustion engines also from a practical point of view.

The validation criteria have been set in order to make the model predictive and adaptable for other applications.

This request underlines the need of working on the improvement of the modeling activity also considering as target of the project, the creation of a standardized methodology to be extended to all the engine families of the company.

The model has been designed in order to be used either in the prototyping phase, to test new technical solutions, or to predict the engine performances within the customer vehicle.

The bench configuration will follow the real prototype development and will be continuously updated in the final version, while for the vehicle configuration some possible applications have been investigated related to the behavior of the engine cooling system with particular environmental conditions.

1.1 NEF67 CNG engine

Specifications

Fuel: CNG
Total Displacement: 6.7 L
Thermodynamic Cycle: 4 strokes
Arrangement: six in line cylinders
Valves per cylinder: 4
Injection System: ECR
Cooling system: liquid
Air Handling: TCA
EGR: -
Dimensions: 1062x687x1049 mm
Dry Weight : 530 kg
Rated power: 132 kW @1800 rpm
Peak Torque: 700 Nm @1500 rpm
Application: Off-Road



FPT Industrial is investing on alternative fuels, especially on natural gas due to the following reasons:

- Fuel cost savings amount to up to 30% compared to Diesel, thanks to the fact that both CNG and LNG are significantly less expensive than Diesel in most European Countries. Adaptation to a wide range of gas quality also maximizes engine flexibility
- Natural gas models adopt air-to-air charge cooler and turbocharger with waste-gate valve, assuring prompt transient response. Multipoint sequential injection guarantees very stable combustion
- To comply with Euro VI standards, natural gas engines do not need EGR, SCR, or DPF but rely on a simple 3-way catalyst: a converter located at the end of the exhaust pipe, based on an integrated structure plated with Platinum, Palladium, and Rodium catalyzers. This compact and cost-effective after-treatment system contributes to make natural gas Total Cost of Ownership very competitive [1]



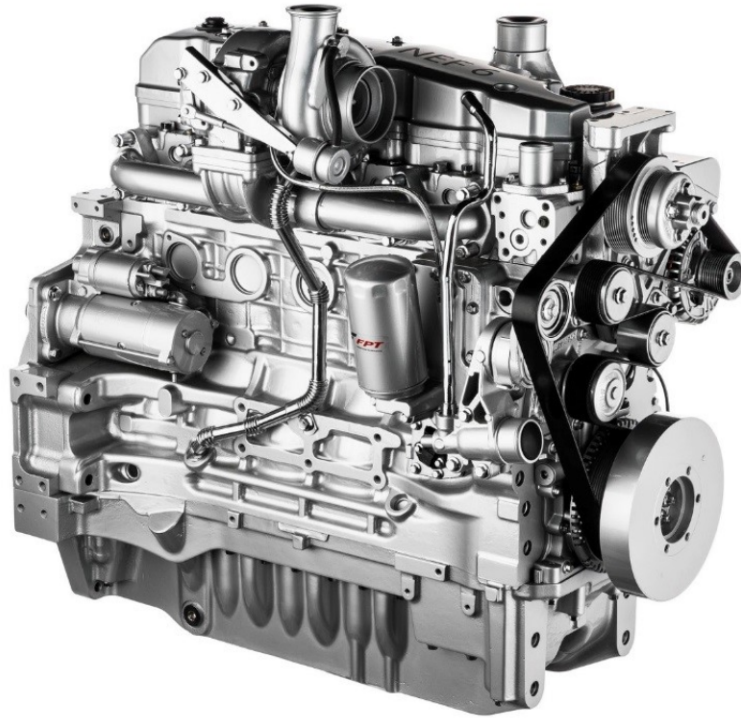


Figure 1.1: NEF67 CNG

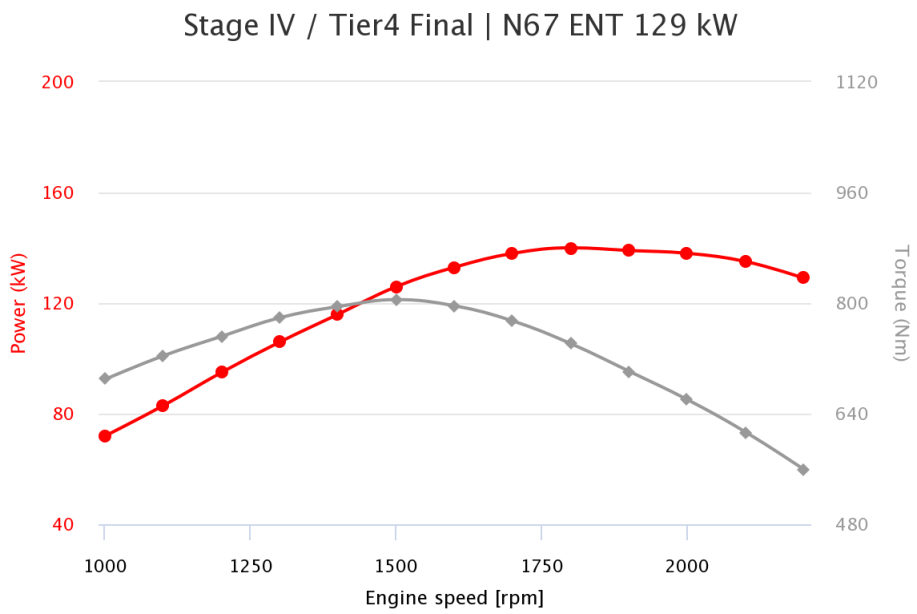


Figure 1.2: Torque-Power characteristics



Figure 1.3: Tactor equipped with NEF67 CNG engine

Chapter 2

The engine cooling system

2.1 Description and main functions

The cooling system [3] main task is to extract the heat produced by the engine and to guarantee that the maximum temperature of each component is below the limit of mechanical integrity at any operating condition. The heat flux to be extracted from the engine depends on rotational speed and load and it's around the 30 % of its useful power.

High temperature is generated by the combustion, with peak values above 2000 °C.

The most critical engine components in terms of temperature are described below.

Combustion chamber walls A very high amount of heat invests the combustion chamber and walls reach very high temperature. Moreover, the pressure of the gases generates high deformations, leading to thermo-mechanical fatigue phenomena. The most critical areas are the one closer to the exhaust valve seats and the spark plug/injector seat (depending on the engine type, CI/SI or direct/indirect injection).

Cylinder liner The mechanical and thermal deformations have a negative effect on the cylinder liners circularity, causing excessive pistons wear, friction enhancement and problems related to blow-by flow and oil consumption. Moreover, the high temperature reached at the liner top , increases the oil evaporation causing lubrication issues and possible seizure.

Piston Piston is the most stressed component, with a temperature profile that decreases from the center to the periphery. For Diesel engines, the most critical area is the piston bowl where combustion occurs. The piston is designed with a slight conical shape to compensate the mechanical and thermal deformations and it is continuously cooled by the oil that both reduces friction with the cylinder liner and dissipates heat.

Exhaust valve The exhaust valve is made with Fe-Ni alloys to withstand high mechanical stresses and thermal loads. Deformations and corrosion have to be reduced in order to guarantee always a perfect sealing.

Spark plug and injector Spark plug and injector are generally located in a very hot region of the combustion chamber. The high temperature can damage either the spark plug tip or the injector solenoids, and can generate undesired detonation of the mixture due to local hot spots.

Lubrication oil As already mentioned, the lubricant oil has two main functions in the engine:

- Reduces friction between components in relative motion
- Dissipates heat in the regions where the coolant fluid cannot work

To reduce the cracking problem, which worsen the lubricant properties, some additives are used to improve the oil performance at high temperature. Moreover, a water/oil heat exchanger can be installed to dissipate the excessive heat, so to extend the oil life.

2.2 Cooling circuit components

The engine block and head contain internal channels where the cooling fluid flows and reaches the walls with highest temperature, extracts heat and flows away to the heat exchangers. The design of the internal geometry is very complicated and it's performed using 3D CFD simulations, trying to give to the fluid always an high speed and avoiding excessive pressure drops and stagnation areas.

The fluid volume, called "water jacket", surrounds the hottest areas of the engine and extracts heat to maintain the temperature always below the prescribed limits for the components.

The engine water jacket is connected to the other components of the circuit in order to extract the excessive heat and prevent overheating:

- Some components are physically connected to the engine and receive the cooling fluid through ports obtained in the engine block or head
- Other components are located in the vehicle side and are connected to the water jacket by pipes.

In the following, are listed and described the main components of the engine cooling system.

2.2.1 Cooling fluid

The cooling fluid is a mixture of water and ethylene glycol, able to evaporate above 100 °C and freeze below 0 °C. This property is required either at high temperature, where the fluid must cool all the components without evaporating, or at low temperature (e.g. cold start operation) where an undesired freezing could affect the right operation of the system. The mixture composition depends on the particular engine thermal requirements and application. A commonly used water-glycol composition is the 50-50.

2.2.2 Centrifugal pump

The centrifugal pump is used to send the cooling fluid inside the engine and reach the other components of the circuit. It is connected to the engine crankshaft using a belt with a transmission ratio

$$\tau = \frac{n_{pump}}{n_{engine}}$$

usually between 1.1 - 2, in order to always provide the circuit with the required flow rate for the heat dissipation and avoid cavitation at the pump inlet port.

Figure 2.1 shows the technical drawing of a typical centrifugal pump for automotive application.

The pump head must be always sufficient to overcome the circuit pressure drop, with a pressure increase usually between 0.5 – 3 bar, depending on engine application.

A typical water pump characteristic (called "pump-map") is shown in Figure 2.2. The working point is the intersection between the pump characteristic at fixed rotational speed and the circuit characteristic, the latter depending on the permeability of all components of the circuit.

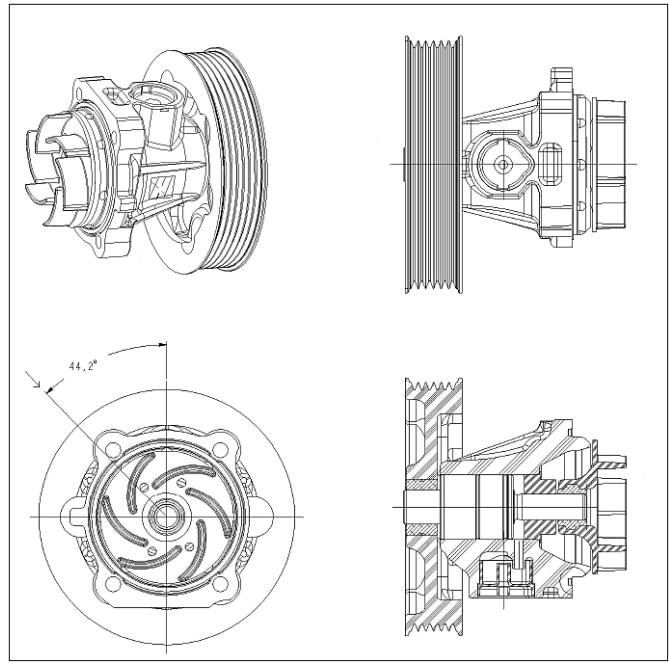


Figure 2.1: Centrifugal water pump technical drawing

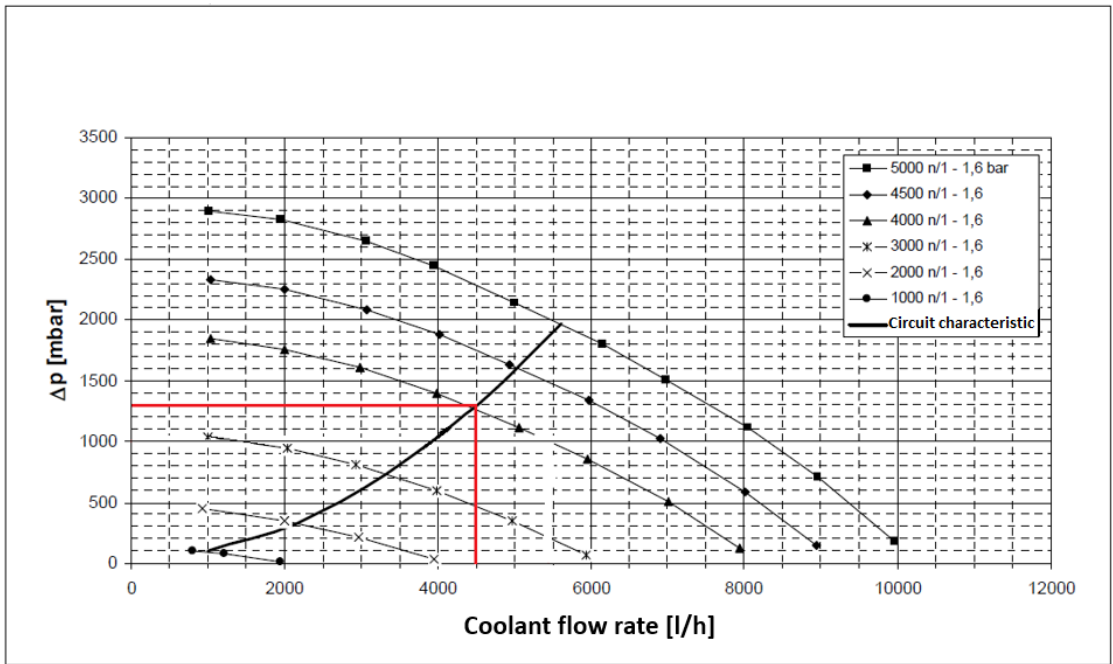


Figure 2.2: Water pump characteristic

2.2.3 Thermostat

The thermostat is a device used to control the temperature difference between the engine inlet and outlet. It is a proportional valve that, changing its position linearly with the increase in temperature, controls the amount of flow rate going into the radiator and thus the heat to be dissipated. The valve, initially closed, starts opening when the coolant temperature reaches a limit value between 80 °C and 100 °C, splitting the flow between the radiator and the by-pass. Three types of configuration are usually adopted, depending on the thermostat location and the by-pass type:

- Engine outlet, fixed by-pass: Cheaper solution. The thermostat controls the flow going into the radiator as a function of the engine outlet temperature. A fixed by-pass is not the best solution at maximum heat dissipation rate, because some flow rate is always subtracted to the radiator.
- Engine outlet, controlled by-pass: Most used solution. The thermostat controls continuously its position opening and closing progressively the ports in order to split the flow between radiator and by-pass.
- Engine inlet, controlled by-pass: Thermostat controls the temperature at the pump inlet, where flows coming from radiator and by-pass mix. It is the less used solution, due to the produced temperature oscillations at the engine inlet.

Figure 2.3 shows a thermostat lift characteristic (valve lift-coolant temperature) with a typical hysteretic behaviour.

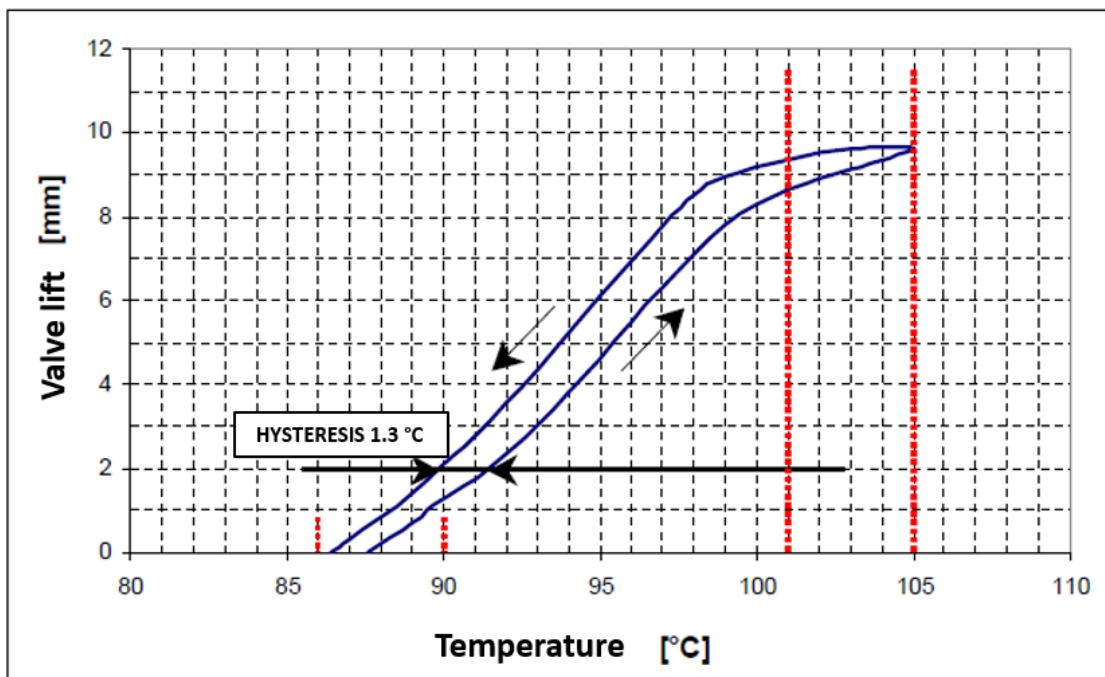


Figure 2.3: Thermostat lift characteristic

2.2.4 Expansion Tank

The expansion tank, located in the top of the circuit, is connected to the degassing line to one side and to the pump inlet to the other side (Figure 2.4). Its main functions are:

- Allowing the fluid to expand due to temperature rise without empty down the circuit
- Filling the circuit keeping the coolant level constant after evaporation
- Creating a barometric head at the pump inlet avoiding cavitation
- Separating liquid and gas phases

A pressurization cap (Figure 2.5), is used to close the expansion tank in order to:

- Pressurize the cooling circuit and increase the dissipation rate
- Set a maximum level of pressure, usually 1.2-1.4 bar, and degas the circuit if required
- Fill the circuit with air after coolant contraction for temperature decrease

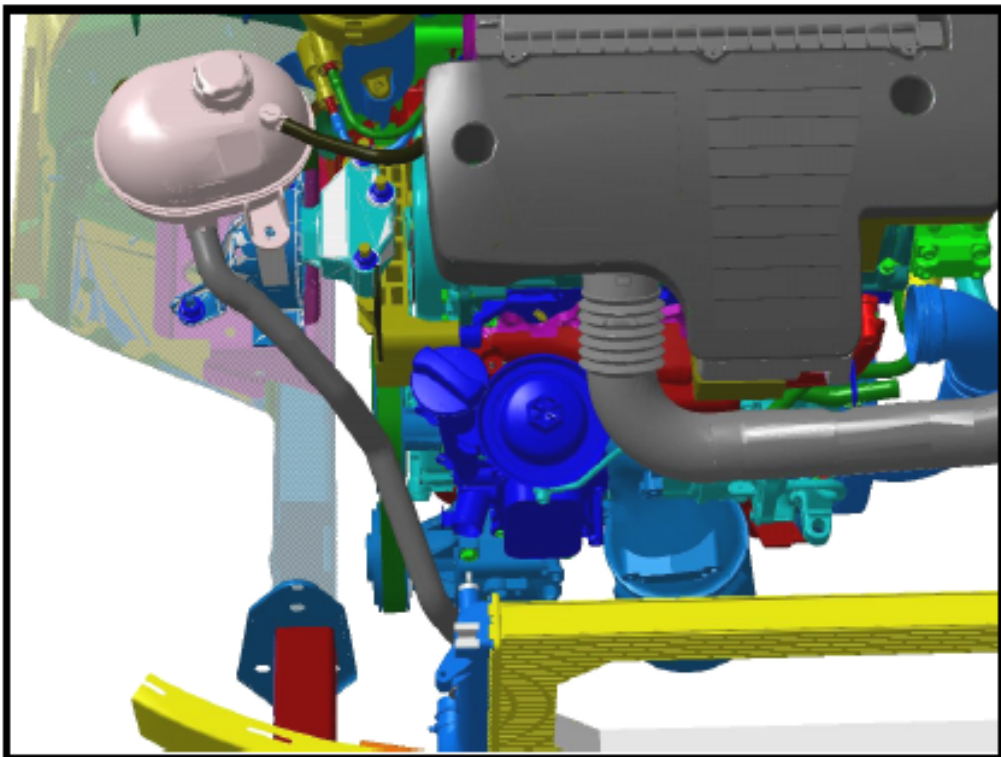


Figure 2.4: Expansion tank location (Top view)

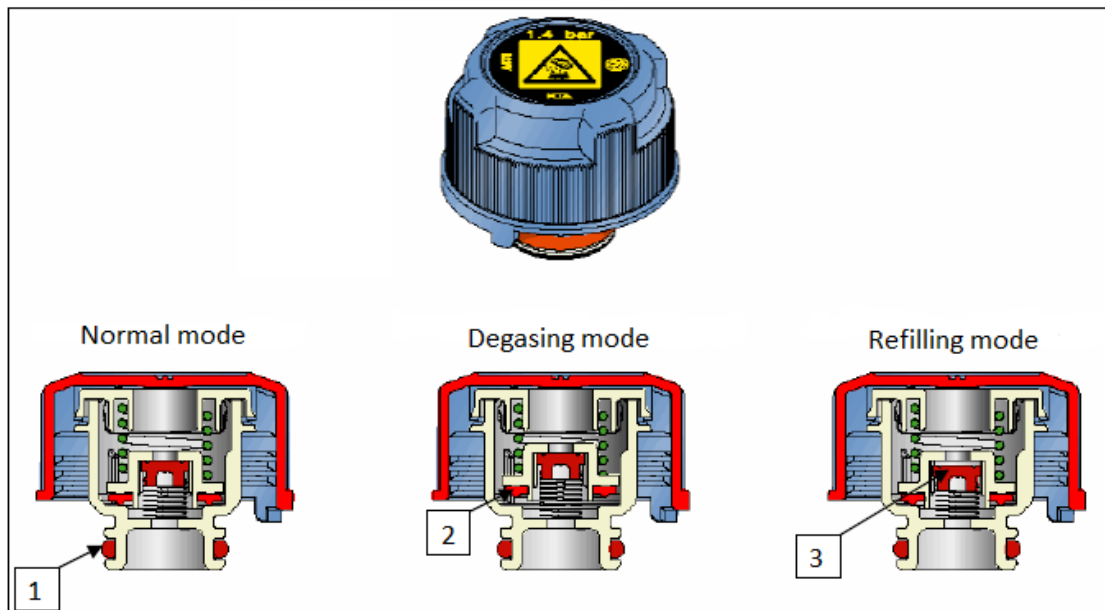


Figure 2.5: Pressurization cap operating modes

The pressurization cap contains three sealing control elements:

1. Toroidal gasket for perfect sealing between the expansion tank and the external environment
2. Elastic spring for maximum pressure control and degassing
3. Control valve for air refilling after coolant fluid contraction

2.2.5 Oil cooler

The oil cooler is a water/oil heat exchanger used to cool down the lubricant oil and prevent overheatings in operation.

The geometry can be of two types:

- Modular with water and oil plates (Figure 2.11)
- With oil plates immersed in water (Figure 2.12)

Figure 2.13 shows the oil cooler heat release performance at different coolant and oil flow rates.

It is worth noting that both oil and coolant flow rates have low effect on the heat release rate. To improve the oil cooler performance is better to work on its internal geometry, finding the right number of plates and reducing pressure losses.

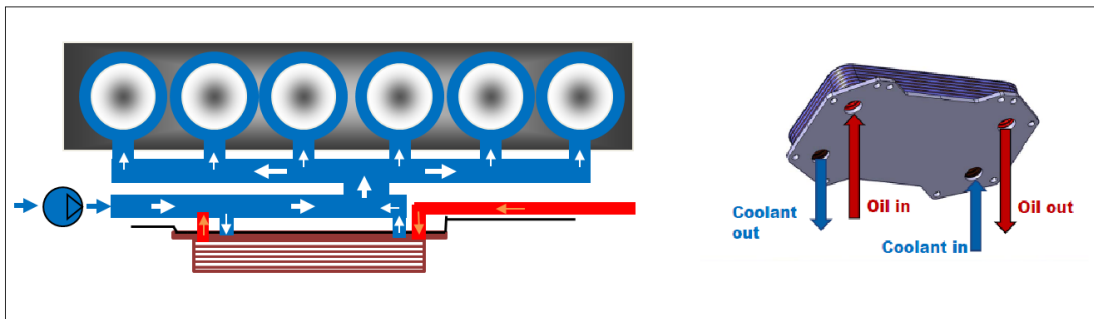


Figure 2.6: Oil cooler (oil and water plates)

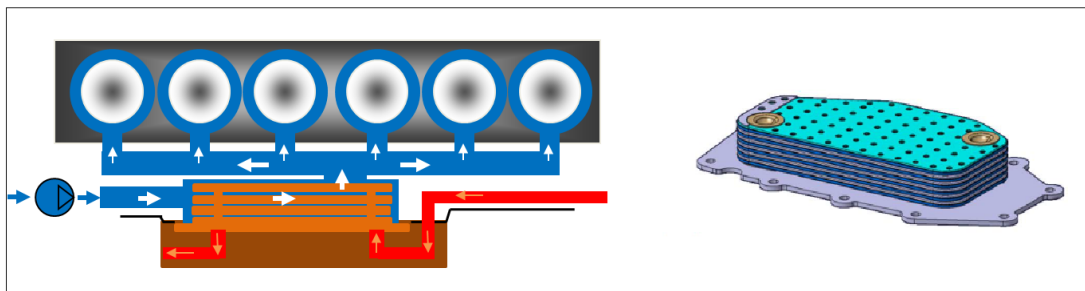


Figure 2.7: Oil cooler (oil plates immersed in water)

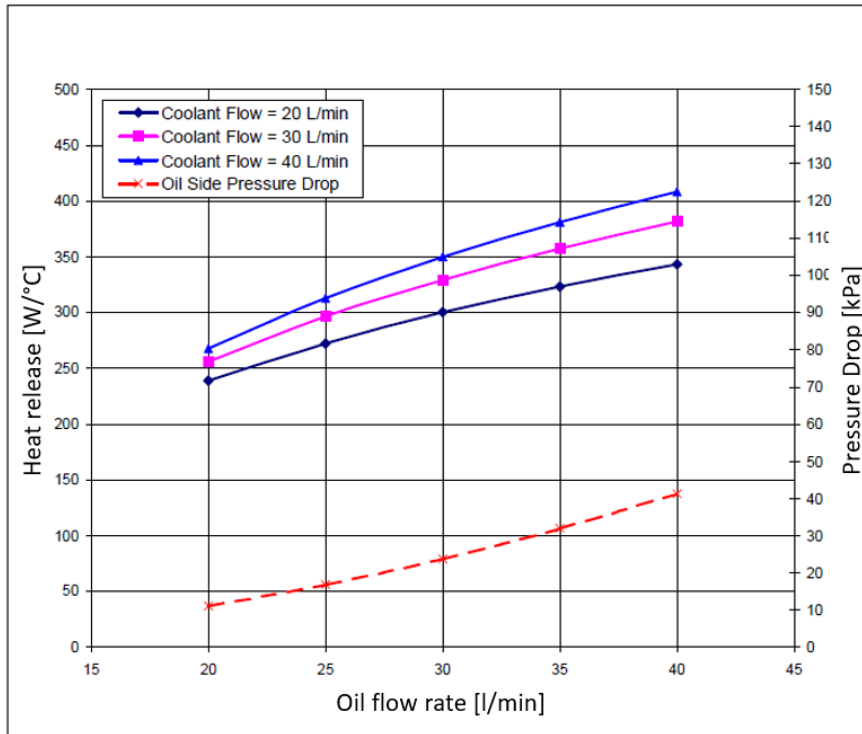


Figure 2.8: Oil cooler heat release performance

2.2.6 Radiator

The radiator, usually located in the vehicle front side, is a water/air heat exchanger used to dissipate the heat released by the engine. It receives hot coolant from the open thermostat and sends the fresh coolant to the pump inlet.

The structure is made of two parts (Figure 2.6) :

- A finned module containing the coolant fluid
- Two tanks for the hot and cold flows distribution

The radiator heat release rate depends on:

- Coolant flow rate
- Coolant temperature
- Air flow rate
- Air temperature

A typical trend of radiator heat release versus water and air flow rates is shown in Figure 2.7.



Figure 2.9: Radiator

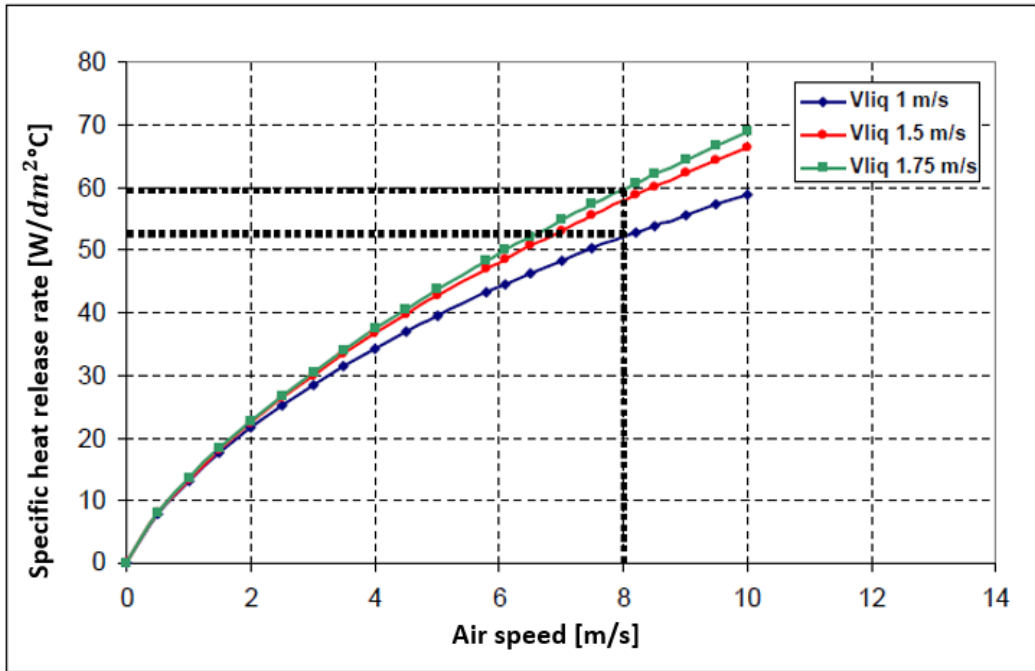


Figure 2.10: Radiator heat release performance

2.2.7 Fan

When the external air flow rate or temperature are not sufficient to dissipate the radiator heat, a fan is activated to force the air flux toward the finned module. The fan is mounted on the engine pulley to have a rotational speed proportional to the engine one.

Four types of joints are used for the fan activation:

- Fixed/Direct connection
- Viscous: an intermediate viscous fluid between pulley and fan produces a friction torque proportional to the relative speed. The transmission ratio is changed proportionally with engine temperature thanks to a bimetallic sheet that changes the internal fluid path according to the required torque.
- Viscronic: same principle of viscous joint with electric control strategy
- Magnetic: an electromagnetic clutch is actuated when required by the system

The control strategy is used to:

- Activate the fan only once needed, reducing the absorbed mechanical power
- Reduce the noise at low engine speed

The most suitable joints for control purposes are the electromagnetic one, which can run also at three different speeds:

- Off
- On 1: Intermediate speed obtained with eddy currents (Foucault effect)
- On 2: Same speed of the engine pulley

The main advantage of having an intermediate speed range is that is possible to reduce the fan power absorption (proportional with the engine speed squared) when the engine runs at low speed and the heat to be dissipated is not too high.

Figure 2.8 shows a magnetic joints with the three speeds characteristic.

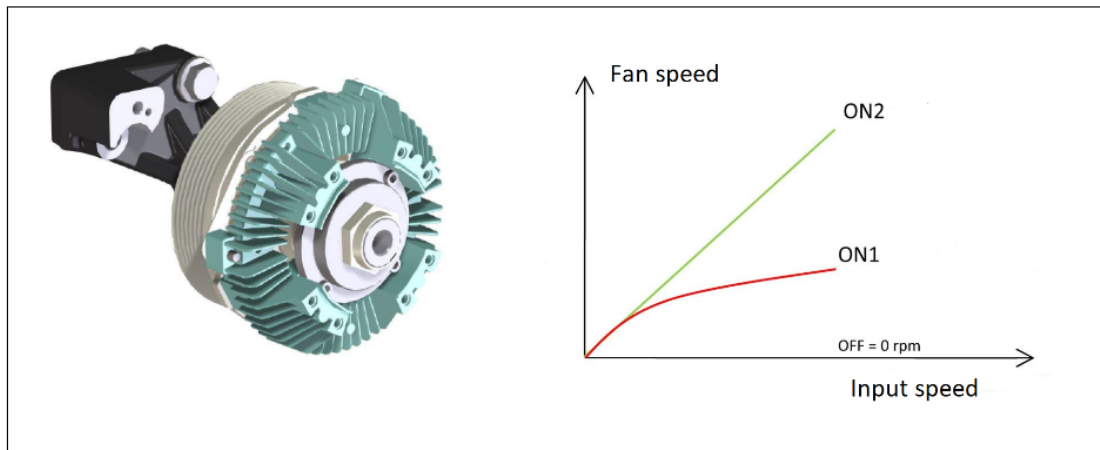


Figure 2.11: Electromagnetic clutch

The fan can be located either behind or in front the radiator (see Figure 2.9), depending on the engine layout and aerodynamic constraints.

A typical air mass flow rate/Head characteristic, measured at the test bench, is reported in Figure 2.10.

The choice for the right fan is determined by its efficiency in the most critical operating condition (low vehicle speed, full load).

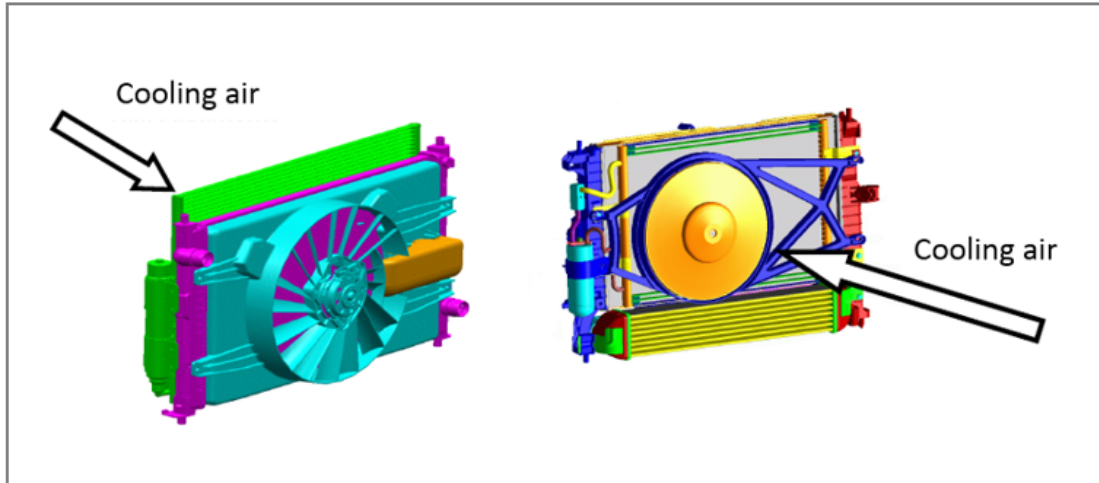


Figure 2.12: Fan location with respect to the radiator

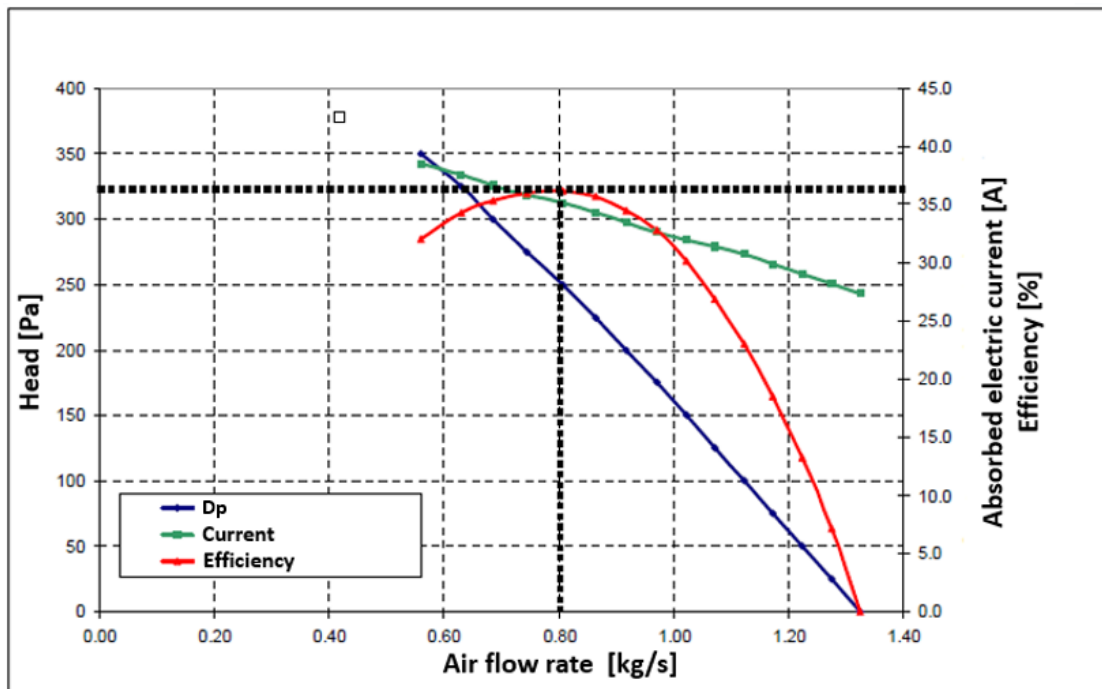


Figure 2.13: Fan characteristic

2.2.8 EGR cooler

The new emissions standards for diesel passenger cars and commercial vehicles can no longer be met with adjustments to the engine alone.

One approach to complying with the new emissions limits is to incorporate cooled exhaust gas recirculation (EGR).

This involves extracting a portion of the main exhaust flow between the engine outlet and the turbine, cooling it in a special heat exchanger, and feeding it back to the intake air downstream of the charge air cooler.

The combustion temperature in the engine is thereby lowered, thus reducing the formation of nitrogen oxides (NO_x) [4].

Figure 2.14 shows a real EGR cooler with the schematic view of gas and coolant ports.

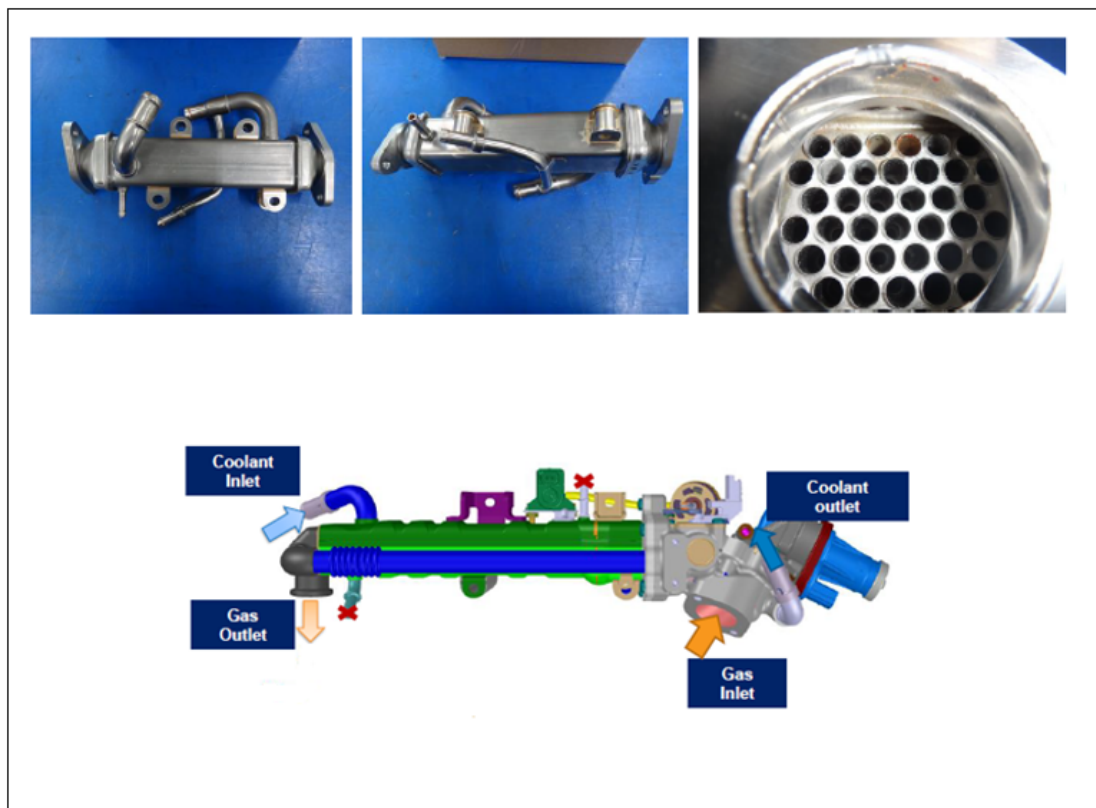


Figure 2.14: EGR cooler

2.2.9 Intercooler

The intercooler is a heat exchanger used to cool down the air at the compressor outlet in turbocharged engines.

The main goal is to increase the air density going into the cylinders, improving the volumetric efficiency. The compressed air at the compressor outlet can reach temperatures near to 200 °C and must be cooled down at 60–50 °C before entering in the combustion chambers.

The intercooler efficiency is defined as:

$$\eta = \frac{T_{ai} - T_{ao}}{T_{ai} - T_{ae}} \quad (2.1)$$

where:

T_{ai} = Air temperature at compressor outlet (intercooler inlet)

T_{ao} = Air temperature at intercooler outlet

T_{ae} = External cooling air temperature

The intercooler is generally an air/air heat exchanger, a typical characteristic curve is shown in Figure 2.15.

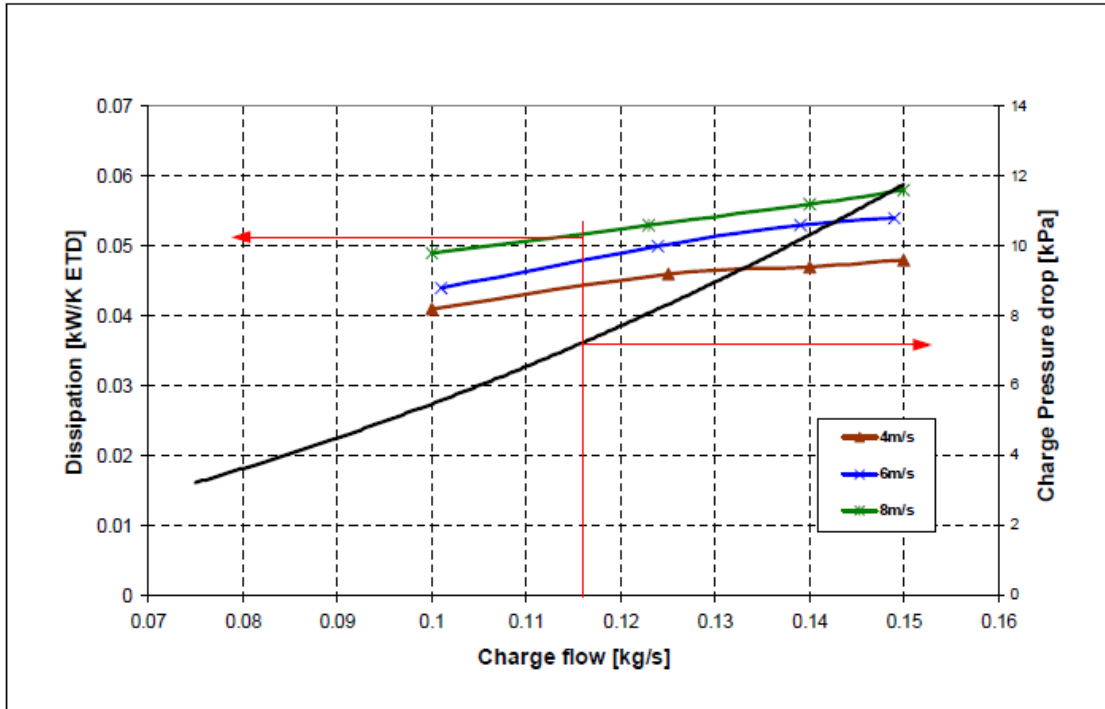


Figure 2.15: Intercooler characteristic

2.3 Heat balance equations

In this section are going to be presented the basic heat balance equations for an internal combustion engine, in order to show the main physical quantities involved in the cooling circuit design.

Starting from the heat generated during the fuel combustion, the generic heat balance equation of the engine is the following:

$$Q_f = Q_u + Q_w + Q_{exh} + Q_{inc} + Q_{rad} \quad [kJ/h] \quad (2.2)$$

where:

Q_f = total heat introduced in the engine with fuel combustion

Q_u = equivalent shaft mechanical power

Q_w = heat released to the cooling fluid

Q_{exh} = heat released to exhaust gases

Q_{inc} = unburned fuel thermal energy

Q_{rad} = heat released with convection and radiation

The total heat introduced with fuel combustion is computed as:

$$Q_f = \dot{m}_f H_i \quad [kJ/h] \quad (2.3)$$

where:

\dot{m}_f = fuel flow rate [kg/h]

H_i = fuel lower heating value [kJ/kg]

The heat released to the cooling fluid is proportional to the engine speed and load, and is the sum of three effects: exhaust gases convection, radiation, and conduction with the walls.

It is computed with the following equation:

$$Q_w = K A_{eq} \Delta T_m \quad [kJ/h] \quad (2.4)$$

where:

K = heat transfer coefficient, depends on gas physical properties and combustion chamber geometry [kJ/m^2Kh]

A_{eq} = equivalent surface of the combustion chamber involved in the heat exchange [m^2]

ΔT_m = temperature difference between combustion chamber walls and cooling fluid [K]

The same heat quantity can be computed looking to the "water side":

$$Q_w = c_w \dot{m}_w (T_{wo} - T_{wi}) \quad [kJ/h] \quad (2.5)$$

where:

c_w = water specific heat capacity at constant pressure [kJ/kgK]

\dot{m}_w = coolant flow rate [kg/h]

T_{wo} = coolant temperature at the engine outlet [K]

T_{wi} = coolant temperature at the engine inlet [K]

If an oil heat exchanger is present in the cooling circuit, the heat released to the coolant is computed with the following equation:

$$Q_w = c_w \dot{m}_w (T_{wo} - T_{wi}) + c_l \dot{m}_l (T_{lo} - T_{li}) \quad [kJ/h] \quad (2.6)$$

where:

c_l = lubricant oil specific heat capacity at constant pressure [kJ/kgK]

\dot{m}_l = lubricant oil flow rate [kg/h]

T_{lo} = lubricant oil temperature at the engine outlet [K]

T_{li} = lubricant oil temperature at the engine inlet [K]

Under the hypothesis of null heat losses along the circuit, the total amount of heat extracted from the engine by the coolant fluid is released to the external environment by the radiator:

$$Q_w = K_r A_r (T_{rm} - T_{ext}) \quad [kJ/h] \quad (2.7)$$

where:

K_r = radiator heat transfer coefficient [kJ/m^2Kh]

A_r = radiator exchange surface [m^2]

T_{rm} = mean coolant temperature inside the radiator [K]

T_{ext} = external environment temperature [K]

The heat released to the exhaust gases is computed as:

$$Q_{exh} = c_{exh} \dot{m}_{exh} (T_{exh,out} - T_{air,in}) \quad [kJ/h] \quad (2.8)$$

where:

c_{exh} = exhaust gases specific heat capacity at constant pressure [kJ/kgK]

\dot{m}_{exh} = exhaust gases flow rate [kg/h]

$T_{exh,out}$ = exhaust gases temperature [K]

$T_{air,in}$ = air inlet temperature [K]

The unburned fuel heat is computed as:

$$Q_{inc} = \lambda \dot{m}_f H_i \quad [kJ/h] \quad (2.9)$$

where:

λ = specific air to fuel ratio

\dot{m}_f = fuel flow rate [kg/h]

H_i = fuel lower heating value [kJ/kg]

Finally, the dissipated thermal power by convection and radiation Q_{rad} , is usually estimated as difference between the total thermal power introduced in the engine with fuel combustion and the total dissipated power already computed.

ATB and ATD parameters

The extreme equilibrium condition for the cooling fluid between the heat received from exhaust gases and the heat released to the external environment is identified by the ATB parameter (Air Temperature to Boiling), which represents, for a specific operating condition of the engine, the ambient temperature for which the coolant starts to boil.

$$ATB = T_{ext} + T_{boil} - T_{ri} \quad [K] \quad (2.10)$$

where:

T_{ext} = external environment temperature [K]

T_{boil} = coolant boiling temperature at the circuit pressurization value [K]

T_{ri} = coolant temperature at the radiator inlet [K]

The ATD parameter (Air Temperature to Derating) represents, for a specific operating condition of the engine, the ambient temperature for which the engine power rating starts to be reduced for safety reasons (e.g. too high coolant temperature reached in operation).

$$ATD = T_{ext} + T_{derating} - T_{ri} \quad [K] \quad (2.11)$$

where:

T_{ext} = external environment temperature [K]

T_{boil} = engine derating temperature [K]

T_{ri} = coolant temperature at the radiator inlet [K]

Chapter 3

Cooling circuit unidimensional modeling

After a brief overview on the engine cooling system main functions and the basic theory of engine thermal management, in this chapter is described in detail the central activity of the project, the unidimensional modeling of the engine cooling circuit.

This activity required lot of time, either to learn the software and acquire the proper skills to create the model in a smart way, or to test new procedures able to refine the results and reduce the computational time.

Lot of interactions with the design engineers have been necessary, to gather all the cooling system components data and implement the proper fluid dynamic and thermal characteristics.

The model is presented in two configurations in order to support the cooling system design and validation in different design phases.

The test bench model to be used during the prototyping to test new design proposals and technical solutions, before running the engine in the test cell.

The vehicle model for testing the engine within the final vehicle, dependent on the client specifications.

3.1 Software

The software used for the project is GT-SUITE by Gamma Technologies, a 0D/1D/3D multi-physics CAE system simulation software used in the automotive field for engine performance, systems validation and control strategies.

For powertrain cooling applications, GT-SUITE models can be used to predict heat rejection to coolant, oil, and ambient, before engine hardware is available for physical testing. Simulations can be performed both in steady state and transient conditions [2].

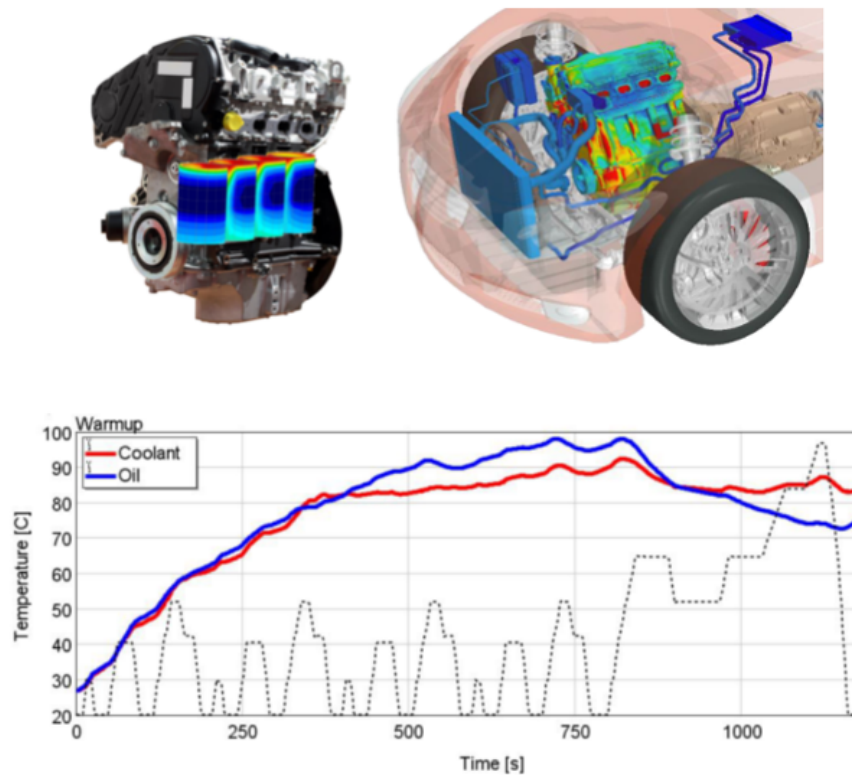


Figure 3.1: GT-SUITE engine cooling system simulations

3.2 Engine water jacket 1D model

The starting point of the modeling activity has been to extract the water jacket volume from the engine cad model and import it as STL file on GEM3D, a graphical pre-processor used to create 1D GT-SUITE models from 3D geometries. The resultant geometry is shown in Figure 3.2.

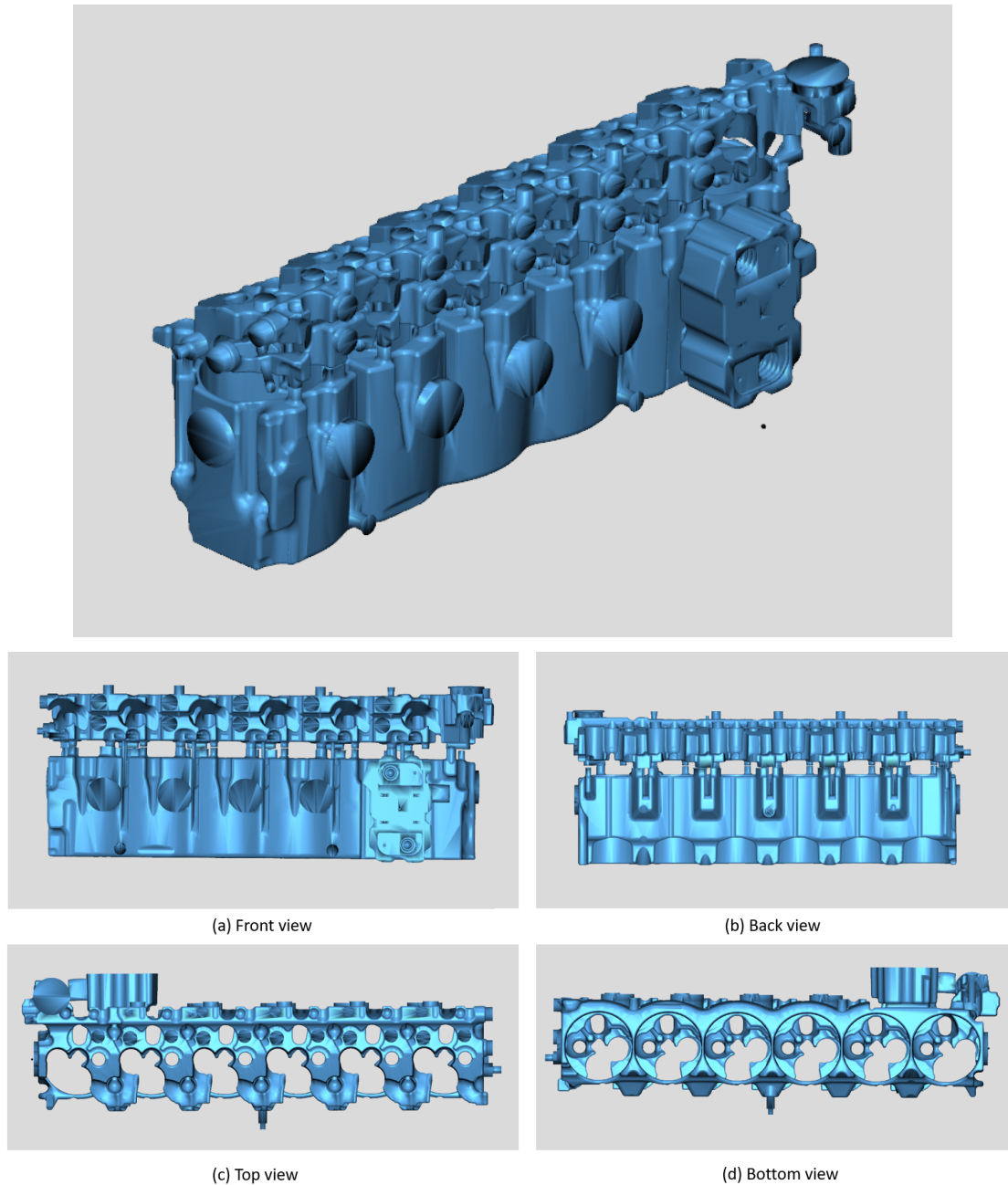


Figure 3.2: Water jacket views

3.2.1 External connections opening

Using the *cutting tool* command, is possible to open the water jacket connections with the external components of the cooling circuits:

- Pump
- Thermostat
- Cabin Heater
- CNG pressure regulator
- Turbocharger

Figure 3.3 shows the water jacket front view and back view with the indication of the inlet and outlet ports.

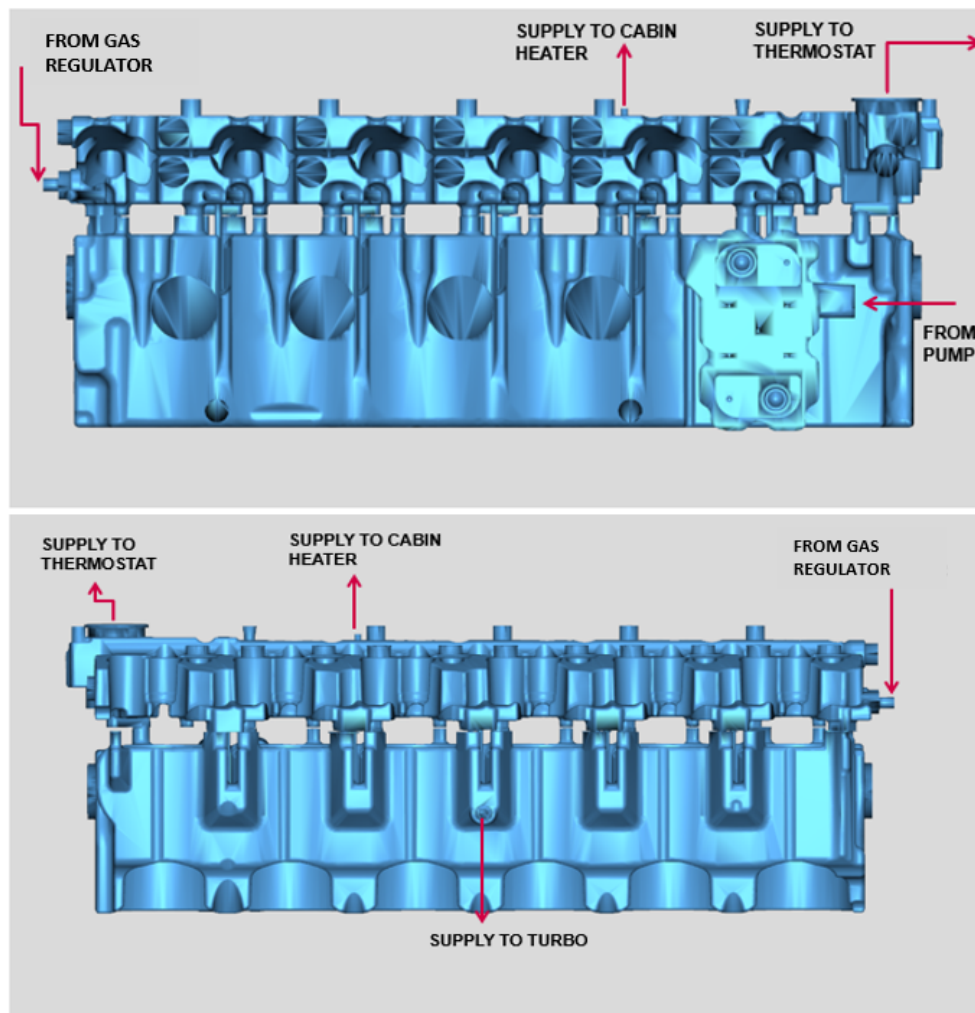


Figure 3.3: Water jacket ports

3.2.2 Geometry discretization

The 3D geometry has been discretized in three main parts (block, cylinder head gasket, and cylinder head) and each part divided in six components, as the engine number of cylinders.

In particular, cylinder 1 and cylinder 2 have been merged in a single component due to the presence of the oil cooler inlet port between the two. Therefore, head 1 and head 2 have been merged too. For what the cylinder head gasket is concerned, each connecting passage between block and cylinder head have been opened in order to be calibrated in the following steps.

The water jacket discretized volumes are the following (Figure 3.4):

BLOCK	C 1-2	C3	C4	C5	C6
HEAD	H 1-2	H3	H4	H5	H6
GASKET	A1,B1,E12,F12 A2,B2,E23,F23	A3,B3,E34,F34	A4,B4,E45,F45	A5,B5,E56,F56	A6,B6

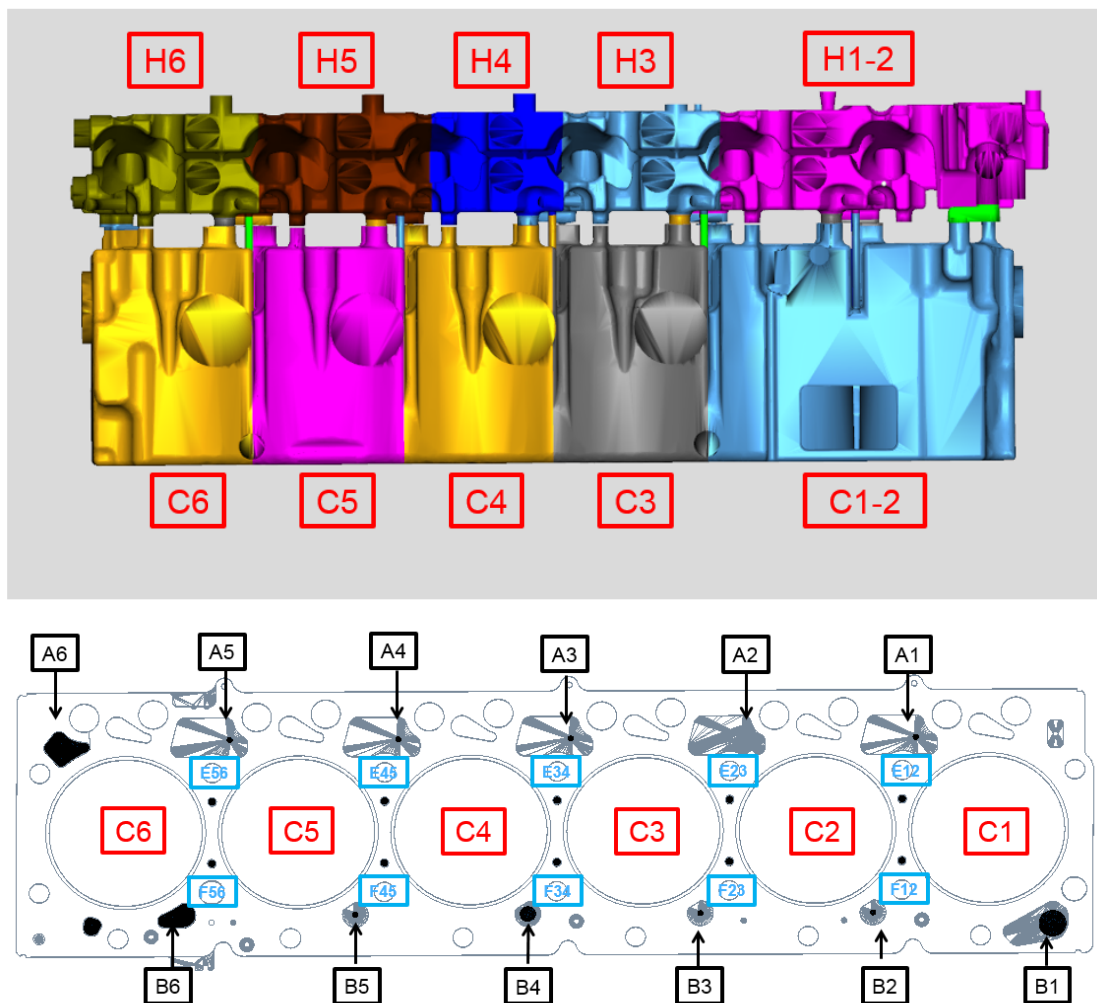


Figure 3.4: Water jacket discretized volumes

3.2.3 Equivalent flow split elements

Using the *Convert shape to component* command, each volume of the discretized 3D geometry has been converted in a flow split element with equivalent ports representing the water connections with adjacent volumes.

Figure 3.5 shows, as an example, how cylinder C6 and head H6 look like after the conversion:

- Ports 3 (A6) and 4 (B6) represent the connections through the head gasket
- Ports 5 (E56) and 6 (F56) represent the vertical cross drills connections
- Ports 1 and 2 represent the connections to the adjacent volumes
- Port 8 represents the external connection of head H6 with the gas pressure regulator

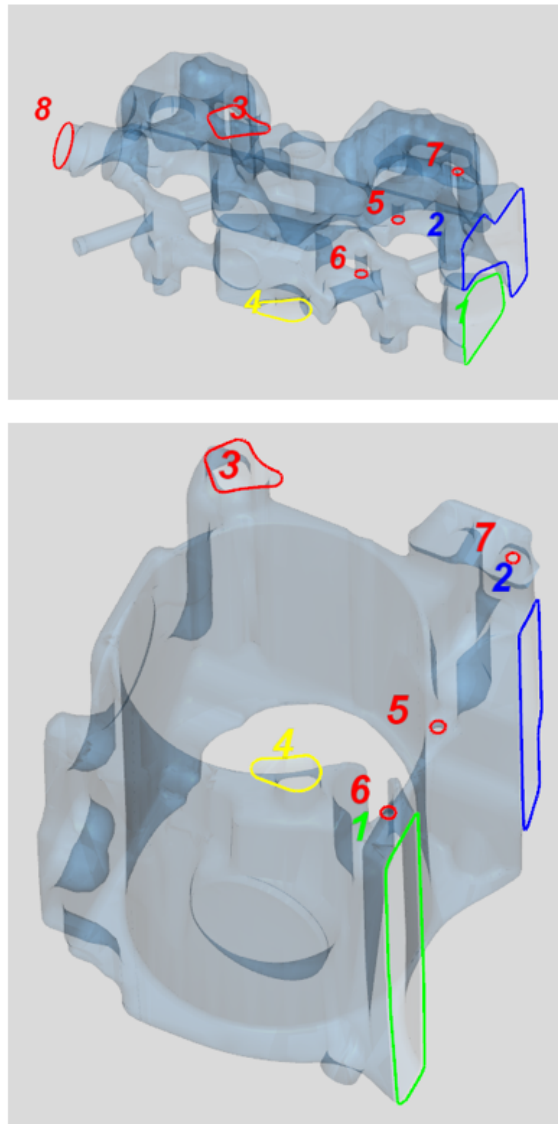


Figure 3.5: H6 and C6 flow split components

3.2.4 GT model

Once the conversion has been completed, the 3D model has been transformed in an equivalent unidimensional circuit made by pipes, orifices and splitters representing the water jacket internal and external connections. The resultant circuit has been organized in order to have an easy understanding of the circuit layout, and each cylinder head gasket orifice has been named according to the followed standard. It is important to highlight at this point, that the 1D circuit obtained with the conversion needs to be calibrated in order to perform the same behavior of the target tridimensional CFD simulation.

Some *End-flow* elements have been added to the circuit in order to represent the water boundary conditions at the external connections.

The boundary data derive from the 3D CFD simulation of the engine running at 2000 rpm, reported in Figure 3.6:

- PUMP-FLOW: Inlet water flow rate coming from the pump equal to 3.25 kg/s
- SUPPLY-THERMOSTAT: Thermostat pressure equal to 1.97 bar and water flow rate almost equal to the 97% of the pump flow rate
- SUPPLY-TURBO: Turbocharger water feeding pressure equal to 2.46 bar and water flow rate almost equal to the 3% of the pump flow rate

The other water jacket external connections have been closed at this phase to match the 3D simulations results. They have been opened later during the water jacket matching with the external cooling circuit and calibrated in order to guarantee the target flow rates for each component.

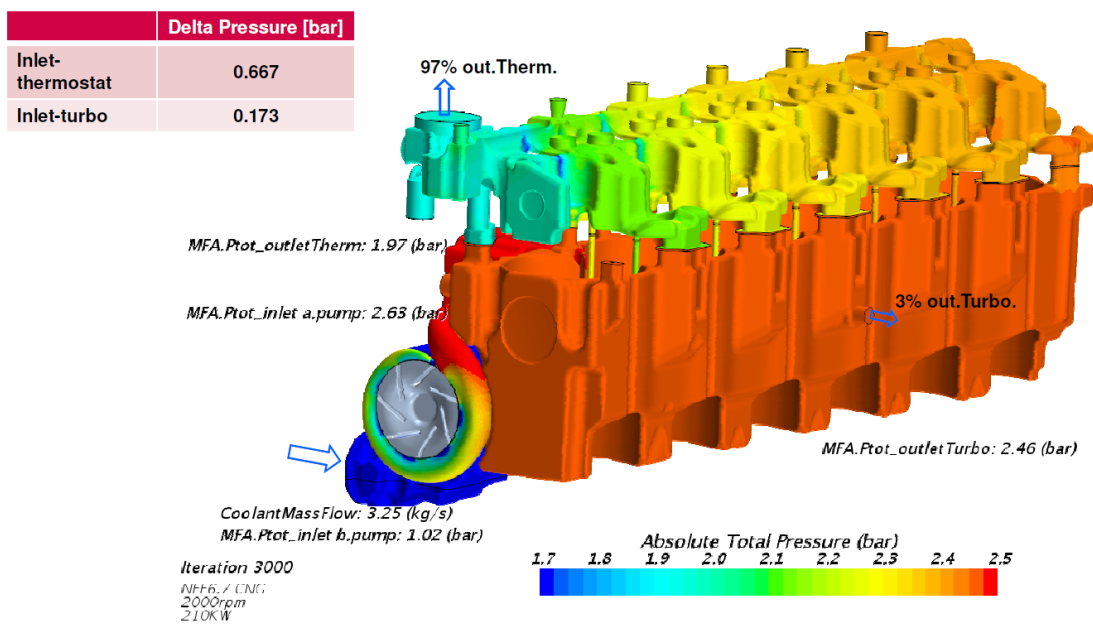


Figure 3.6: 3D CFD simulation boundary data

The first step cooling circuit model is shown in Figure 3.7 with the highlighted regions:

- BLOCK REGION (green)
- GASKET REGION (red)
- HEAD REGION (yellow)

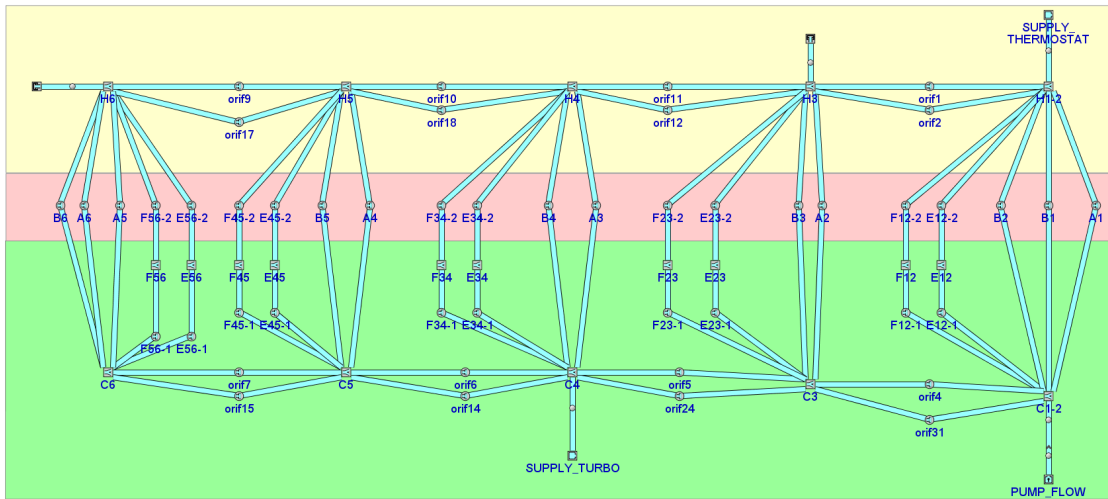


Figure 3.7: Water jacket GT model

3.3 Engine water jacket 1D model calibration

The resulting 1D water jacket model did not show the same fluid dynamic performance of the 3D model after conversion.

The circuit branches showed different pressure drops and flow rates.

The following step has been to perform a head/gasket orifices calibration based on the target flow rates of the 3D CFD simulation (Figure 3.8).

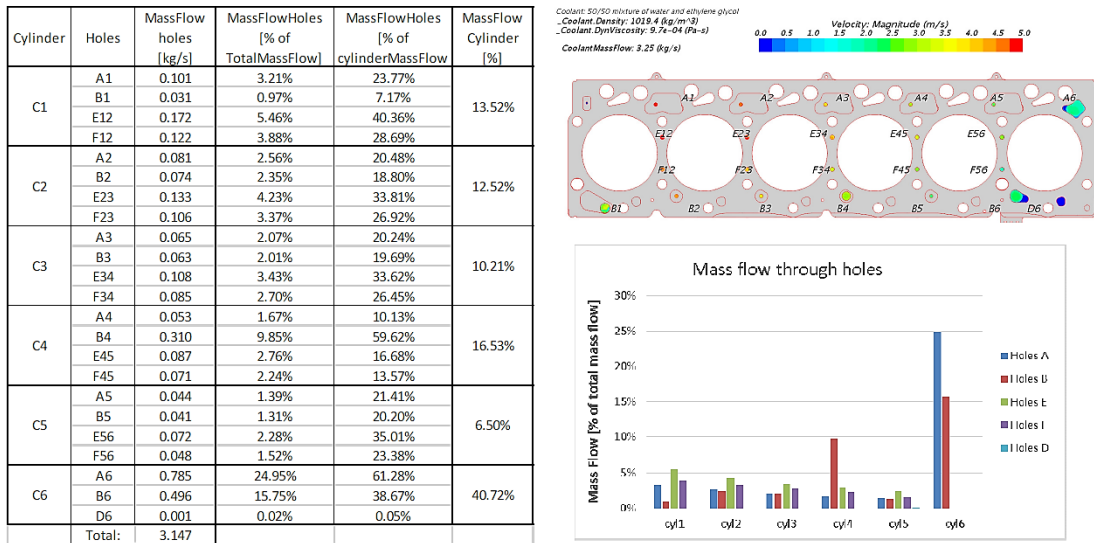


Figure 3.8: 3D CFD simulation target flow rates

In the following, are presented two different approaches used to achieve that target:

- A standard procedure
- An alternative procedure I have proposed in order to get precise results in a short time

The basic idea of both procedures is to parametrize the head orifices diameters in the model *Case Setup* and change them iteratively until the target flow rates are reached.

3.3.1 Standard procedure

The standard iterative procedure is done basically by hand, using an Excel file. Each orifice diameter is changed manually in order to reach the target flow rate with a maximum tolerance of 10 %.

The main disadvantage of this procedure is that any change requires a new simulation, more setup cases are required with the updated values and the time to reach the tolerance increases exponentially with the increasing number of variables to be controlled.

Below is reported the excel table used to calibrate the model (Figure 3.9).

At least ten iterations have been performed to reach the tolerance and the results were not so precise (a finer calibration would require even more time).

Cylinder	Water hole	Star	CASE 1		CASE 2		CASE 3		CASE 4		CASE 5		CASE 6		CASE 7		CASE 8		CASE 9		CASE 10			
			Mass flow kg/s	Diameter [mm]	Mass flow kg/s	Change wet Star %	Diameter [mm]	Mass flow kg/s	Change wet Star %	Diameter [mm]	Mass flow kg/s	Change wet Star %	Diameter [mm]	Mass flow kg/s	Change wet Star %	Diameter [mm]	Mass flow kg/s	Change wet Star %	Diameter [mm]	Mass flow kg/s	Change wet Star %	Diameter [mm]	Mass flow kg/s	Change wet Star %
C1	A1	0.11	27.565	3.9	13.7025	0.81	10.81	6.89	0.20	7.6	4.00	0.07	1.6	4.50	0.08	3.7	3.00	0.30	3.3	3.00	0.30	3.3	3.00	0.30
	B1	0.001	17.382	0.36	8.991	0.33	14.4	4.50	0.08	2.7	4.00	0.07	1.6	2.00	0.02	1.0	6.50	0.00	3.9	6.50	0.00	3.9	6.50	0.00
	E12	0.10	5.988	0.18	2.4	3.988	0.19	1.4	5.99	0.19	1.4	5.99	0.19	1.4	6.00	5.99	0.19	6.00	5.99	0.19	6.00	5.99	0.19	
C2	F56	0.10	5.988	0.18	2.4	3.994	0.06	4.00	0.07	4.00	5.99	0.19	1.4	5.99	0.19	1.4	5.99	0.19	1.4	5.99	0.19	1.4	5.99	0.19
	A2	0.09	27.89	0.10	13.845	0.10	13.4	13.00	0.10	13.2	8.00	0.10	7.7	8.00	0.10	7.8	8.00	0.10	7.8	8.00	0.10	7.8	8.00	0.10
	E2	0.05	17.418	0.10	8.9	17.418	0.10	8.9	17.00	0.10	8.9	15.00	0.10	8.9	14.00	0.10	8.9	13.00	0.10	8.9	12.00	0.10	8.9	11.00
C3	E23	0.15	5.988	0.18	4.2	5.988	0.18	5.9	5.99	0.18	6.1	5.99	0.18	6.1	5.99	0.18	6.1	5.99	0.18	6.1	5.99	0.18	6.1	5.99
	F93	0.31	5.988	0.18	2.4	3.994	0.06	4.00	0.07	4.00	5.99	0.19	1.4	5.99	0.19	1.4	5.99	0.19	1.4	5.99	0.19	1.4	5.99	
	A3	0.07	27.889	0.11	13.945	0.11	13.4	13.00	0.11	13.2	8.00	0.11	7.9	8.00	0.11	7.8	8.00	0.11	7.8	8.00	0.11	7.8	8.00	
C4	B3	0.06	17.431	0.09	8.1	8.7155	0.09	7.0	7.00	0.08	7.0	3.00	0.07	3.0	4.80	0.07	4.8	4.80	0.07	4.8	4.80	0.07	4.8	4.80
	F34	0.08	5.988	0.08	2.4	5.988	0.08	2.4	5.99	0.08	2.4	5.99	0.08	2.4	5.99	0.08	2.4	5.99	0.08	2.4	5.99	0.08	2.4	5.99
	A4	0.00	27.893	0.10	13.9415	0.10	13.4	13.00	0.10	13.2	8.00	0.10	8.1	8.00	0.10	8.1	8.00	0.10	8.1	8.00	0.10	8.1	8.00	
C5	B4	0.12	17.416	0.04	11.4	8.909	0.06	5.9	8.71	0.06	5.9	8.71	0.06	5.9	8.71	0.06	5.9	8.71	0.06	5.9	8.71	0.06	5.9	8.71
	E45	0.09	5.988	0.13	4.1	2.994	0.04	3.4	4.50	0.07	2.9	4.50	0.09	3.9	4.50	0.09	3.9	4.50	0.09	3.9	4.50	0.09	3.9	4.50
	F96	0.05	5.988	0.10	2.4	3.994	0.06	4.00	0.07	4.00	5.99	0.19	1.4	5.99	0.19	1.4	5.99	0.19	1.4	5.99	0.19	1.4	5.99	
C6	A5	0.05	27.899	0.10	13.9495	0.10	13.4	13.00	0.10	13.2	8.00	0.10	8.1	8.00	0.10	8.1	8.00	0.10	8.1	8.00	0.10	8.1	8.00	
	B5	0.04	16.438	0.10	13.1	8.219	0.10	13.1	4.11	0.05	4.0	4.00	0.05	4.0	3.00	0.04	11.8	3.20	0.04	4.0	3.20	0.04	4.0	3.20
	E06	0.07	5.988	0.10	2.4	3.994	0.06	4.00	0.07	4.00	5.99	0.19	1.4	5.99	0.19	1.4	5.99	0.19	1.4	5.99	0.19	1.4	5.99	
C6	F45	0.05	5.988	0.13	4.1	2.994	0.04	3.4	4.00	0.07	3.4	4.00	0.05	3.4	4.00	0.05	3.4	4.00	0.05	3.4	4.00	0.05	3.4	4.00
	A6	0.77	22.809	2.40	11.3	13.965	0.51	13.0	12.00	0.40	13.0	12.50	0.65	13.0	13.00	0.72	6.4	13.00	0.72	6.4	13.00	0.72	6.4	13.00
C6	B6	0.36	17.398	2.28	8.699	0.52	11.7	10.00	0.40	10.0	9.00	0.34	4.9	9.00	0.34	5.0	9.00	0.34	5.0	9.00	0.34	5.0	9.00	

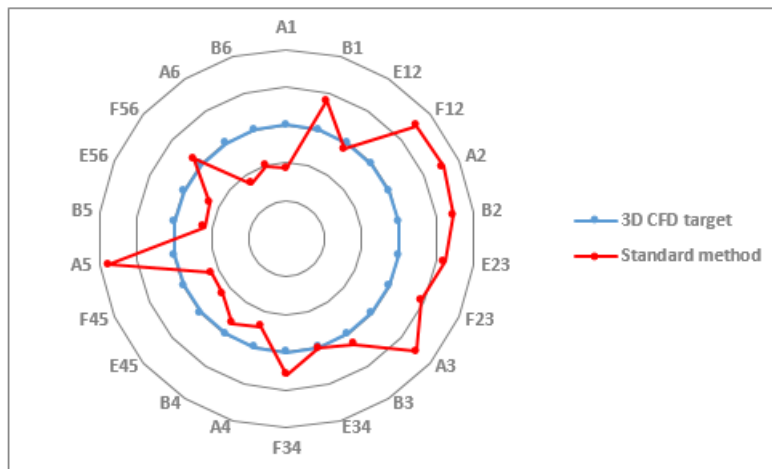


Figure 3.9: Excel table used for manual calibration

Starting from these results, I have worked on building a new procedure able to improve both results precision and time.

3.3.2 New procedure

The main property of the proposed procedure is to be completely automatic, only one simulation is required and the target is reached without error.

The idea is to use a PID control for each orifice able to automatically tune the diameter and reach the target flow rate.

The PID control can be implemented on GT-Suite using the *PIDController* component.

The *Help* tool has been used as guide for the settings definition and the theoretical information acquisition.

PID control

The PID control [5] purpose is to achieve and maintain a target value of some sensible quantity from the system (also known as the "plant") by controlling some input to the plant.

The sensed value from the plant is the input signal to the controller, and the output signal from the *PIDController* is used to control some device on the plant that is to be actuated.

This type of control configuration is known as closed-loop control because the signals make a loop between the plant and the controller.

It needs as main input data:

1. Target for the Input Signal
2. Gains (Proportional, Derivative, Integral)
3. Initial Output Signal
4. Output range (Minimum, Maximum)
5. Convergence criteria (Type of Steady State Error and Tolerance)
6. Solution control (Sampling and ODE Integration Accuracy)

The objective of the controller is to hit a target value as quickly as possible while maintaining stability (an unstable controller is one that continually overshoots the target back and forth) .

At every time step, the *PIDController* calculates the error, which is defined as the difference between the specified Reference Signal and the input signal.

The controller attempts to make its input signal equal Reference Signal by minimizing the error over time.

While PID controllers have great flexibility, they also can be difficult to use because suitable gains have to be found to work for the given situation.

The following equations are solved in the *PIDController* :

$$\frac{dx_1}{dt} = u \quad (3.1)$$

$$\frac{dx_2}{dt} = \frac{u - x_2}{\tau} \quad (3.2)$$

$$y = \left(K_P + \frac{K_D}{\tau} \right) u + K_I x_1 - \frac{K_D}{\tau} x_2 \quad (3.3)$$

where:

K_P = proportional gain

K_I = integral gain

K_D = derivative gain

τ = derivative time constant

y = controller output

u = difference between the Reference Signal value and the input signal value

x_1, x_2 = state variables

If the initial input signal value is known, the user can control the initial output value through the State 1 Initial Value and State 2 Initial Value attributes.

The user may modify the controller gain values depending on the controller behavior using the procedure reported in the following:

- The output should gradually reach its steady value, and may oscillate around that value before settling down. If the response is unstable, reduce the Proportional Gain and Integral Gain values until a stable response is obtained
- If the output takes a long time to reach its final steady, both the Proportional Gain and the Integral Gain values can be increased to speed up the response
- If the output reaches a value, then gradually increases or decreases to the final steady the Integral Gain value can be increased to shorten the time required to reach the steady value
- If the output reaches the steady value quickly, but oscillates around it for a long time, the Derivative Gain value may be increased. A larger Derivative Gain value will damp out oscillations in a shorter time

Settings

Due to the high number of orifices to be calibrated (one for each water passage) and to the type of control (equal for each passage) the data have been implemented using:

- One *Receive Signal* component for the mass flow rate measurement (input)
- One *Send Signal* component for the diameter definition (output)

Settings have been implemented using the *Edit Parts in Spreadsheet* command.

Main

- Target for the input signal: mass flow rates coming from the 3D CFD simulation
- Proportional gain: $K_P = 2$
- Integral gain: $K_I = 6$
- Derivative gain: neglected. It would cause instability due to the variable nature of the input quantity.

Proportional and derivative gains have been chosen using the before mentioned procedure.

Attribute	Object Name	Target for the Input Signal	Gains Specification / Calculation		Gains Specified	Proportional Gain	Integral Gain	Derivative Gain
Unit								
1	PID_A1	0.11 ...	Gains Specification / Calculation	<input checked="" type="radio"/>		2 ...	6 ...	ign ...
2	PID_A2	0.09 ...		<input checked="" type="radio"/>		2 ...	6 ...	ign ...
3	PID_A3	0.07 ...		<input checked="" type="radio"/>		2 ...	6 ...	ign ...
4	PID_A4	0.06 ...		<input checked="" type="radio"/>		2 ...	6 ...	ign ...
5	PID_A5	0.05 ...		<input checked="" type="radio"/>		2 ...	6 ...	ign ...
6	PID_A6	0.77 ...		<input checked="" type="radio"/>		2 ...	6 ...	ign ...
7	PID_B1	0.001 ...		<input checked="" type="radio"/>		2 ...	6 ...	ign ...
8	PID_B2	0.08 ...		<input checked="" type="radio"/>		2 ...	6 ...	ign ...
9	PID_B3	0.06 ...		<input checked="" type="radio"/>		2 ...	6 ...	ign ...
10	PID_B4	0.32 ...		<input checked="" type="radio"/>		2 ...	6 ...	ign ...
11	PID_B5	0.04 ...		<input checked="" type="radio"/>		2 ...	6 ...	ign ...
12	PID_B6	0.36 ...		<input checked="" type="radio"/>		2 ...	6 ...	ign ...
13	PID_E12	0.19 ...		<input checked="" type="radio"/>		2 ...	6 ...	ign ...
14	PID_E23	0.15 ...		<input checked="" type="radio"/>		2 ...	6 ...	ign ...
15	PID_E34	0.11 ...		<input checked="" type="radio"/>		2 ...	6 ...	ign ...
16	PID_E45	0.09 ...		<input checked="" type="radio"/>		2 ...	6 ...	ign ...
17	PID_E56	0.07 ...		<input checked="" type="radio"/>		2 ...	6 ...	ign ...
18	PID_F12	0.12 ...		<input checked="" type="radio"/>		2 ...	6 ...	ign ...
19	PID_F23	0.11 ...		<input checked="" type="radio"/>		2 ...	6 ...	ign ...
20	PID_F34	0.08 ...		<input checked="" type="radio"/>		2 ...	6 ...	ign ...
21	PID_F45	0.07 ...		<input checked="" type="radio"/>		2 ...	6 ...	ign ...
22	PID_F56	0.05 ...		<input checked="" type="radio"/>		2 ...	6 ...	ign ...

Figure 3.10: PID Controller settings (Main)

Limits

Minimum and maximum diameter dimensions set to comply with mass flow rate targets.

Attribute	Object Name	Minimum Output	Maximum Output
Unit			
1	PID_A1	0.4 ...	50 ...
2	PID_A2	0.4 ...	50 ...
3	PID_A3	0.4 ...	50 ...
4	PID_A4	0.4 ...	50 ...
5	PID_A5	0.4 ...	50 ...
6	PID_A6	0.4 ...	50 ...
7	PID_B1	0.4 ...	50 ...
8	PID_B2	0.4 ...	50 ...
9	PID_B3	0.4 ...	50 ...
10	PID_B4	0.4 ...	50 ...
11	PID_B5	0.4 ...	50 ...
12	PID_B6	0.4 ...	50 ...
13	PID_E12	0.4 ...	50 ...
14	PID_E23	0.4 ...	50 ...
15	PID_E34	0.4 ...	50 ...
16	PID_E45	0.4 ...	50 ...
17	PID_E56	0.4 ...	50 ...
18	PID_F12	0.4 ...	50 ...
19	PID_F23	0.4 ...	50 ...
20	PID_F34	0.4 ...	50 ...
21	PID_F45	0.4 ...	50 ...
22	PID_F56	0.4 ...	50 ...

Figure 3.11: PID Controller settings (Limits)

Initialization

- Dwell duration: duration for which the output signal will be held at Initial Output
- Initial Outputs: equal to the orifices diameters of the not-calibrated model, reported as variables in the Case Setup

Attribute	Object Name	Dwell Duration Type	Dwell Duration	Initial Output
Unit				
1	PID_A1	seconds ▼	5 ...	[A1] ...
2	PID_A2	seconds ▼	5 ...	[A2] ...
3	PID_A3	seconds ▼	5 ...	[A3] ...
4	PID_A4	seconds ▼	5 ...	[A4] ...
5	PID_A5	seconds ▼	5 ...	[A5] ...
6	PID_A6	seconds ▼	5 ...	[A6] ...
7	PID_B1	seconds ▼	5 ...	[B1] ...
8	PID_B2	seconds ▼	5 ...	[B2] ...
9	PID_B3	seconds ▼	5 ...	[B3] ...
10	PID_B4	seconds ▼	5 ...	[B4] ...
11	PID_B5	seconds ▼	5 ...	[B5] ...
12	PID_B6	seconds ▼	5 ...	[B6] ...
13	PID_E12	seconds ▼	5 ...	[E12] ...
14	PID_E23	seconds ▼	5 ...	[E23] ...
15	PID_E34	seconds ▼	5 ...	[E34] ...
16	PID_E45	seconds ▼	5 ...	[E45] ...
17	PID_E56	seconds ▼	5 ...	[E56] ...
18	PID_F12	seconds ▼	5 ...	[F12] ...
19	PID_F23	seconds ▼	5 ...	[F23] ...
20	PID_F34	seconds ▼	5 ...	[F34] ...
21	PID_F45	seconds ▼	5 ...	[F45] ...
22	PID_F56	seconds ▼	5 ...	[F56] ...

Figure 3.12: PID Controller settings (Initialization)

Convergence

- Type of Steady State Error: type of steady state error that must be achieved before the controller convergence criterion is met
- Steady State Tolerance: the error tolerance that will be used in conjunction with the above two attributes to determine if the controller convergence criterion is met

Attribute	Object Name	Type of Steady State Error	Type of Steady State Error Tolerance	Steady State Error Tolerance	Consecutive Cycles/RLT Update Intervals for Steady-State
Unit					
1	PID_A1	max_over_RLT_interval	percentage	0.5	4
2	PID_A2	max_over_RLT_interval	percentage	0.5	4
3	PID_A3	max_over_RLT_interval	percentage	0.5	4
4	PID_A4	max_over_RLT_interval	percentage	0.5	4
5	PID_A5	max_over_RLT_interval	percentage	0.5	4
6	PID_A6	max_over_RLT_interval	percentage	0.5	4
7	PID_B1	max_over_RLT_interval	percentage	0.5	4
8	PID_B2	max_over_RLT_interval	percentage	0.5	4
9	PID_B3	max_over_RLT_interval	percentage	0.5	4
10	PID_B4	max_over_RLT_interval	percentage	0.5	4
11	PID_B5	max_over_RLT_interval	percentage	0.5	4
12	PID_B6	max_over_RLT_interval	percentage	0.5	4
13	PID_E12	max_over_RLT_interval	percentage	0.5	4
14	PID_E23	max_over_RLT_interval	percentage	0.5	4
15	PID_E34	max_over_RLT_interval	percentage	0.5	4
16	PID_E45	max_over_RLT_interval	percentage	0.5	4
17	PID_E56	max_over_RLT_interval	percentage	0.5	4
18	PID_F12	max_over_RLT_interval	percentage	0.5	4
19	PID_F23	max_over_RLT_interval	percentage	0.5	4
20	PID_F34	max_over_RLT_interval	percentage	0.5	4
21	PID_F45	max_over_RLT_interval	percentage	0.5	4
22	PID_F56	max_over_RLT_interval	absolute	0.5	4

Figure 3.13: PID Controller settings (Convergence)

Solution control

A continuous sampling interval has been selected.
The resultant PID controller is shown below (Figure 3.14).

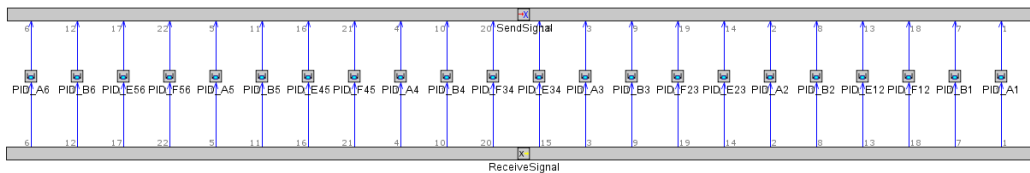


Figure 3.14: PID controller

Run Setup

Simulation is solved using an Explicit Runge-Kutta integrator as recommended in the GT guide for cooling applications. Due to the fluid dynamic nature of the problem (at this phase the main targets are pressures and flow rates in the circuit), the thermal control has been switched off.

Results

The model calibration is completed in few seconds without errors.

The controller reaches the target mass flow rate in less than 25 seconds of simulation time, without oscillations. The output value is the diameter of the calibrated orifice. In the following, are reported the diameter values after calibration (Figure 3.15) and the PID controllers converged solutions (Figure 3.16).

Cylinder	Orifice	Target mass flow [kg/s]	Calibrated diameters [mm]
C1	A1	0,101	4,6
	B1	0,031	2,55
	E12	0,172	5,27
	F12	0,122	4,6
C2	A2	0,081	4,13
	B2	0,074	3,94
	E23	0,133	4,77
	F23	0,106	4,37
C3	A3	0,065	3,7
	B3	0,063	3,65
	E34	0,108	4,41
	F34	0,085	4
C4	A4	0,053	3,35
	B4	0,31	8,1
	E45	0,087	4,05
	F45	0,071	3,73
C5	A5	0,044	3,05
	B5	0,041	2,94
	E56	0,072	3,74
	F56	0,048	3,13
C6	A6	0,785	12,89
	B6	0,496	10,25

Figure 3.15: Head/gasket calibrated orifices diameters

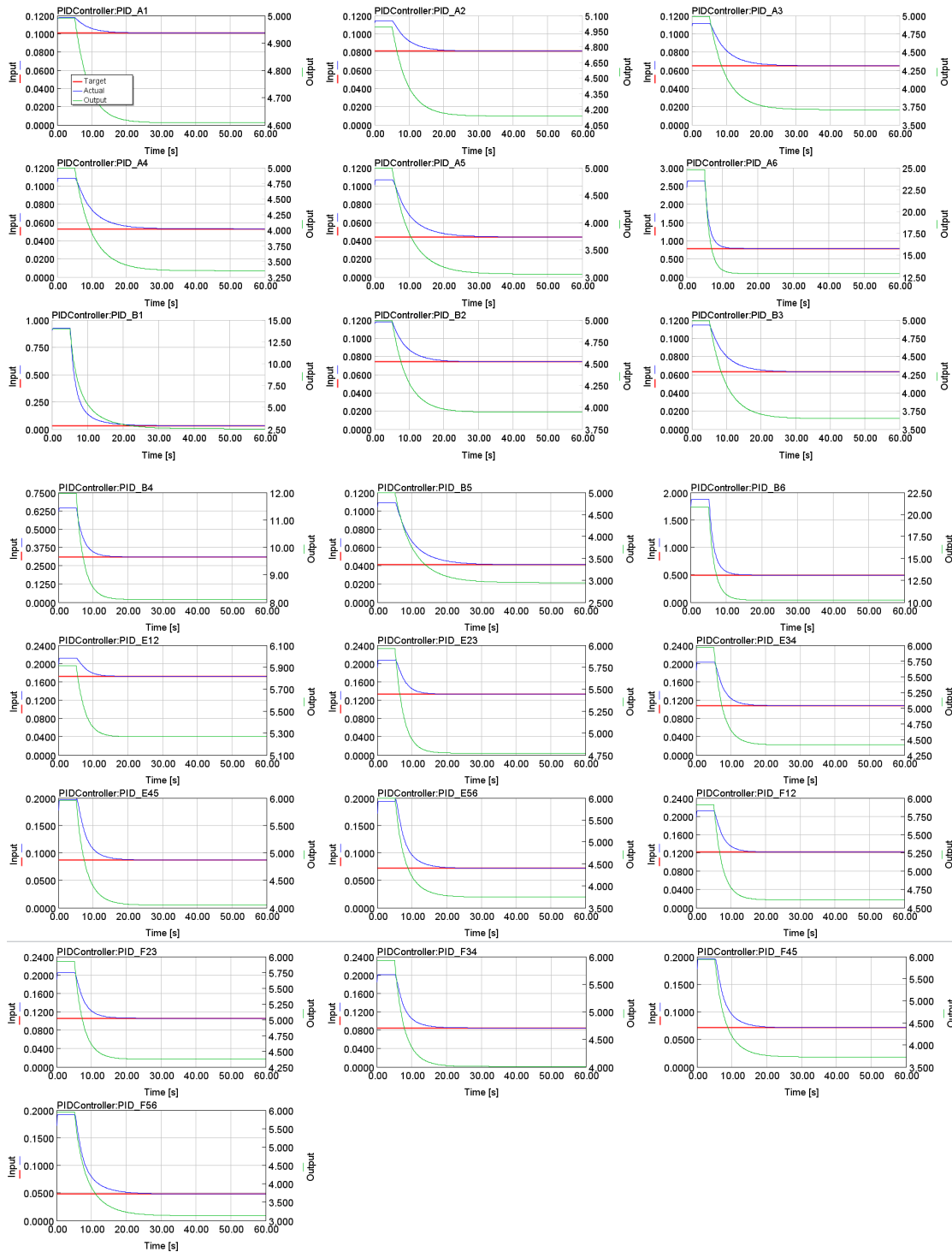


Figure 3.16: PID controllers converged solutions

In order to validate the calibration, it is important to verify that the pressure and mass flow distributions in the 1D model are equal to the one coming from the 3D CFD simulation.

Figure 3.17 and Figure 3.18 show respectively the average pressure and coolant mass flow rate distribution of the water jacket equivalent model.

The new procedure shows the following advantages:

- 100 % target achievement
- Single simulation required
- Automatic model calibration
- Simulation time reduction
- Flexibility and easy adaptation to other engines cooling circuits

With the new procedure based on PID control, the water jacket orifices calibration activity can be performed in a very efficient way, due to its capability to reduce the effort of a manual procedure and obtain exactly the flow rates of the target simulations.

The proposal is also interesting because can be applied to other engines families and used as reference method for similar calibration activities, due to the PID controller flexibility. It can be tuned for specific applications and adapted to reach the desired physical quantities.

Finally, Figure 3.19, shows the comparison between the results obtained with the two different approaches and the error from the target.

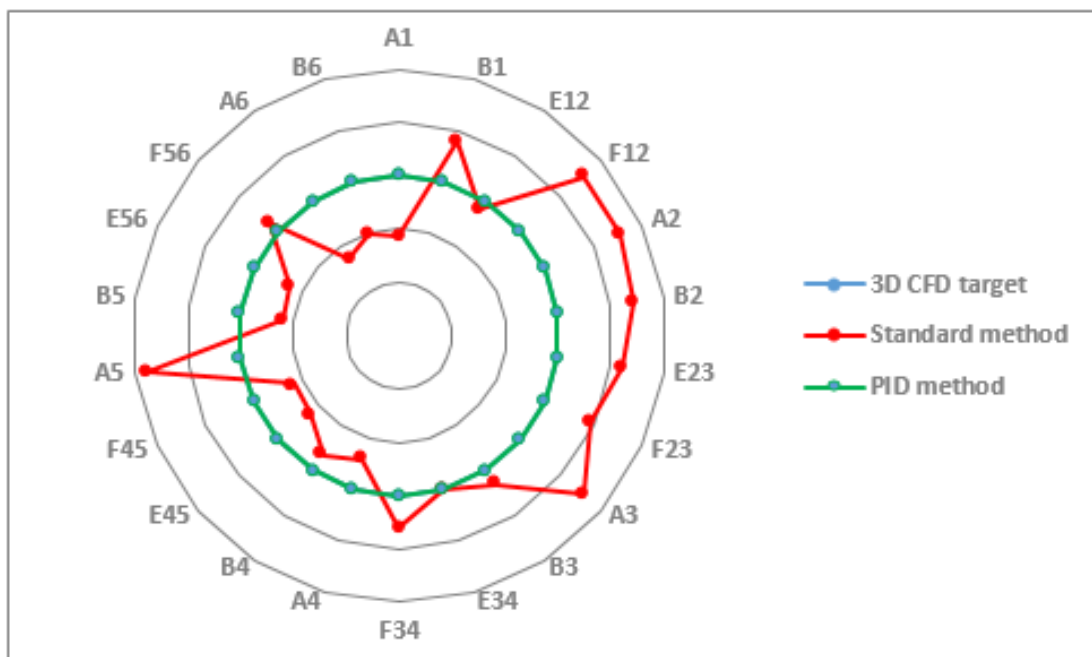


Figure 3.19: Comparison between standard and new calibration procedures

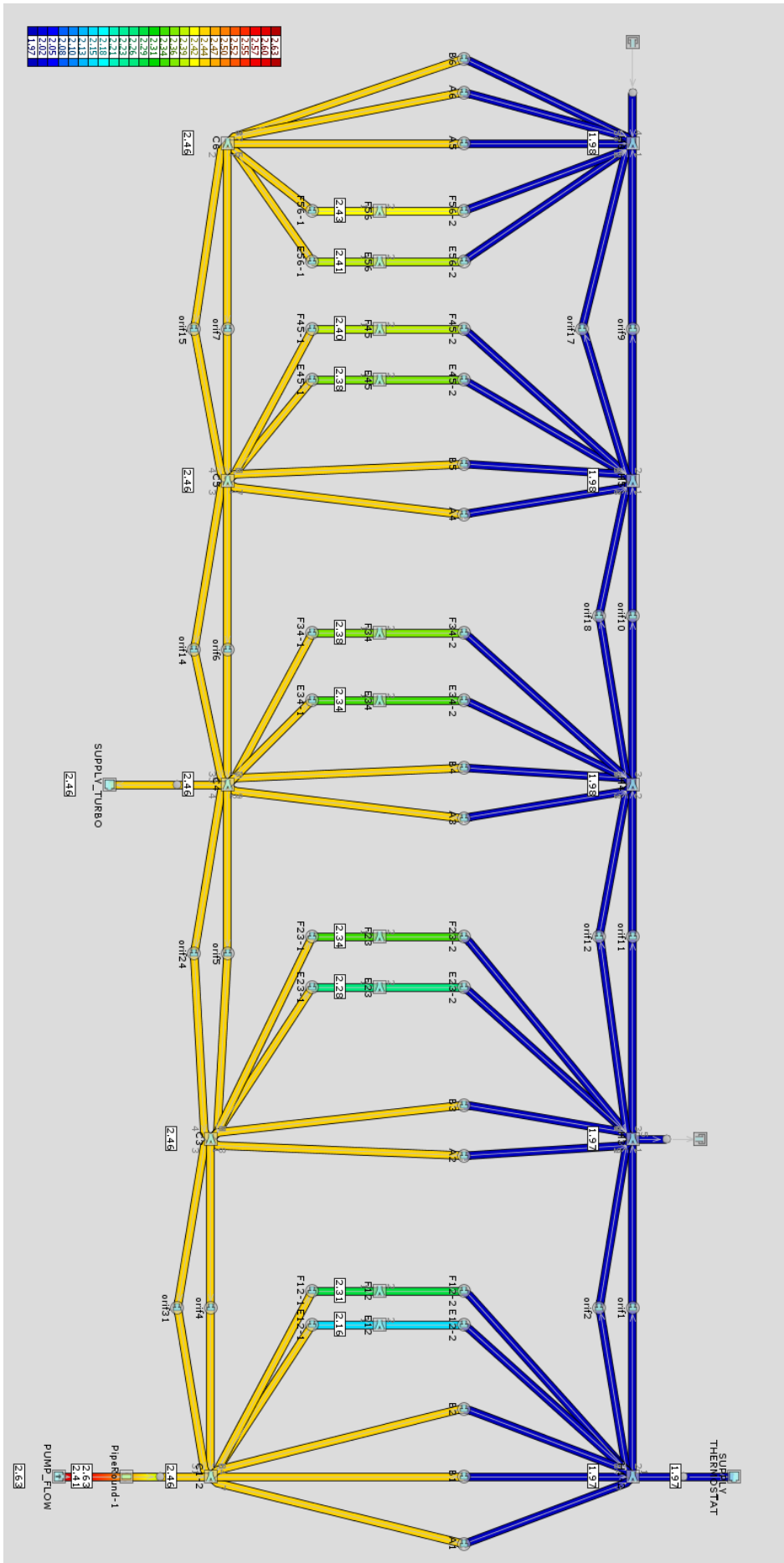


Figure 3.17: Average pressure distribution

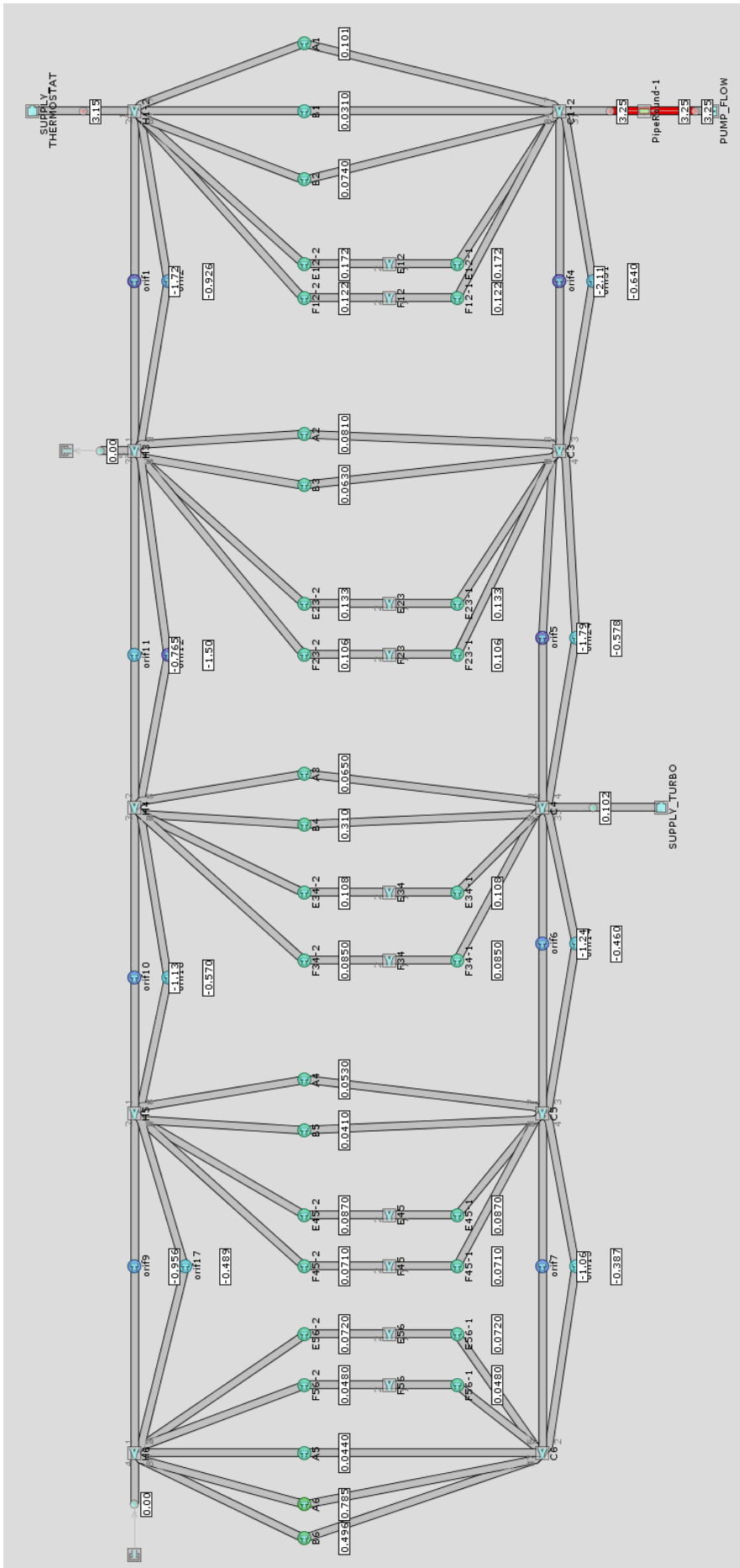


Figure 3.18: Coolant mass flow rate distribution

3.4 Cooling circuit components integration

The next step of the project has been to add to the 1D engine water jacket model, the other cooling circuit components:

- Pump
- Thermostat and by-pass valve
- Oil cooler
- Radiator
- Cabin Heater
- Turbocharger water jacket
- CNG pressure regulator
- Expansion tank
- Pipes and junctions

In Figure 3.20 is highlighted in red, the cooling circuit layout on the NEF67 CNG engine cad model. In particular, are reported only the engine components, while the vehicle components (e.g. radiator and cabin heater) are missing, because depending on clients specifications.

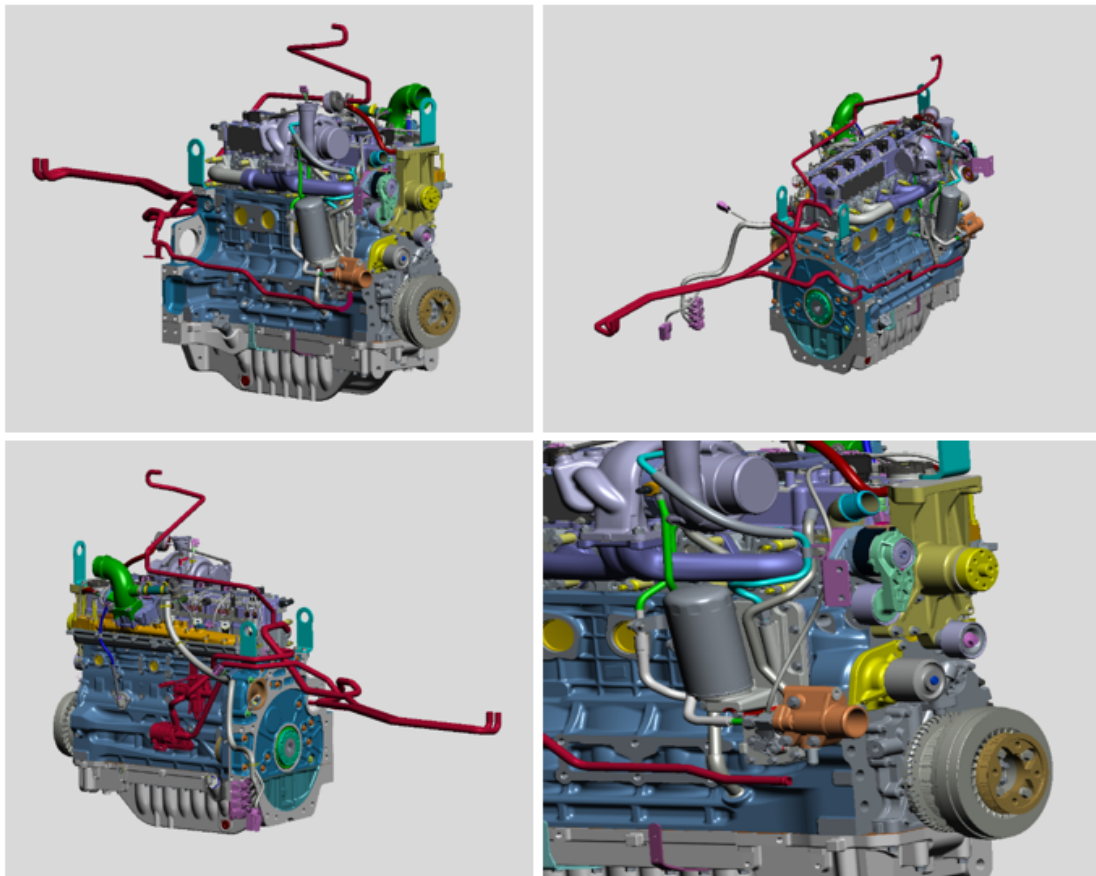


Figure 3.20: NEF67 CNG cooling circuit layout

Pump

In order to model the pump, it is mandatory to have the real pump characteristic provided by the supplier.

Using a *Pump* component, that characteristic has been implemented in the model (Figure 3.21).

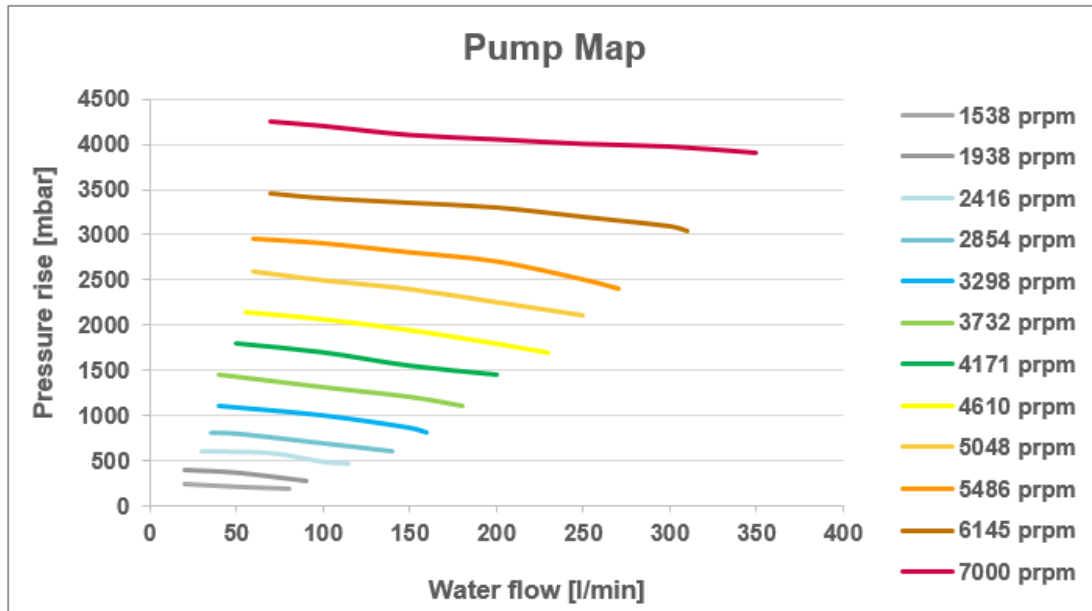


Figure 3.21: Pump map

A *SpeedBoundaryConn* component has been used to run the pump at a certain rotational speed and a *GearConn* component for the transmission ratio indication.

$$\tau = 1.96$$

Engine rotational speed has been set as a variable in *Case Setup* window in order to exploit the pump performance at different speeds and flow rates.

Thermostat and by-pass valve

The thermostat behaviour can be described in two different ways:

1. Imposed lift: to be used if the thermostat lift has to be imposed
2. Fluid conditions dependent (used one)

A *Thermostat* component has been created with the following data:

- Initial thermostat temperature: coolant temperature at simulation start [*InitialCoolant – temperature*] = 90 °C in *Case Setup*
- Initial thermostat state: Average, this will use the average lift calculated between the Temp-Lift (Opening) and Temp-Lift (Closing) profiles
- Temperature time constant (opening and closing): speed response of the component (0.4)
- Sensitive part for Temperature: pipe outlet section before thermostat

The real thermostat temperature-lift characteristics are reported in Figure 3.22, while by-pass characteristics in Figure 3.23.

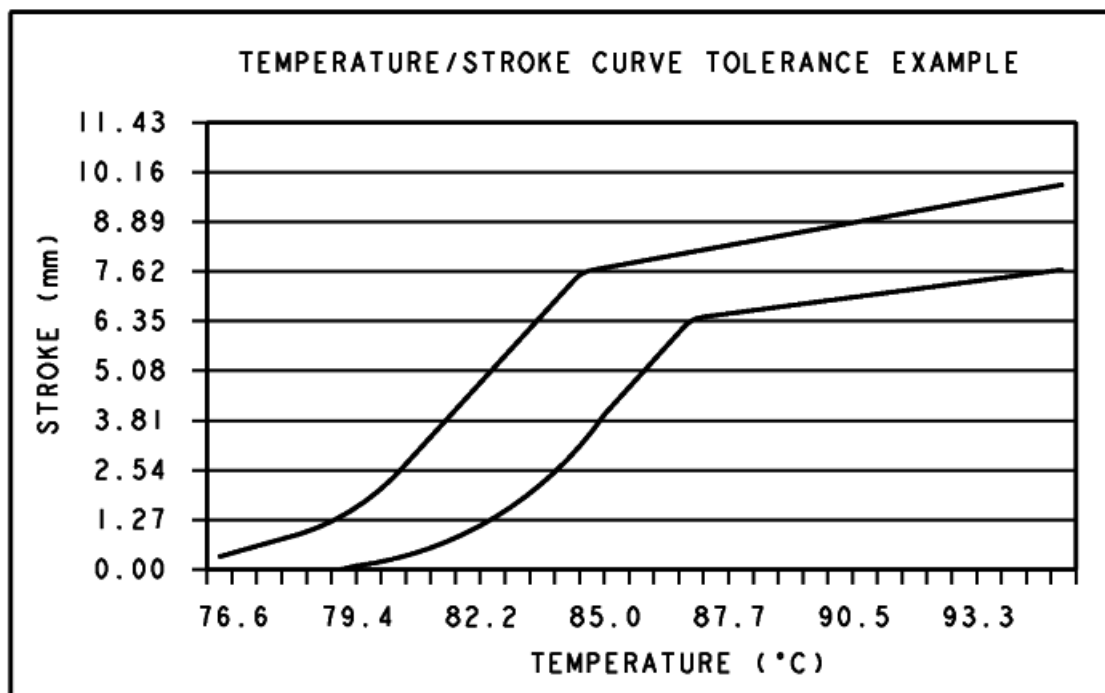


Figure 3.22: Thermostat temperature-lift characteristic

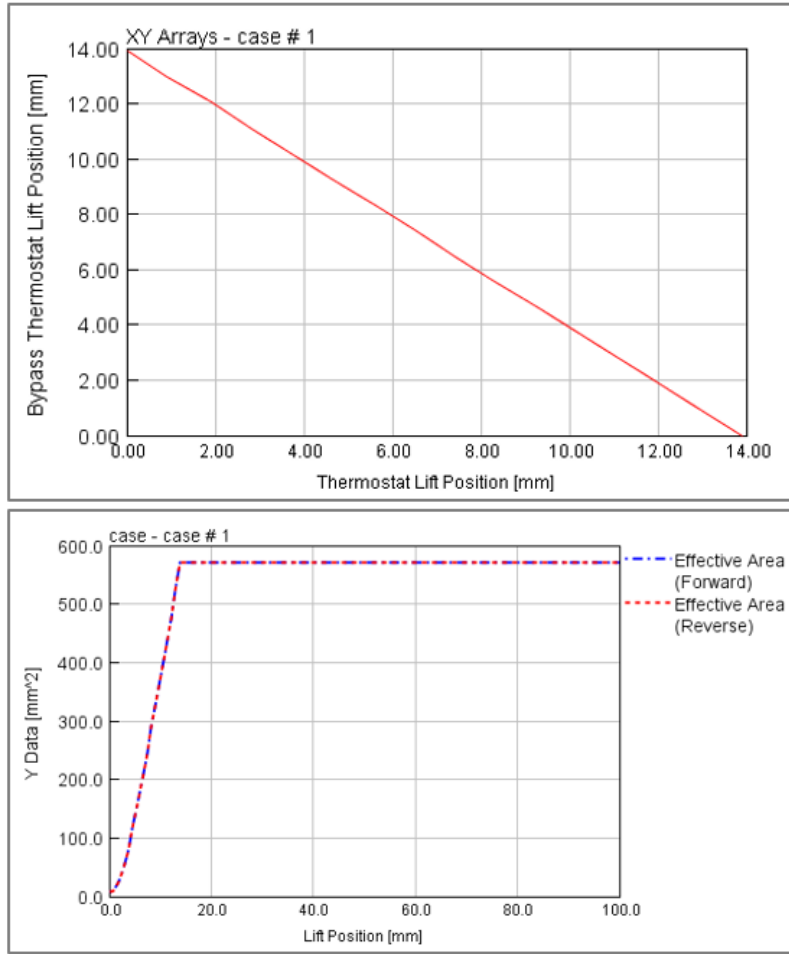


Figure 3.23: By-pass temperature-lift characteristics

Oil cooler

The oil cooler has been modeled as *Heat Addition* component, with related fluid-dynamic and thermal characteristics:

- Permeability, taken from CFD simulations (Figure 3.24)
- Heat release rate, estimated as function of engine speed and power (Eq 3.4)

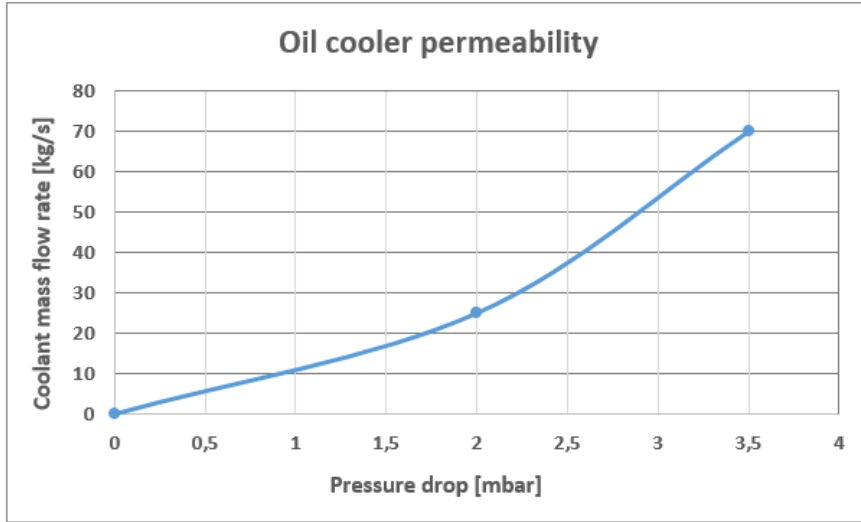


Figure 3.24: Oil cooler permeability

The heat release rate has been computed using an empirical formula obtained from company experimentation results:

$$\frac{P_{th}}{P_{MAXengine}} = \left[0.219 \left(\frac{P_{engine}}{P_{MAXengine}} \right)^3 - 0.358 \left(\frac{P_{engine}}{P_{MAXengine}} \right)^2 + 0.227 \left(\frac{P_{engine}}{P_{MAXengine}} \right) - 0.003 \right] \quad (3.4)$$

Radiator

The radiator has been modeled considering [6] :

- A *HxMaster* component for the water side
- A *HxSlave* component for the air side

The *HxMaster* is internally made up of flow volumes and a thermal mass. The configuration of the flow volumes, and the options available for characterizing the pressure loss in the heat exchanger, depend on the geometry object selected in the *HeatExchangerSpecs* reference object.

The selected *HxGeomTubeFin* template is specific to tube-fin heat exchangers, and the master (tube) side will consist of three volumes (tank + "pipe bundle" + tank). The *HxSlave* contains the cooling air properties (chemical composition, flow rate, temperature).

The required radiator data have been taken from the supplier specifications :

- Geometry: dimensions and material, pass details and fins geometry, tank details (Figure 3.25)
- Permeability: Master(coolant) flow rate/pressure drop characteristic (Figure 3.26)
- Heat transfer: Thermal characteristics as function of coolant and air flow rates (Figure 3.27)

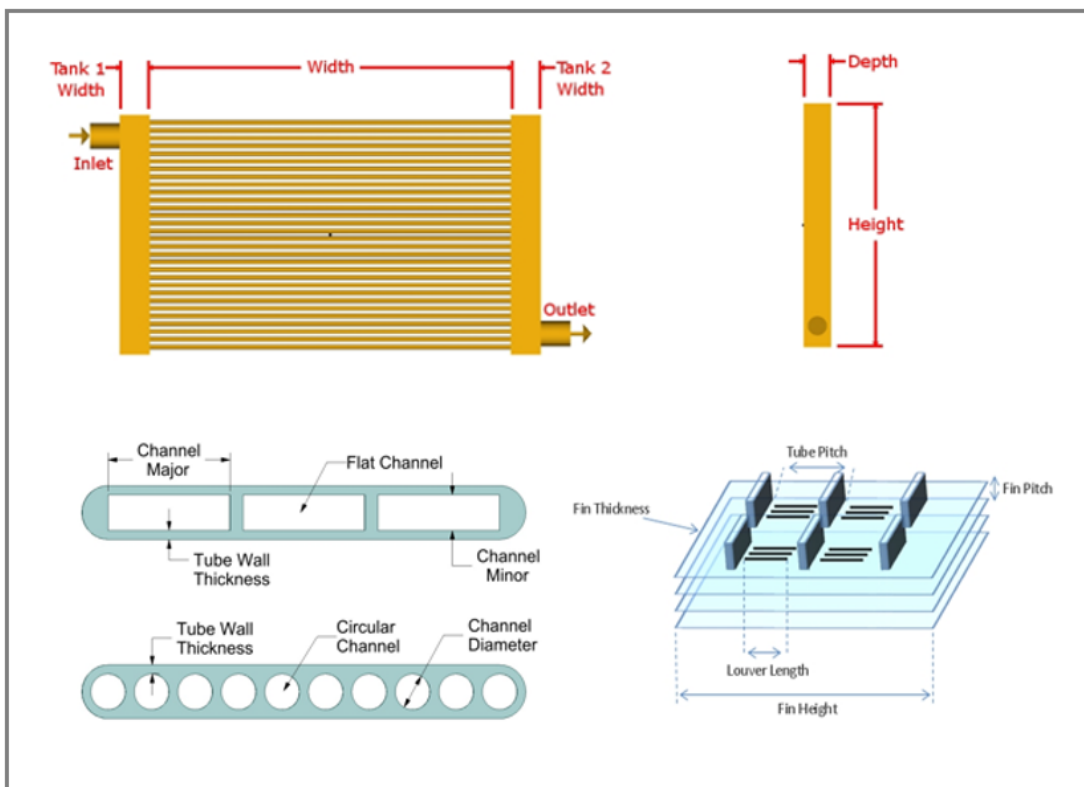


Figure 3.25: Radiator geometrical details

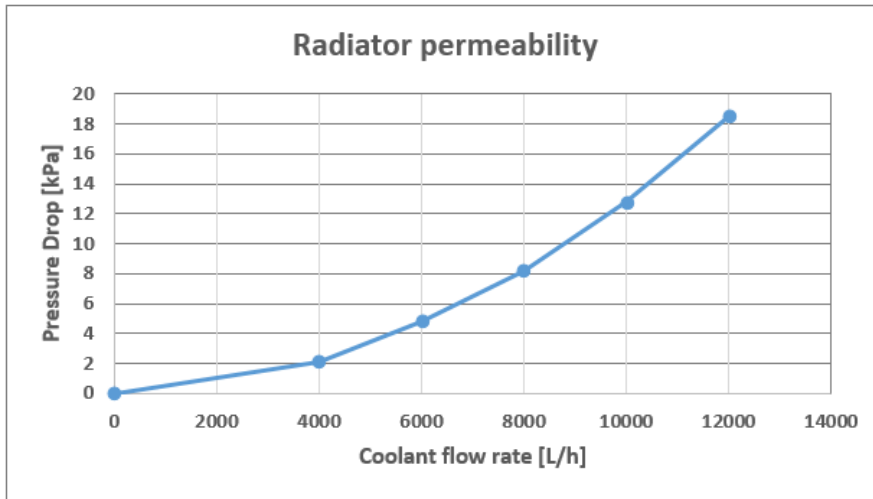


Figure 3.26: Radiator permeability

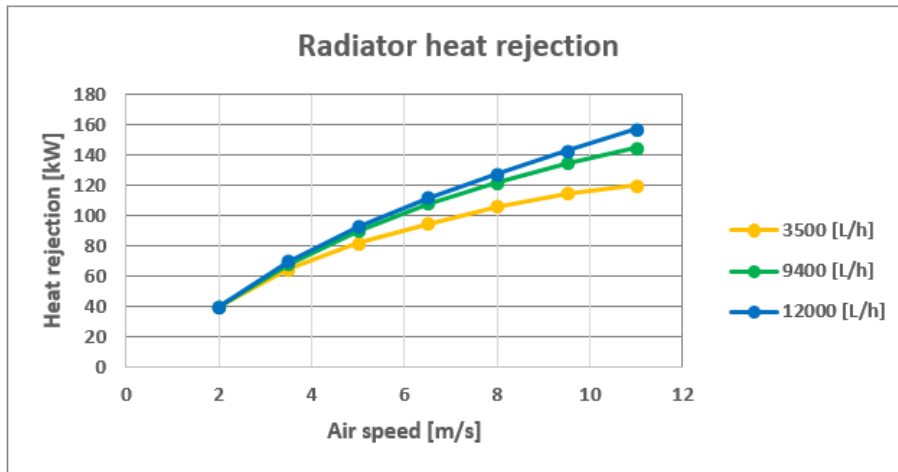


Figure 3.27: Radiator heat rejection

Cabin Heater

The cabin heater has been modeled as *Heat Addition* component, with related fluid-dynamic and thermal characteristics:

- Permeability, taken from CFD simulations (Figure 3.28)
- Heat request (Figure 3.29)

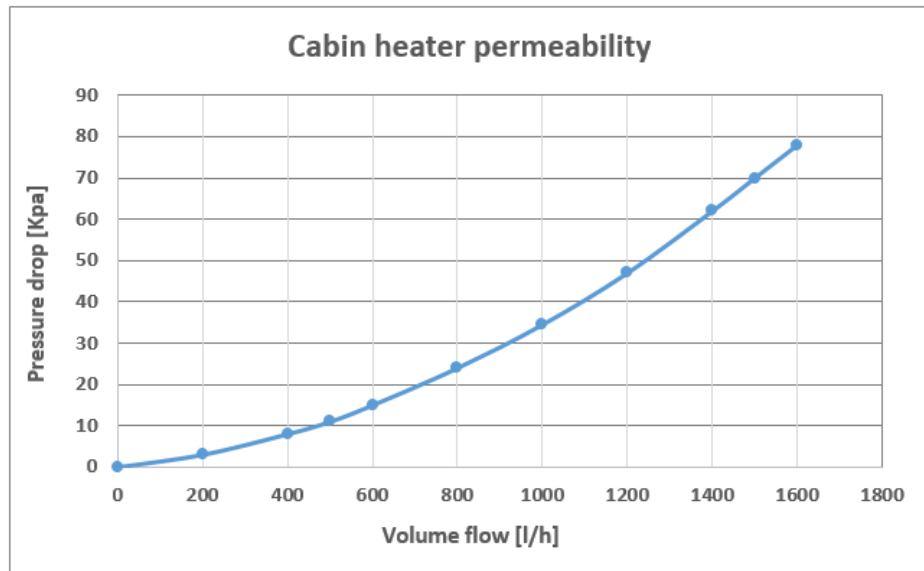


Figure 3.28: Cabin heater permeability

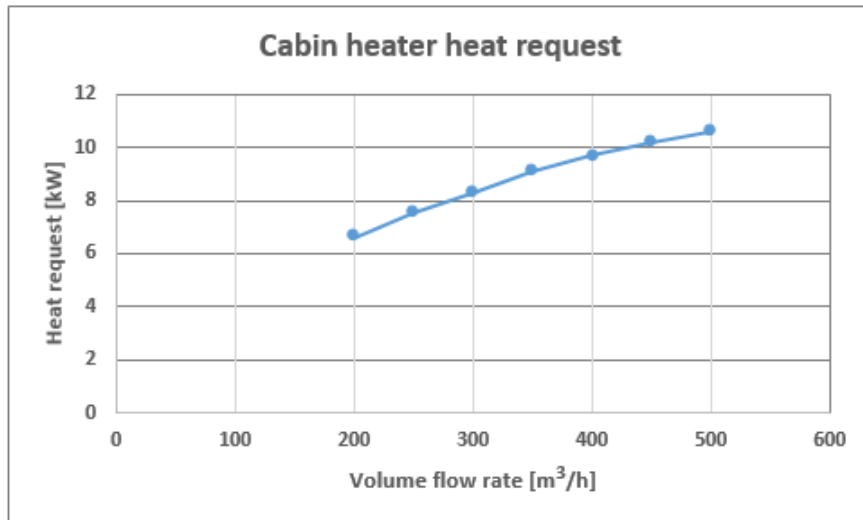


Figure 3.29: Cabin heater heat request (at constant coolant flow rate 500 l/h)

Turbocharger water jacket

The turbocharger is a critical component due to the high temperatures reached in operation. Oil is normally used to cool down the center housing preventing bearings and seals failure but, for specific applications (i.e. marine and NG engines), a water line is added to the cartridge to remove the excessive heat produced, especially after the engine shut off when some heat still remains in the center housing area. The water, coming from the engine head, is sent through a pipe to the turbocharger center housing and then delivered to the pump inlet port.

The turbocharger water jacket has been modeled as *Heat Addition* component, with related fluid-dynamic and thermal characteristics:

- For what the fluid characteristic is concerned, the turbocharger permeability has been taken from the component specifications
- The general rule of thumbs to estimate, as first guess, the turbocharger heat rejection is:

$$P_{Thermal,Turbo} = 2.5\%P_{engine} \quad [kW] \quad (3.5)$$

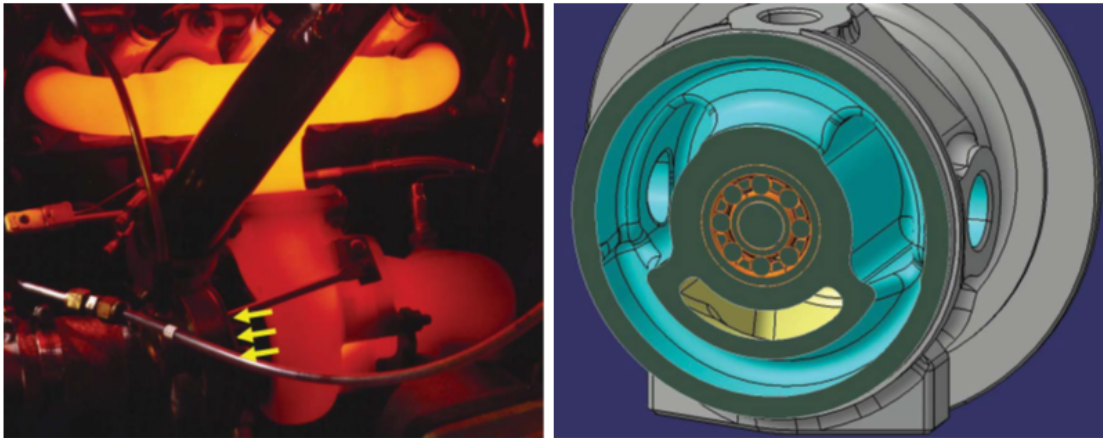


Figure 3.30: Water cooled turbocharger

CNG pressure regulator

The CNG pressure regulator is a device used in CNG engines to reduce the gas pressure from the tank level to the injector feeding level. Due to the gas expansion, a temperature decrease affects the component (Joule-Thomson effect), with the risk of freezing during low ambient temperature operations. For this reason, a water line is added to warm up the gas pressure regulator, avoiding excessive temperature drops.

Water coming from the engine head is sent to the component and then delivered through return lines to the pump inlet port.

The gas pressure regulator has been modeled as *Heat Addition* component, with related fluid-dynamic and thermal characteristics:

- Fluid-dynamic characteristic has been taken from component measurements at the supplier test bench (Figure 3.31)
- Heat rejection data have been estimated under the hypothesis of fuel mass flow rate in full load conditions:

$$P = \Delta H_{vap} \dot{m}_f \quad [kW] \quad (3.6)$$

where:

- $\Delta H_{vap} = 510$ fuel enthalpy of vaporization [kJ/kg]
- $\dot{m}_f =$ fuel mass flow rate [kg/s]

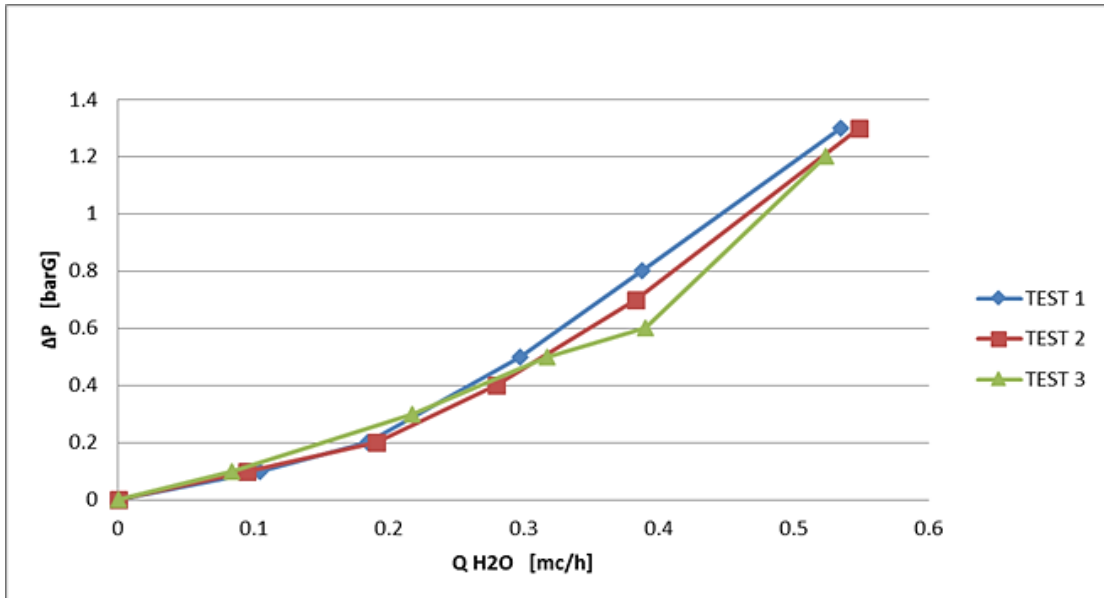


Figure 3.31: Gas pressure regulator tested permeability

Expansion tank

The expansion tank has been modeled as *Accumulator* component with check valves representing the pressurized cap.

The total volume in the accumulator is always conserved, but the distribution of volume between the two parts freely changes, as necessary to maintain a balance of pressure.

The specified data are the following:

- Cap safety valve opening pressure: 1.4 barg
- Initial air volume 2.5 L
- Initial air temperature 20 °C (steady state simulation)
- Initial coolant volume 8.5L.
- Initial coolant temperature 90 °C (steady state simulation)
- Flow coefficients define the pressurized cap opening law, discharge coefficient as a function of pressure drop across the check valve (Figure 3.32)

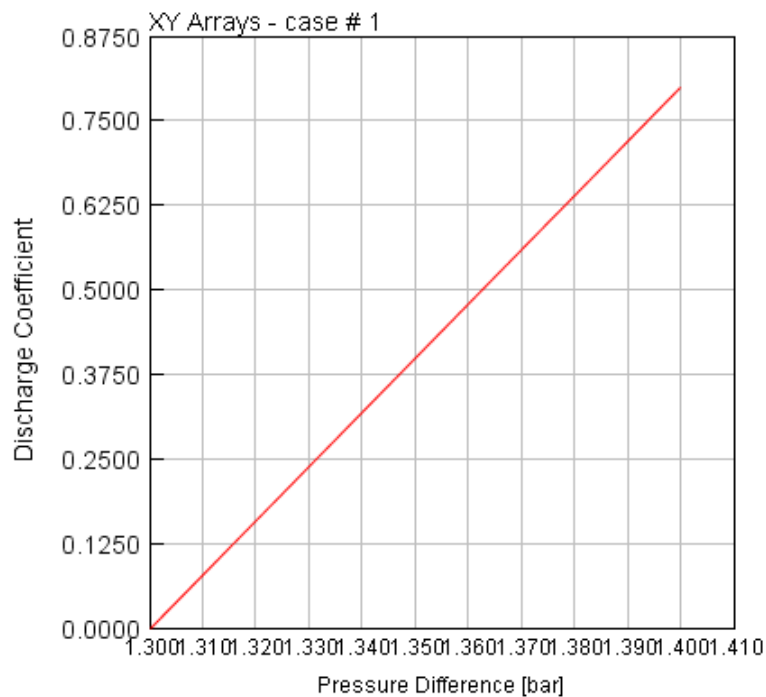


Figure 3.32: Pressurized cap discharge coefficient characteristic

Pipes and junctions

To model in a more realistic way the circuit, each pipe has been discretized using GEM3D and converted into an equivalent GT model, with the same technique used for the water jacket.

Each pipe portion has been converted in a *pipe* element with inlet and outlet ports and curvature as the one reported in Figure 3.33.

In this way, is possible to take into account the effect of pipe bends and restrictions on the coolant pressure drop and to make the equivalent model behavior closer to the real one.

This procedure have been performed for all the circuit pipes. At the end, all the equivalent 1D pipes have been implemented into the cooling circuit GT model. The final geometries (3D and 1D) are shown in Figure 3.34.

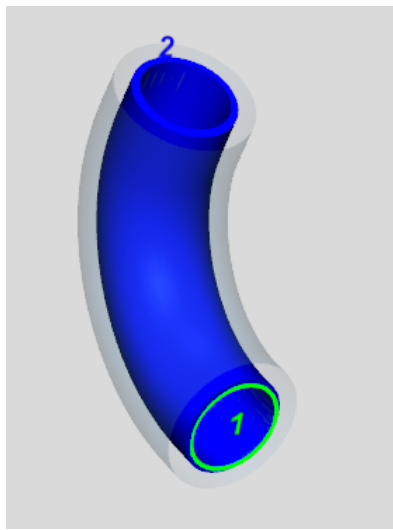


Figure 3.33: Equivalent pipe element

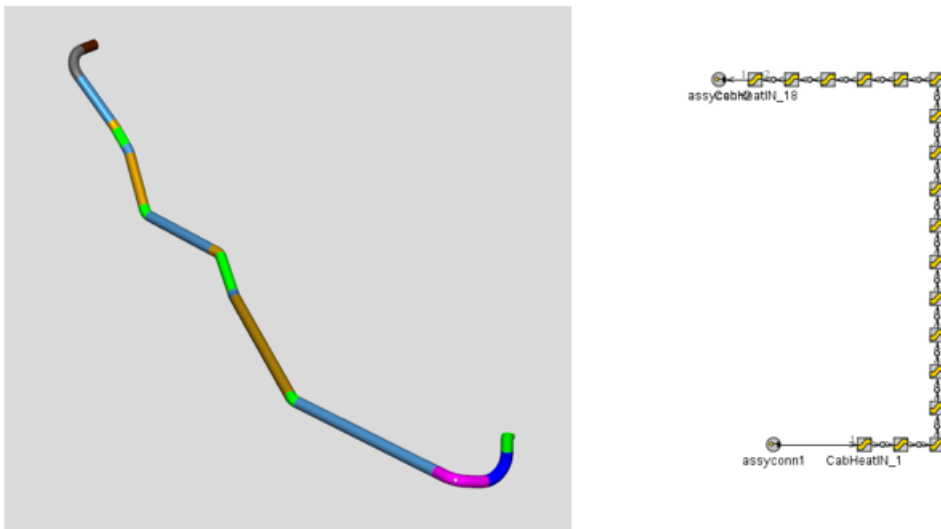


Figure 3.34: Discretized pipe: 3D-1D conversion

The same procedure has been followed for the junctions, which are local points of the circuit where pressure losses are concentrated.

They are used to connect different branches of the circuit.

Figure 3.35 shows an example of flow split element for a generic junction of the circuit.

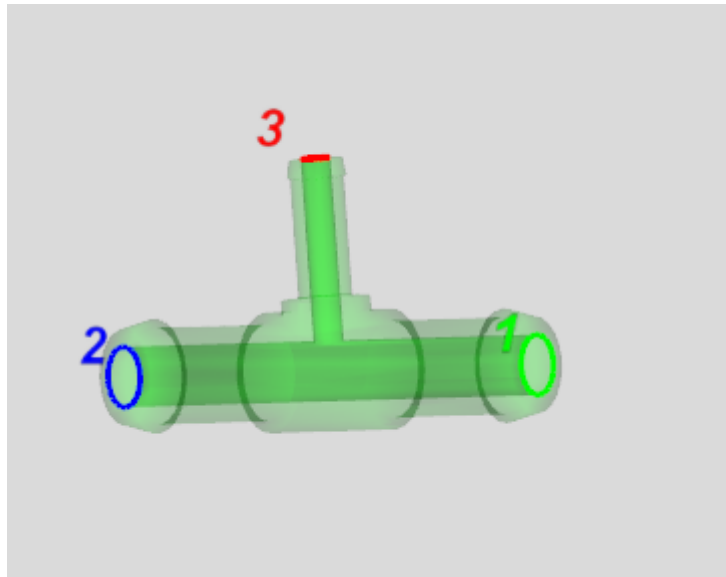


Figure 3.35: Junction equivalent flow split element

3.5 Steady state thermal modeling

Once the components fluid-dynamic and thermal characteristics have been implemented, the following step has been to make the model sensible to the combustion heat rejection.

To define the thermal power to be rejected to the coolant fluid, two different methods can be used:

- As preliminary estimation, in case no measured data are available, it is possible to estimate it as

$$P_w = (0.25 - 0.3)P_u \quad [kW] \quad (3.7)$$

- If measured data are available, it is preferable to use them in order to have a more precise estimation

Following the second approach, the measured coolant thermal power and engine useful power have been set as variables in the *Case setup* window as function of the engine speed.

To estimate the thermal power produced during combustion inside the engine, the thermal power absorbed by the oil cooler (Eq. 3.4) and turbocharger (Eq. 3.5) have been subtracted from the total thermal power rejected to the coolant fluid:

$$P_{head} = P_{th} - P_{th,oilcooler} - P_{th,turbocooler} \quad [kW] \quad (3.8)$$

The estimated thermal power has been distributed among the head gasket coolant passages linearly with the mass flow rates, with respect to the overall flow rate passing between the engine block and head.

Heat addition components have been introduced setting the thermal power associated to each branch:

$$P_{head,n} = P_{head} \frac{\dot{m}_n}{\sum \dot{m}} = P_{head} \frac{\dot{m}_n}{\dot{m}_{pump}} \quad [kW] \quad (3.9)$$

Using the *Edit parts in Spreadsheet* window (see Figure 3.36), to each *Heat Addition* component have been specified:

- Volume of fluid inside the component: in order not to modify the total coolant volume and concentrate the rejected heat in the head gasket region, 0.01 L has been set for each component
- Initial state name: Initial state pressure (1 bar) and initial state temperature (90 °C)
- Heat input Rate: as function of coolant mass flow rate for each branch
- Pressure drop: in order to not modify the model permeability, pressure drops have been neglected (ign)

Attribute	Object Name	Volume of Fluid Inside Component	Initial State Name	Heat Input Rate	Heat Input Rate Multiplier	Pressure Drop Reference Object
Unit		L		W		
1	Cabin_heater	0.5	init	=[CabinHeater_HR(W)]	def (=1.0)	Cabin_heater
2	Gas-Press_Regulator	0.1	init	=-[FuelRegulator_HR(W)]	def (=1.0)	PressureRegulatorDP
3	HA_A1	0.01	init	=[P_head(W)]*0.0322	def (=1.0)	ign
4	HA_A2	0.01	init	=[P_head(W)]*0.0258	def (=1.0)	ign
5	HA_A3	0.01	init	=[P_head(W)]*0.0207	def (=1.0)	ign
6	HA_A4	0.01	init	=[P_head(W)]*0.0168	def (=1.0)	ign
7	HA_A5	0.01	init	=[P_head(W)]*0.0140	def (=1.0)	ign
8	HA_A6	0.01	init	=[P_head(W)]*0.2489	def (=1.0)	ign
9	HA_B1	0.01	init	=[P_head(W)]*0.0099	def (=1.0)	ign
10	HA_B2	0.01	init	=[P_head(W)]*0.0236	def (=1.0)	ign
11	HA_B3	0.01	init	=[P_head(W)]*0.02	def (=1.0)	ign
12	HA_B4	0.01	init	=[P_head(W)]*0.0985	def (=1.0)	ign
13	HA_B5	0.01	init	=[P_head(W)]*0.0130	def (=1.0)	ign
14	HA_B6	0.01	init	=[P_head(W)]*0.1573	def (=1.0)	ign
15	HA_E12	0.01	init	=[P_head(W)]*0.0549	def (=1.0)	ign
16	HA_E23	0.01	init	=[P_head(W)]*0.0337	def (=1.0)	ign
17	HA_E34	0.01	init	=[P_head(W)]*0.0343	def (=1.0)	ign
18	HA_E45	0.01	init	=[P_head(W)]*0.0245	def (=1.0)	ign
19	HA_E56	0.01	init	=[P_head(W)]*0.0203	def (=1.0)	ign
20	HA_F12	0.01	init	=[P_head(W)]*0.0345	def (=1.0)	ign
21	HA_F23	0.01	init	=[P_head(W)]*0.0377	def (=1.0)	ign
22	HA_F34	0.01	init	=[P_head(W)]*0.0270	def (=1.0)	ign
23	HA_F45	0.01	init	=[P_head(W)]*0.0225	def (=1.0)	ign
24	HA_F56	0.01	init	=[P_head(W)]*0.0152	def (=1.0)	ign
25	Oil_cooler	1	init	=[OilCooler_HR(W)]	def (=1.0)	OC_daCFD
26	Radiator	5	init	=-[Radiator_HR(W)]	def (=1.0)	waterside_DP
27	Turbo-cooler	0.3	init	=[Turbo_HR(W)]	def (=1.0)	TurboDp

Figure 3.36: Water jacket heat addition components specifications

The resultant water jacket model is shown in Figure 3.37.

3.6 Vehicle and test bench model configurations

The last step of the modeling has been to connect all the components of the cooling circuit according to the actual engine layout.

Two configurations have been created, in order to investigate the system performance at different project steps:

- Test bench configuration
- Vehicle configuration

The test bench model has been created to be used during the prototyping to test new design proposals and technical solutions, before running the engine in the test cell. It can support the validation activity, being a fast tool to use for answering practical problems and reduces both time and cost of a real prototype.

In order to be in line with the actual engine configuration at the test bench, the model needs to be updated continuously to be always ready for answering new design solutions or technical proposals.

The vehicle model has been created to test the engine performances within the final vehicle, dependent on the client specifications.

It can be useful for both sides, either to find common solutions for the final product or to choose the best components for the engine between different market competitors.

For the particular application of the thesis, the bench model has been calibrated using measured data from of real engine running at the testing facility.

Calibration has been performed in order to reach the target measured quantities with a maximum tolerance of $\pm 10\%$.

The vehicle model have been used instead, to discuss about previsions on the real engine cooling circuit performances on clients vehicles.

Test bench configuration

The test bench configuration presents the following differences with respect to the vehicle one:

- No cabin heater installed (vehicle side)
- No CNG pressure regulator heat exchanger
- No turbocharger water jacket degassing pipe installed
- Fully open thermostat (no by-pass line)
- water/water bench radiator

Figure 3.38 shows the cooling circuit model in the test-bench configuration.

Vehicle configuration

Due to the high dependence on the client vehicle specifications and purpose, the vehicle configuration has been modeled in the most general way, considering all the above mentioned components (in a real configuration some devices may not be included).

Figure 3.39 shows the cooling circuit model in the vehicle configuration. Coolant pipes are highlighted in green, air path in light blue while degassing pipes in yellow. The latter, used to send vapor bubbles to the expansion tank formed up at high temperature, are connected to:

- Engine head
- Radiator
- Turbocharger cooler

The ENGINE WATER-JACKET *Subassembly* contains the unidimensional water jacket model.

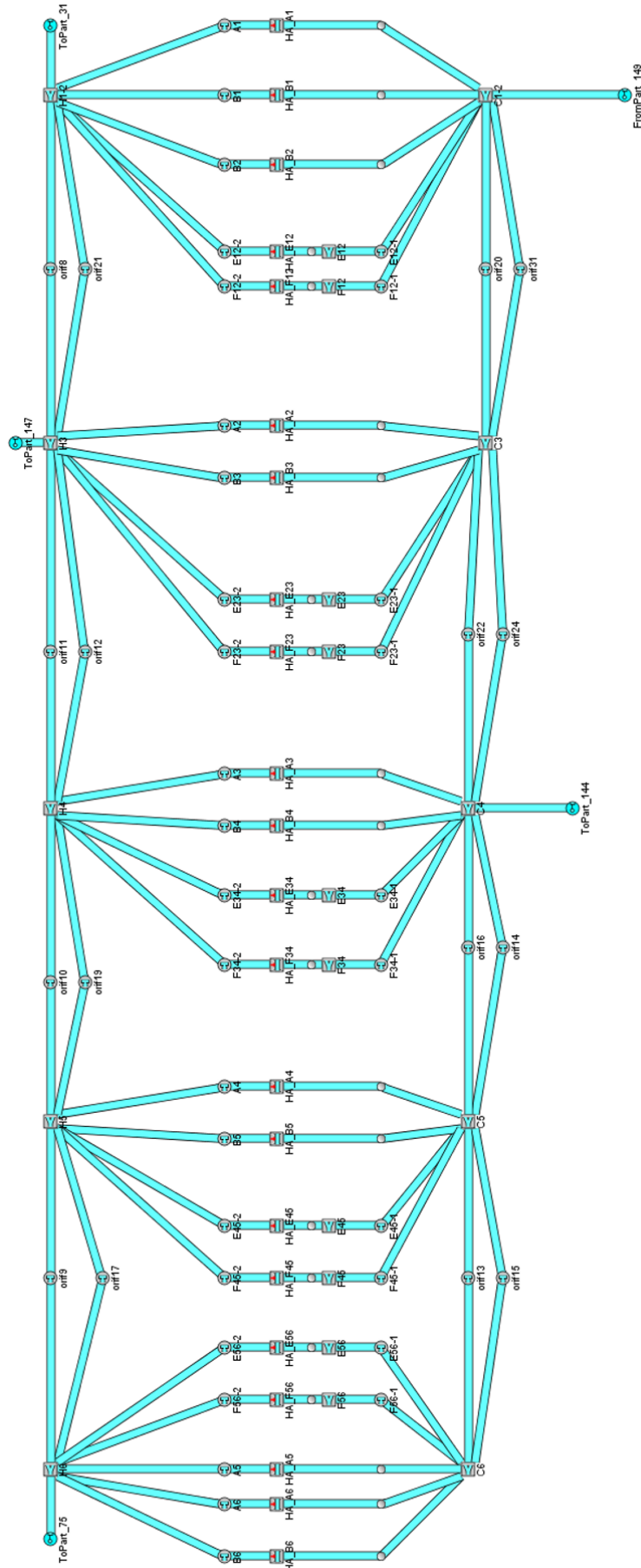


Figure 3.37: Complete water jacket model

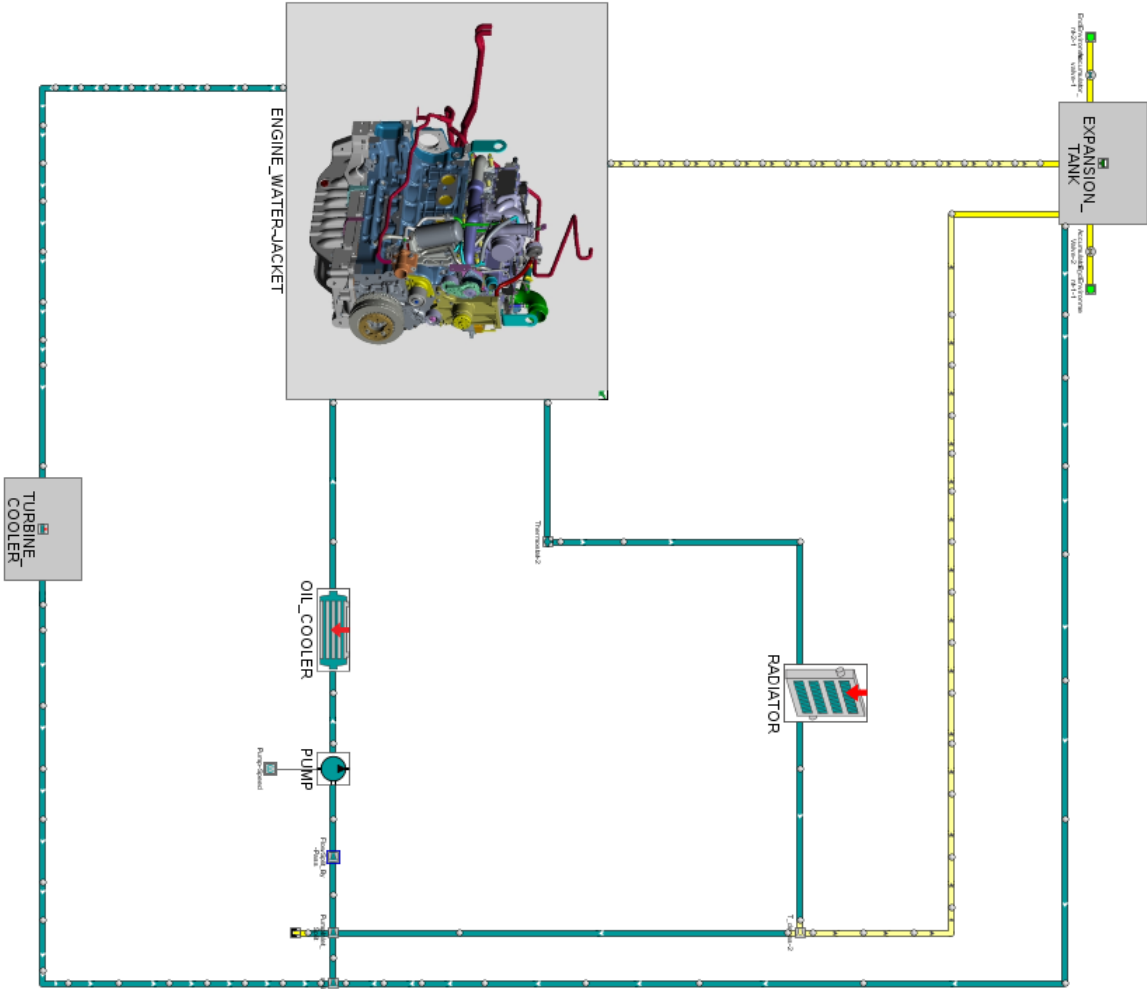


Figure 3.38: Cooling circuit unidimensional model (test bench configuration)

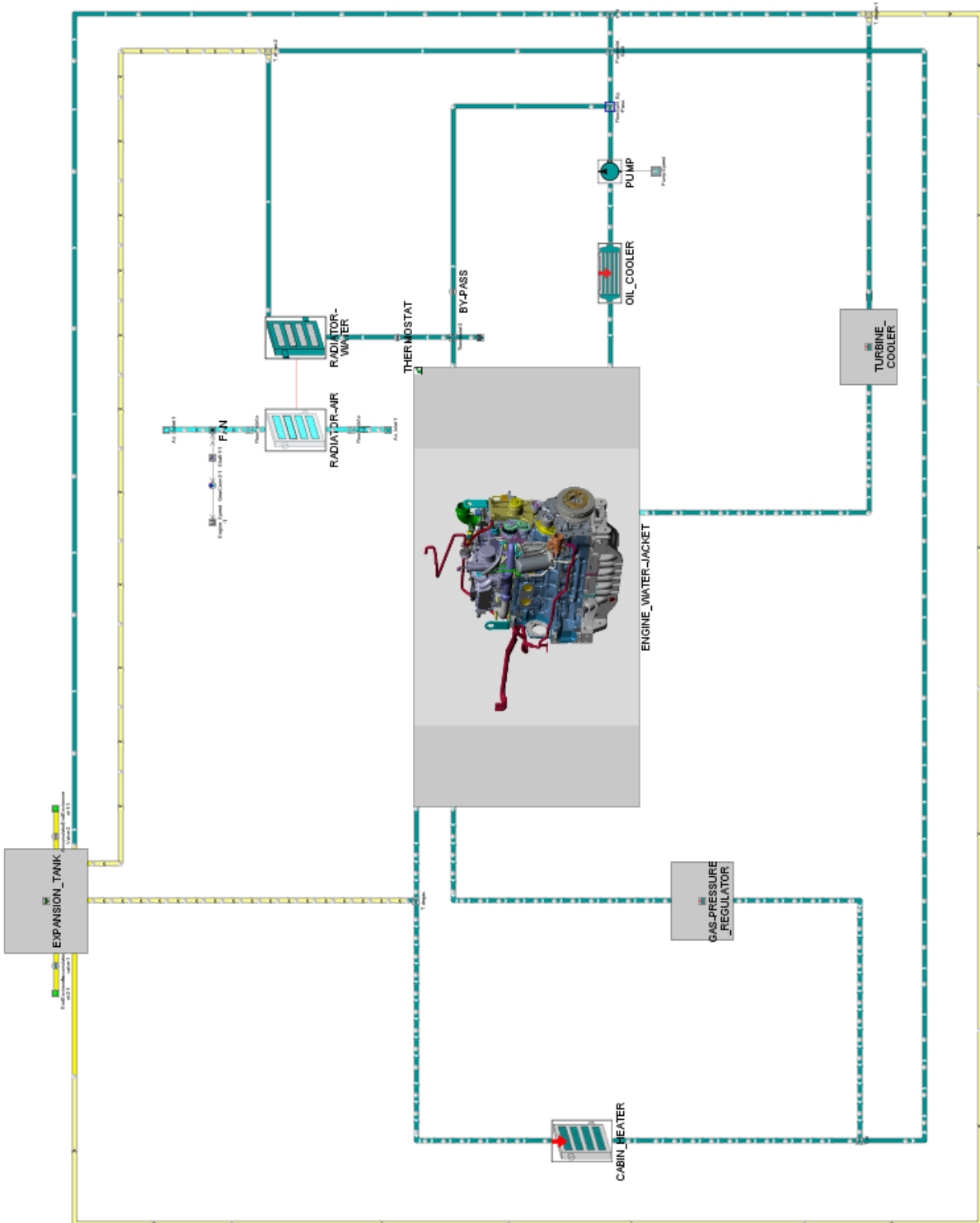


Figure 3.39: Cooling circuit unidimensional model(vehicle configuration)

Chapter 4

Test bench model calibration

Once the modeling activity has been completed, the following important step has been to calibrate the cooling system model in order to reproduce the same performance of the real one.

An experimental campaign has been organized at the FPT testing center to collect some useful data on the real prototype and tune the model in order to improve its predictive capability.

The activity turned out to be the most interesting of the project, and fundamental for linking the virtual model simulations with the real engine behavior.

Working on the prototype on the definition of the sensor locations, and attending the test to collect data for the post processing, made the physical phenomena understanding easier and contributed to enhance the knowledge on the internal combustion engines also from a practical point of view.

After a brief presentation of the engine test bench experimental activities and a detailed description of the cell instrumentation and the data acquisition methodology, the measured data have been compared with the simulated one and the model improved in order to reach the requested target tolerance.

The plots will not show numerical values, as required by FPT Industrial S.p.A to preserve confidentiality.

4.1 Engine test bench

The engine test bench [7] is a facility used to test, develop and calibrate internal combustion engines.

Typical fields of application of engine test benches are:

- Combustion development and basic research
- Performance and emission development
- Parameterization and calibration
- Emission certification of engines for heavy-duty applications
- Endurance testing and aging of components for exhaust gas after-treatment
- Component testing near the engine
- Mechanics and function development

The data management system located locally at the testbed allows parameters, measurements and data to be handled in a structured manner.

Results are post-processed with dedicated software and used to analyze the engine performances at different loading conditions.



Figure 4.1: Engine test bench

4.2 Experimental measurements campaign

The test bench model has been created referring to the actual test bench configuration of the engine. In particular, the experimental activity have been carried out on an alpha-phase prototype, installed in the testing cell of the company, dedicated to CNG technology development.

The engine components, at this prototyping stage, are not the same of the final engine and does not show the same performance and characteristics of the latters. Moreover the results obtained cannot be frozen, because of further changes in the engine project.

Therefore creating a model to make simulations on the engine, even in the prototyping phase, can be useful to boost the design process, to make hypothesis and creating new solutions before installing the real engine on the bench and run the measurement activities.

In order to make the model equivalent with the engine test bench configuration, a measurement campaign at the FPT Industrial testing center has been planned to get the following data:

- Engine performance curves (Torque and Power)
- Heat rejection
- Components permeability
- Coolant flow rate
- Pressure drop across the engine

The activity has been carried out after a practical insight on the engine disassembling, to study the engine architecture and the particular cooling system layout. The obtained quantities have been used either to exactly know the components performance curves to be implemented in the model, or to have the reference values for the further calibration of the model.

4.2.1 Instrumentation

To have a correct estimation of the components fluid dynamic and thermal characteristics, it was necessary to measure pressures, temperatures and flow rates in specific points of the cooling circuit.

To measure the desired quantities, has been asked to be installed on the engine test bench some extra pressure sensors, thermocouples and flow meters , before running the test.

Temperature sensors

Resistance thermometers, also called resistance temperature detectors (RTDs), are sensors used to measure temperature [8].

Many RTD elements consist of a length of fine wire wrapped around a ceramic or glass core but other constructions are also used. The RTD wire is a pure material, typically platinum, nickel, or copper. The material has an accurate resistance/temperature relationship, which is used to provide an indication of temperature. In particular, for metals the resistivity can be expressed linearly as function of temperature:

$$\rho(T) = \rho_0[1 + \alpha(T - T_0)] \quad [\Omega m] \quad (4.1)$$

where:

T = temperature [K]

$\rho(T)$ = material resistivity at temperature T [Ωm]

ρ_0 = material resistivity at temperature T0 [K]

α = proportional coefficient dependent on material thermal properties [K^{-1}]

Referring the resistivity to the resistance (considering section S and length L of the conductor)

$$R = \frac{\rho L}{S} \quad [\Omega] \quad (4.2)$$

the following equation is obtained:

$$R(T) = R_0[1 + \alpha(T - T_0)] \quad [\Omega] \quad (4.3)$$

From the latter, is possible to estimate the temperature from the measure of the resistance.

Furthermore, a more complex model can be used to take into account the change of conductor section and length with temperature:

$$R(T) = R_0[1 + \alpha_1(T - T_0) + \alpha_2(T - T_0)^2 + \alpha_3(T - T_0 - 100)T^3] \quad [\Omega] \quad (4.4)$$

where:

$R_0 = \text{resistance at } 273K \text{ (} 100 \Omega \text{ for PT100)}$

$\alpha_1 = 3.9083 \cdot 10^{-3} \text{ [K}^{-1}\text{]}$

$\alpha_2 = -5.775 \cdot 10^{-7} \text{ [K}^{-2}\text{]}$

$\alpha_3 = -4.183 \cdot 10^{-12} \text{ [K}^{-4}\text{]}$

The selected sensor for the temperature measurement at the test bench is a PT100 sensor [9], where PT stands for platinum and 100 indicates the resistance value at 0 °C.

Platinum is the best metal for RTDs due to its linear resistance/temperature relationship, highly repeatable over a wide temperature range.

The unique properties of platinum make it the material of choice for temperature standards over the range of -272.5 °C to 961.78 °C. It is also chosen because of its chemical inertness.

Figure 4.2 shows the construction scheme of the PT100 sensor.

These elements nearly always require insulated leads attached. PVC, silicone rubber or PTFE insulators are used at temperatures below about 250 °C.

Above this, glass fiber or ceramic are used (e.g. MgO).

The measuring point, and usually most of the leads, require a housing or protective sleeve, often made of a metal alloy that is chemically inert to the process being monitored.

Selecting and designing protection sheaths can require more care than the actual sensor, as the sheath must withstand chemical or physical attack and provide convenient attachment points.

The sensor specifications are reported in Figure 4.3.

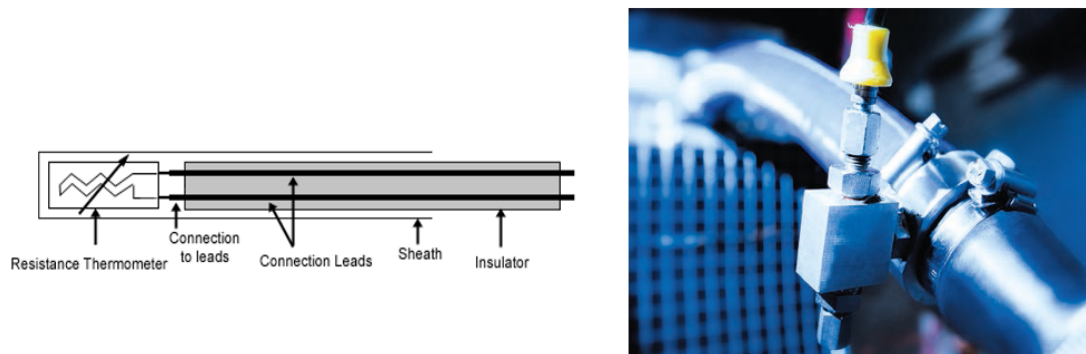


Figure 4.2: PT100 temperature sensor

THERMISTOR PT100 D= 4mm, L= 100mm	
Resistance	Platinum-100 Ohm at 0°C
Temperature Range	-30 °C < T < 250 °C
Tolerance	$\pm (0,15 + 0,002) \text{ } ^\circ\text{C}$
Insulation	MgO
Sheath Material	AISI 316
Transition	Inox- D=6 mm, L=50 mm
Spring	Inox- L=50 mm
Cable	Teflon- sect=0,35 mm ² , Copper wire- sect=0,35 mm ²

Figure 4.3: PT100 temperature sensor specifications

Pressure transducers

A pressure transducer [10] is a device that converts an applied pressure into a measurable electrical signal. It consists of two main parts, an elastic material that deforms when exposed to a pressurized medium and an electrical device that detects the deformation.

The elastic material can be formed into many different shapes and sizes depending on the sensing principle and range of pressures to be measured. The most common method is to form it into a thin flexible membrane called diaphragm.

The electrical device, which is combined with the diaphragm to create a pressure transducer, can be based on a resistive, capacitive or inductive principle of operation.

Pressure transducers can be classified in terms of pressure ranges, temperature of operation, and the type of pressure they measure:

- Absolute pressure sensors: measure the pressure relative to perfect vacuum
- Gauge pressure sensors: measure the pressure relative to atmospheric pressure
- Differential pressure sensors: measures the difference between two pressures, one connected to each side of the sensor
- Sealed pressure sensors: These sensors are similar to gauge pressure sensors except that they measures pressure relative to some fixed pressure rather than the ambient atmospheric pressure (which varies according to the location and the weather)

The selected sensor for the pressure measurement is a silicon pressure transducer UNIK PTX 5072 [11] (Figure 4.4).



Figure 4.4: UNIK PTX 5072 pressure transducer

Silicon pressure sensors have silicon based sensing diaphragms, which have a very high elasticity and semiconductor strain gauges implanted in the silicon substrate which produce a high span sensitivity.

They have a high mV/V output signal, high overpressure and very good non-linearity, hysteresis and measurement repeatability.

The sensor specifications are reported in Figure 4.5.

PRESSURE TRANSDUCER UNIK PTX 5072	
Accuracy	± 0,1 % f.s. BSL
Overpressure	4 times f.s value
Material	Steel AISI 316L
Power Supply	7 - 32 V DC
Frequency response	5 kHz
Working Temperature Range	-55 °C < T < 125 °C
Rated temperature	-20 °C < T < 80 °C
Rated Temperature Error	± 1 % f.s TEB
Connection	G 1/4 female
Stability	±0, 1 % f.s (per year)
Electric Connection	4-20 mA, M12x1 4-Pin (IP65)
Measure Field	70 mbar-700 bar

Figure 4.5: UNIK PTX 5072 pressure transducer specifications

Flow meters

The flow meter [12] is a device used to measure fluid (liquid/gas) flow rates. Due to the high number of technical solutions shared in the market, just a brief classification is presented in the following, before introducing the specific technology adopted in the project:

- Mechanical flow meters (piston meter/rotary piston, gear meter, turbine flow meter, single/multiple jet meter, current meter)
- Pressure-based meters (Venturi meter, orifice plate, Dall tube, Pitot tube, cone meters, linear resistance meters)
- Variable-area flow meters
- Optical flow meters
- Open-channel flow meters
- Thermal mass flow meters
- Vortex flow meters
- Sonar flow meters
- Electromagnetic, ultrasonic and Coriolis flow meters
- Laser Doppler flow meters

The selected flow meter used to estimate the coolant flow rate at the test bench is a MUT2200EL magnetic sensor [13]. (Figure 4.6)

This flanged sensor bases its operation on the "Faraday Principle", by which a conductor crossing a magnetic field generates a potential perpendicularly orientated to the same field. The flow tube made in stainless steel AISI 304 is equipped with carbon steel or stainless steel flanges, two coils are installed on the top and inferior part; the magnetic field, generated by the electric current crossing the coil, induces in the electrodes a difference in the potential proportional to the flow rate. With the aim of measuring such potential of very low values, the interior of the flow tube is electrically insulated, thus the process liquid is no longer in contact neither with the material of the flow tube nor with that of the flange. The converter used (MC608A) [13], generates the current supplying the coil, acquires the electrodes difference of potential, processes the signal to calculate the flowrate and administers the communication with the exterior. (Figure 4.7)

Electromagnetic flowmeters are the best solution to measure conductive liquids with minimum conductivity of 5 microS/cm, as they offer rapid response time, high measuring accuracy and long term stability. No moving parts in the pipe and no obstruction to the liquid, with great advantage of no-pressure loss and virtually maintenance free system.

The sensor specifications are reported in Figure 4.8.



Figure 4.6: MUT2200EL magnetic sensor



Figure 4.7: MC608A converter

MAGNETIC FLOW METER MUT2200EL	
Flow tube material	AISI 316
Flanges material	AISI 316
Electrodes material	Hastelloy B, Titanium, Tantalio, Platinum
Internal lining	PTFE
Liquid temperature	-40 < T < 130 °C
Protection degree	IP68 1.5 m continuous immersion
Converter	MC608A
Electrical connection	Cable glands M20 x 1.5
Diameter	DN 40
Measuring range	22 m ³ /h
Flux velocity	5 m/s

Figure 4.8: MUT2200EL magnetic sensor specifications

4.2.2 Sensors location

The sensors location has been set in order to:

- Build the components fluid-dynamic (permeability) and thermal (heat rejection) characteristics
- Have easy access for the installation
- Avoid incorrect estimation of measured quantities (e.g. effect of exhaust manifold position on temperature)

Figure 4.9 shows the sensors location on the engine test bench.

The measured data are the following:

1. Engine inlet (Pump) : p_1 , T_1 , m_1
2. Engine outlet (Thermostat): p_2 , T_2 , m_2
3. Turbocharger inlet: p_3 , T_3
4. Turbocharger outlet: p_4 , T_4

where p stands for pressure [bar] , T temperature [°C] and m flow rate [L/h].

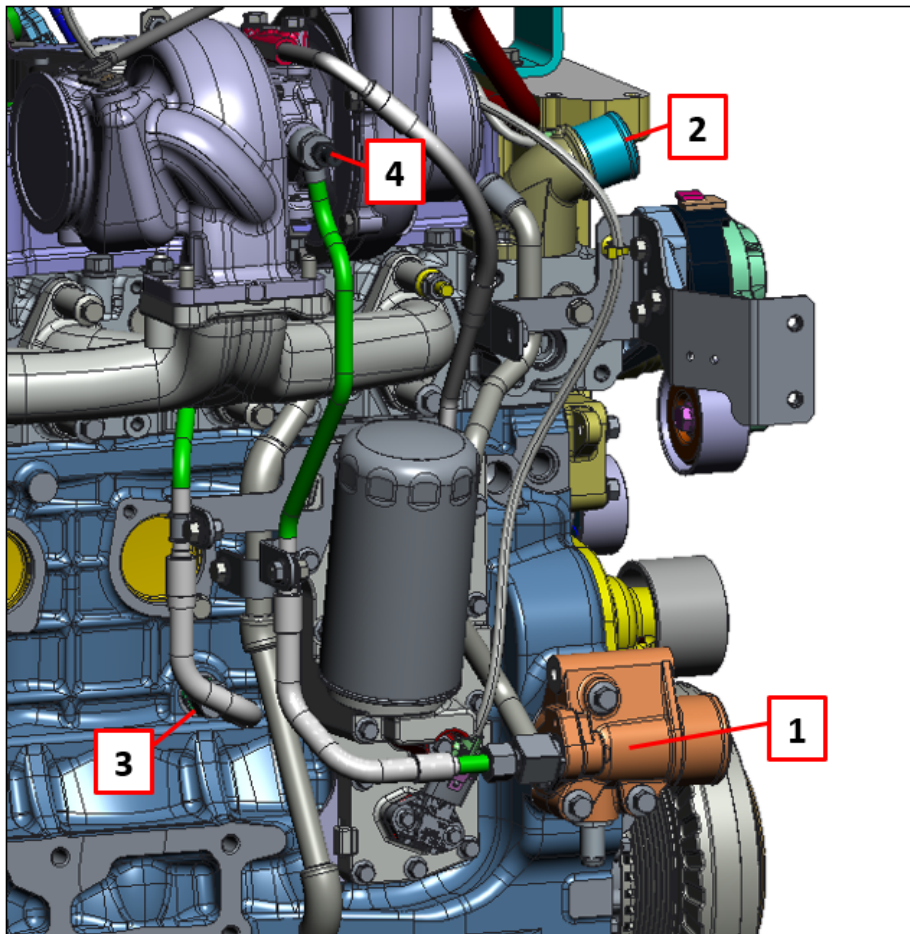


Figure 4.9: Sensors location at the engine test bench

4.2.3 Engine setup and data acquisition

The test bench control system has been set in order to:

- keep a constant intake air temperature downstream from the intercooler
- keep the thermostat completely open and control the water/water heat exchanger flow rate in order to set the engine outlet water temperature equal to 97 °C

The engine has been run in full load from 2300-800 rpm in steady state conditions. Following the maximum power curve, data have been acquired each 100 rpm with a sampling time of 60 seconds.

Moreover, in order to stabilize the engine at the specific working point, each acquisition have been performed every 10 minutes.

The test results have been finally collected for the post-processing.

Among the whole data acquired, the following have been used for the heat rejection estimation and the model calibration:

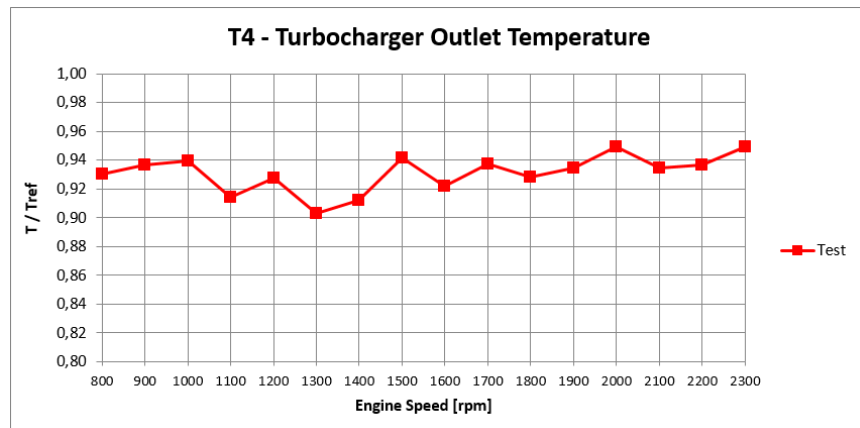
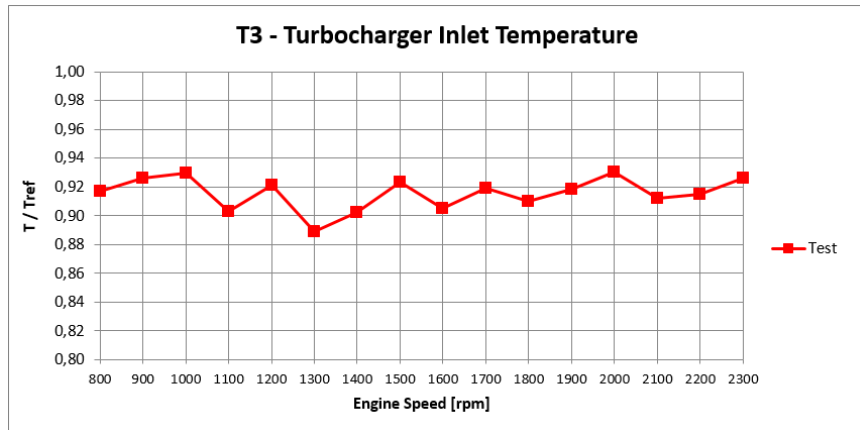
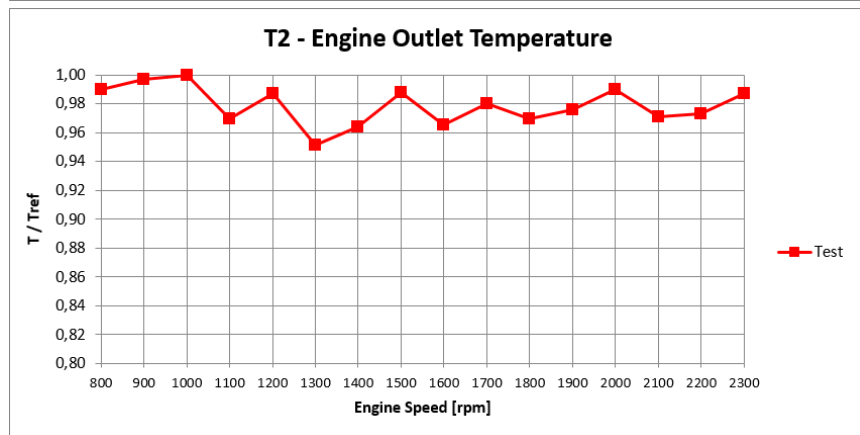
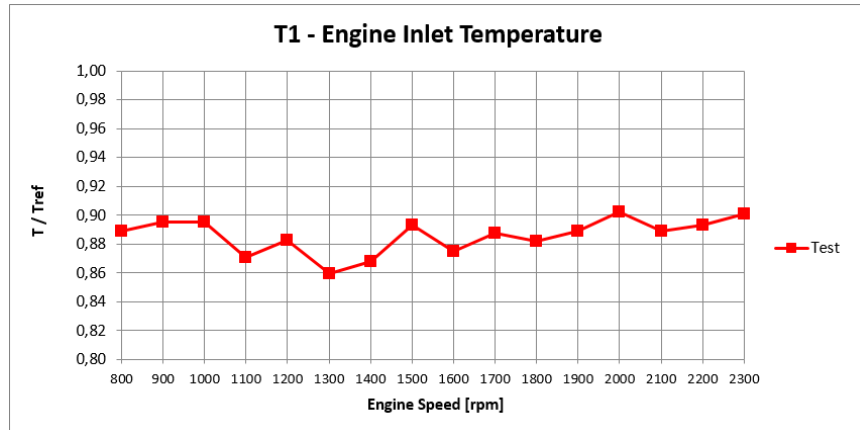
- Torque and useful power
- Fuel consumption and air to fuel ratio
- Coolant flow rate
- Air temperature and flow rate
- Exhaust gases temperature and flow rate
- Temperatures and pressures in the prescribed locations

The measured temperatures, pressures and flow rates are normalized with respect to the corresponding maximum value and reported in the following as function of engine rotational speed.

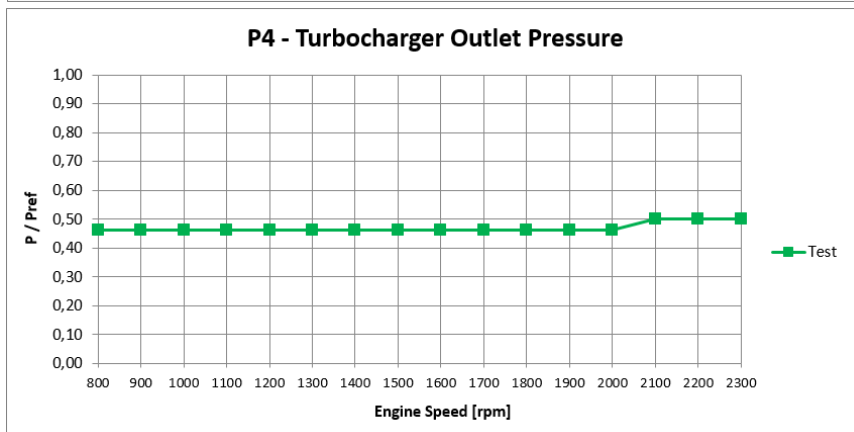
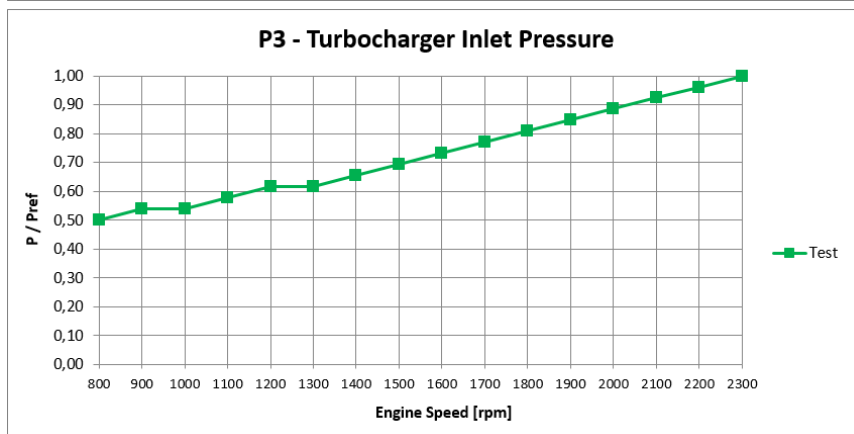
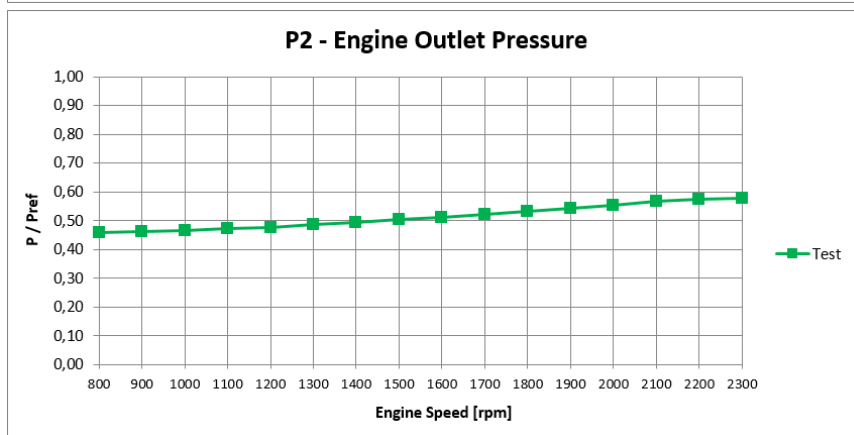
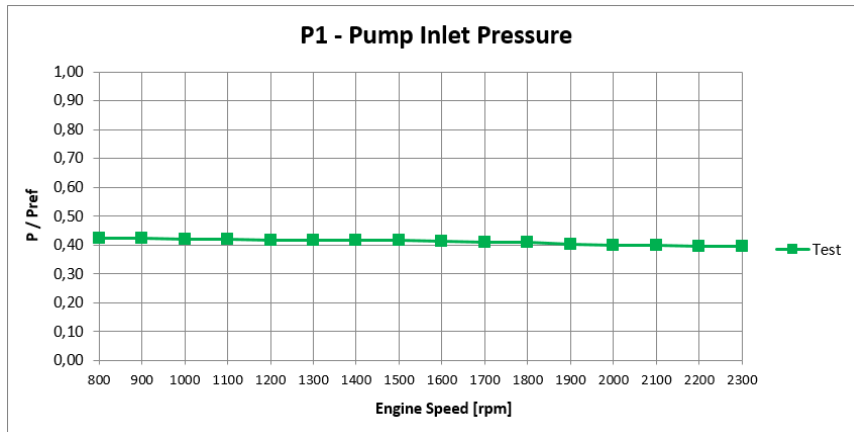
Temperatures turn out to be the most oscillating quantities among the measured ones, maybe due to the sensor instability.

It's also easy to detect the measurement error of the turbocharger outlet pressure.

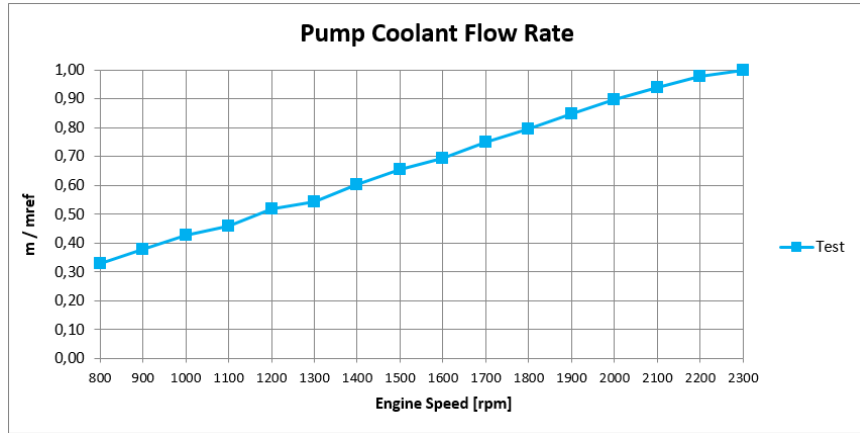
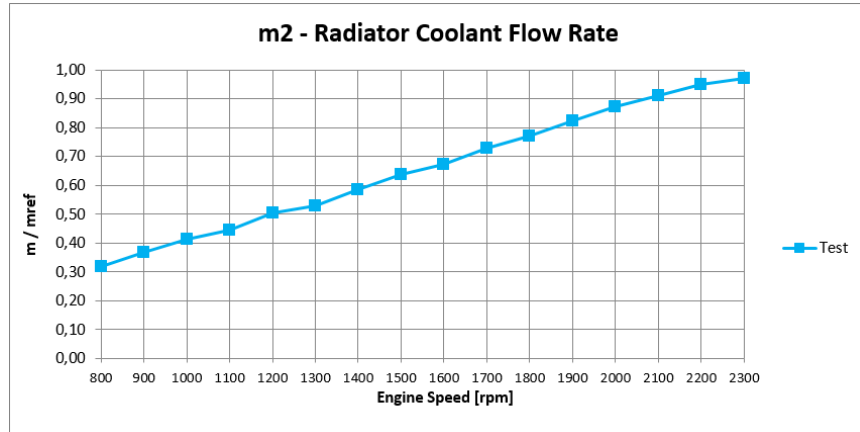
Temperatures



Pressures



Coolant flow rates



4.2.4 Simulation results

Simulation results have been finally compared with test results to show the model capability to predict the engine cooling system performance in the test bench configuration.

Temperatures, pressures and flow rates, evaluated in the prescribed locations for the sensors, have been considered as target values for the cooling system model validation.

The maximum error tolerance accepted is $\pm 10\%$ of the target value.

This choice has been made to make the model adaptable to different engine cooling systems and preferring an higher flexibility to an higher precision.

For what temperatures is concerned, simulation results are quite good with an error tolerance well below the limit.

Test results show an oscillating behavior, probably due to stabilization issues, but they are quite in line with the simulated ones.

Among the four measurements, T2 shows an offset between the simulation and the test results.

The reason is that during the test the temperature at the engine outlet is kept constant by a control system that, controlling the water flow rate in the water/water heat exchanger, keeps the thermostat completely open.

Pressures turned out to be the most difficult quantities to reach with simulations because of the sensor precision and accuracy.

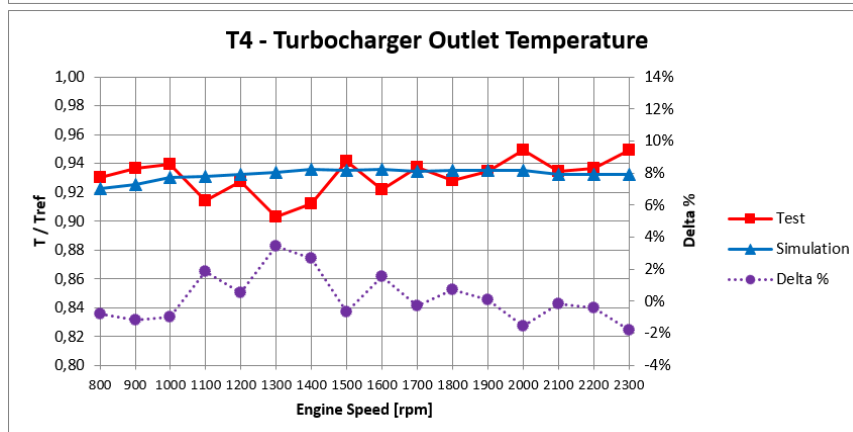
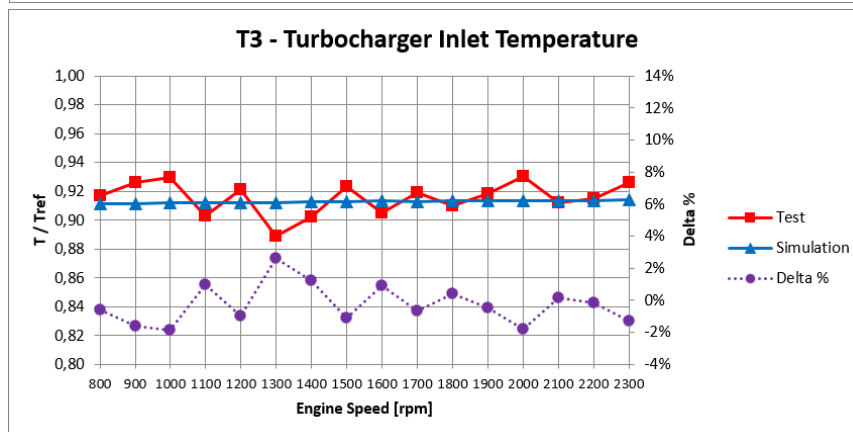
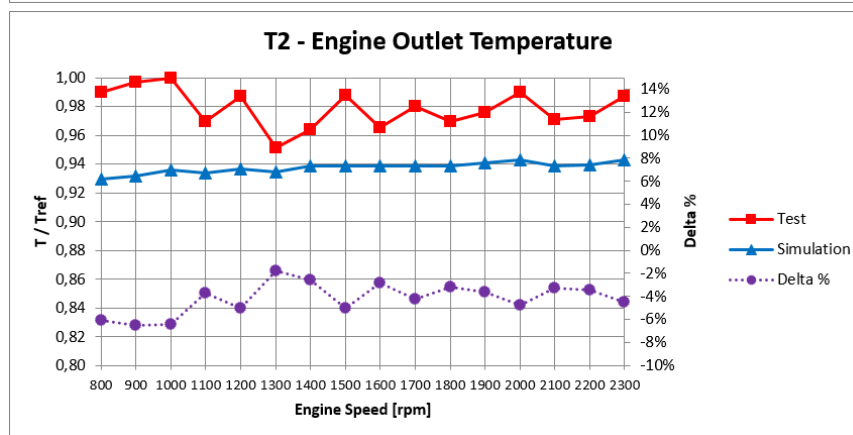
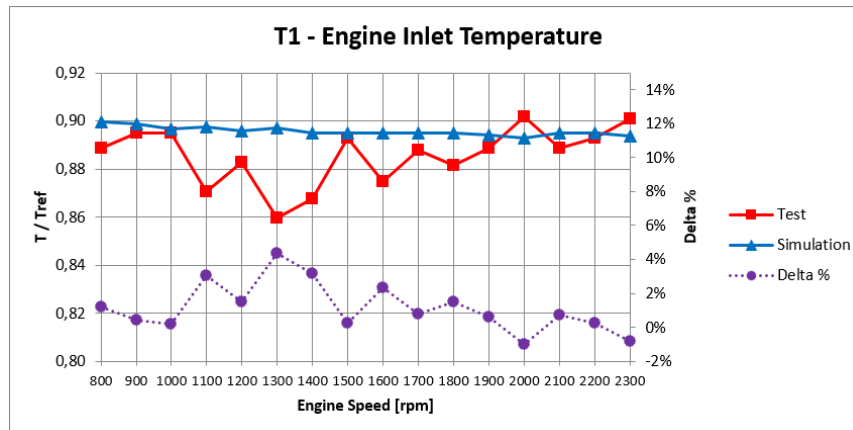
Except for P2, which is simulated with very good precision, the limit error tolerance is overcome in all the others quantities, especially for P4, due to an incorrect measurement of the sensor.

Anyway, results are acceptable if considering the obtained radiator and turbocharger permeabilities, with an error tolerance below the limit.

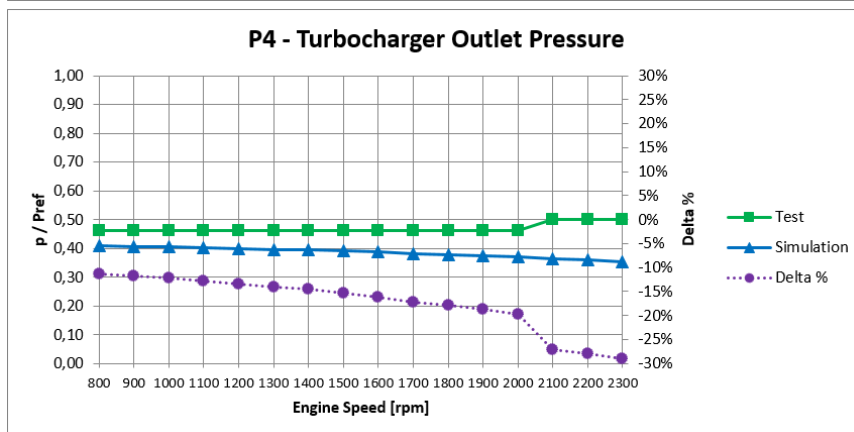
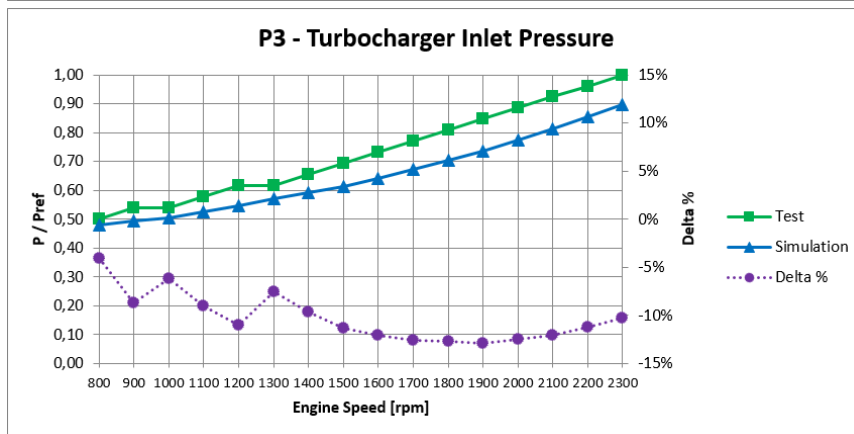
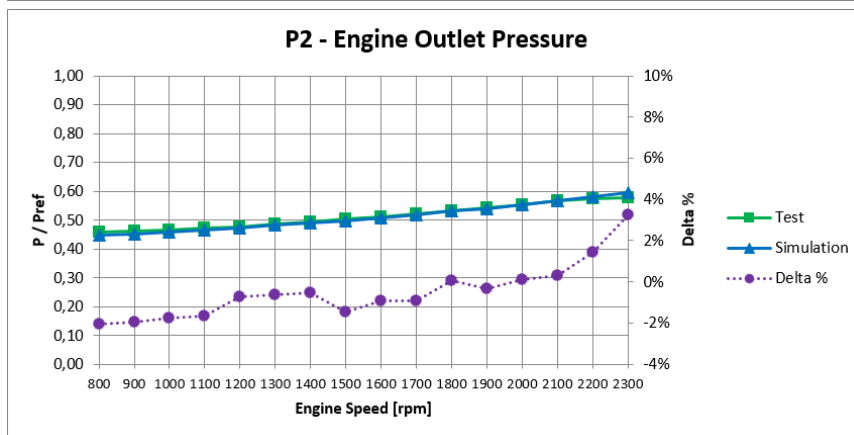
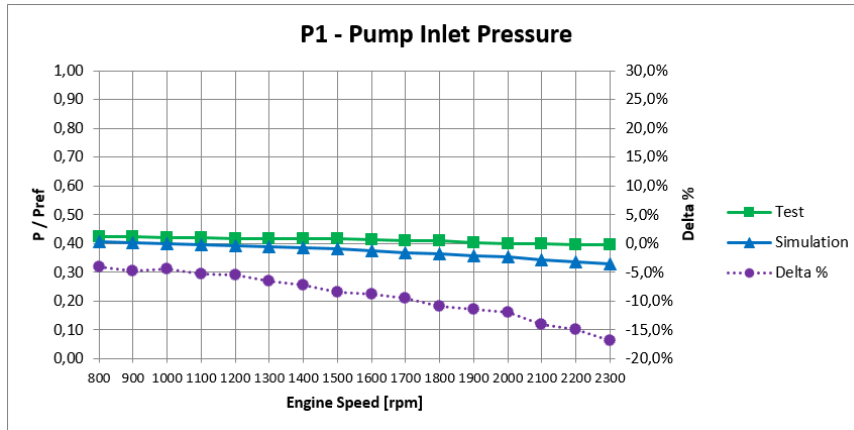
Moreover, a simulated pump inlet pressure lower than the measured one, can be useful to avoid cavitation.

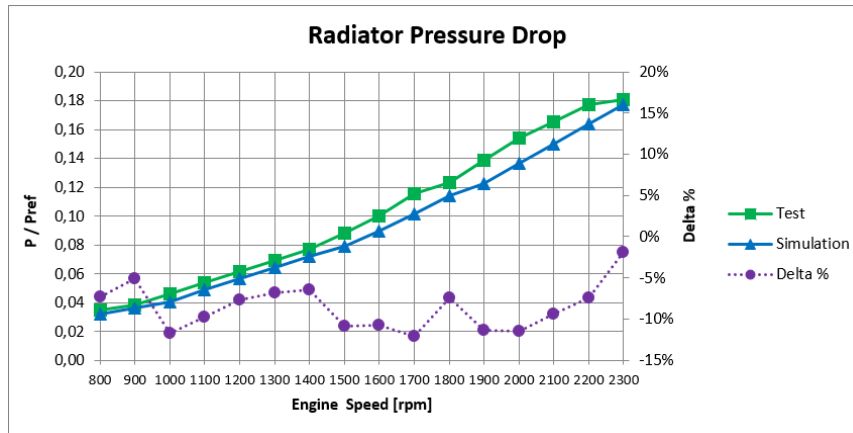
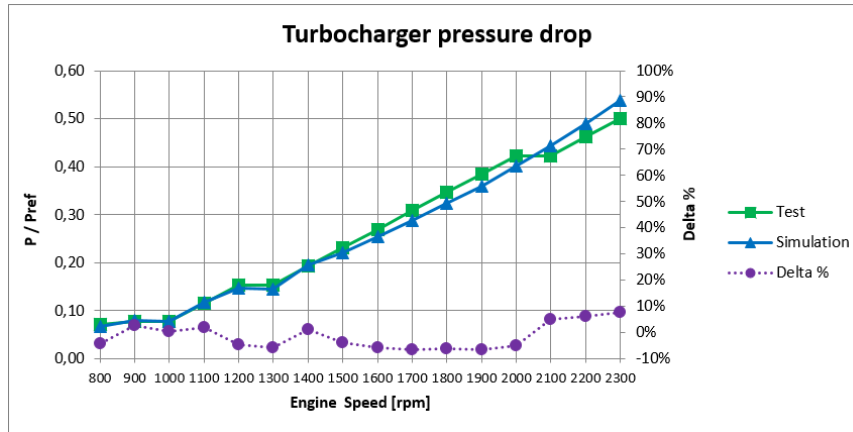
Finally, simulated coolant flow rates show a behavior very close to the measured ones, suggesting that the cooling circuit model permeability is quite close to the real one on the test bench.

Temperatures

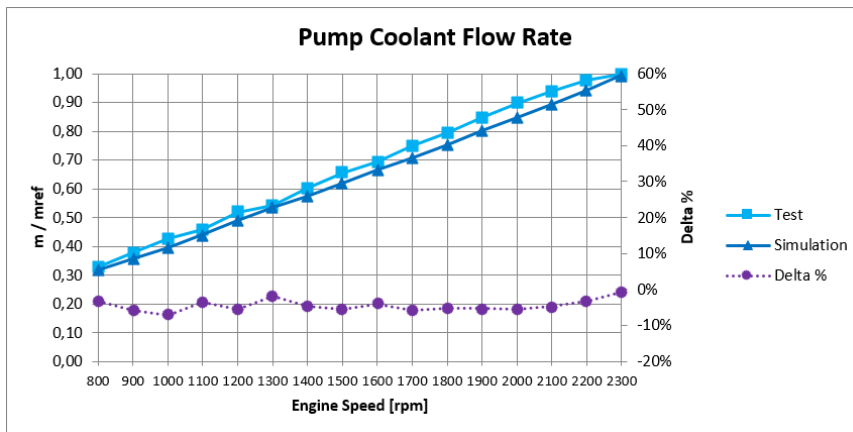
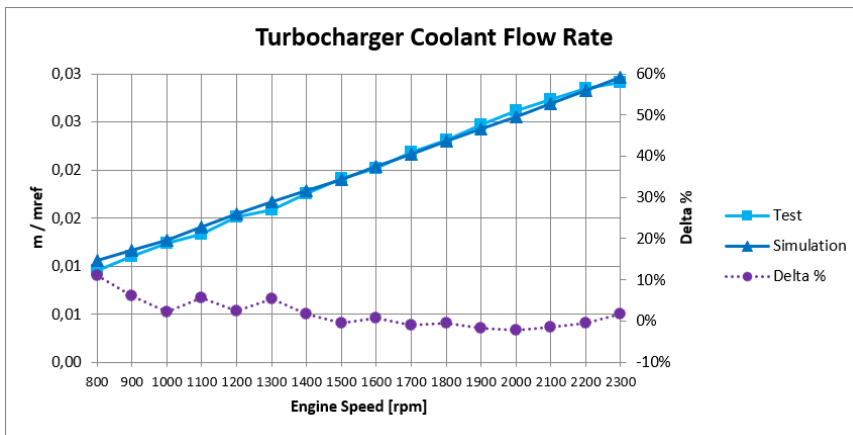
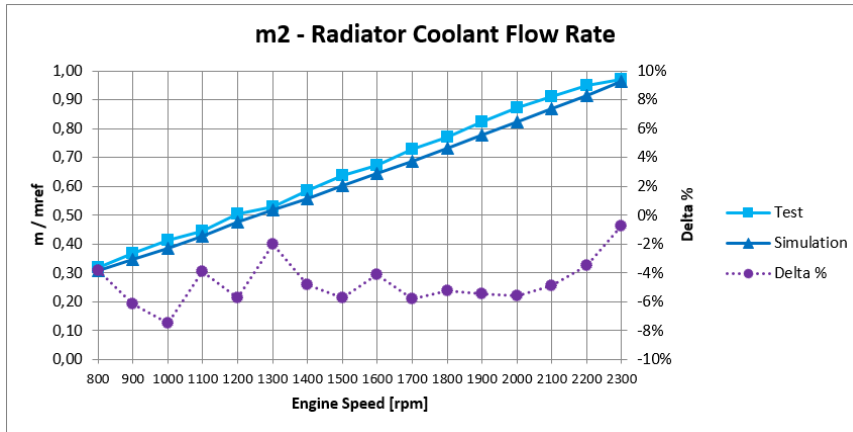


Pressures





Coolant flow rates



4.2.5 Heat rejection

The total heat balance gives information on how the total available energy produced by the combustion is split towards the engine (see Eq. 2.2).

The results obtained at the engine test bench have been used to compute the following quantities, as function of engine rotational speed:

- Useful Power
- Dissipated power by engine coolant
- Dissipated power by air intercooler
- Dissipated power by incomplete combustion
- Dissipated power by exhaust gases
- Dissipated power by lubricant oil
- Dissipated power by convection and radiation
- Turbocharger cooler heat rejection

They can be used either to estimate some relevant quantities of the engine performance directly at the testing cell, or to validate the cooling system model after the calibration.

Useful Power

$$P_u = C \omega \quad [kW] \quad (4.5)$$

where:

C = measured engine torque [Nm]

ω = engine rotational speed [rad/s]

Dissipated power by the engine coolant

$$Q_w = c_w \dot{m}_2 (T_{rad,out} - T_2) \quad [kW] \quad (4.6)$$

where:

c_w = coolant specific heat capacity [kJ/kgK]

\dot{m}_2 = measured engine outlet flow rate going into the radiator [kg/s]

$T_{rad,out}$ = computed radiator outlet temperature [K]

T_2 = measured engine outlet temperature (thermostat) [K]

$T_{rad,out}$ has been computed by means of a thermal balance at the pump inlet flow split (see Figure 4.10), using the First Principle of Thermodynamics (unfeasible sensor installation due to water/water radiator location):

$$\dot{m}_2 c_w T_{rad,out} + \dot{m}_{turbo} c_w T_4 + \dot{m}_{degas} c_w T_{degas} = \dot{m}_1 c_w T_1 \quad (4.7)$$

Being the coolant flow rate in the degassing pipe negligible with respect to the total flow rate of the circuit, the final equation for the radiator outlet temperature is the following:

$$T_{rad,out} = \frac{\dot{m}_1 T_1 - \dot{m}_{turbo} T_4}{\dot{m}_2} \quad [K] \quad (4.8)$$

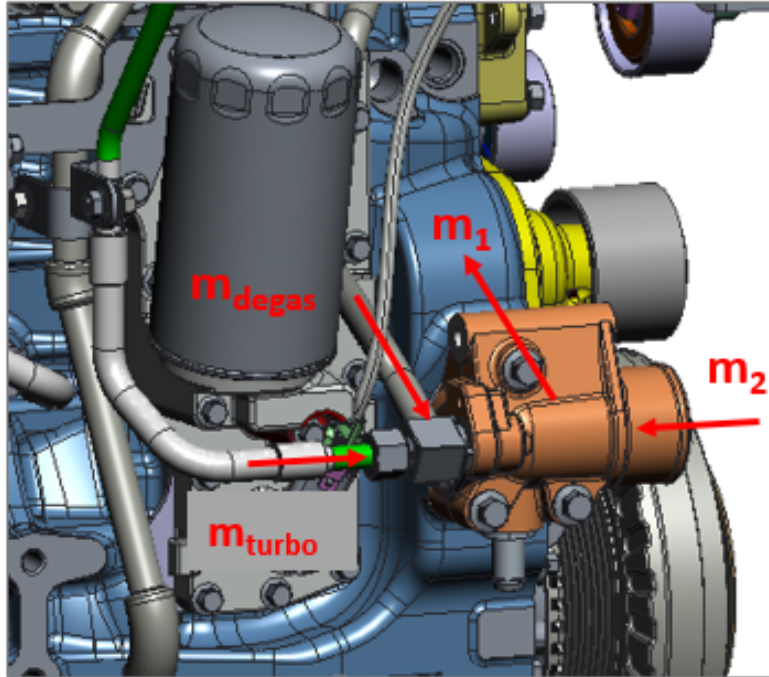


Figure 4.10: Pump inlet flow split

Dissipated power by air intercooler

$$Q_{int} = c_{air} \dot{m}_{air} (T_{int,out} - T_{int,in}) \quad [kW] \quad (4.9)$$

where:

c_{air} = air specific heat capacity [kJ/kgK]

\dot{m}_{air} = air flow rate [kg/s]

$T_{int,out}$ = intercooler outlet temperature [K]

$T_{int,in}$ = intercooler inlet temperature [K]

Dissipated power by incomplete combustion

$$Q_{inc} = \lambda \dot{m}_f H_i \quad [kW] \quad (4.10)$$

where:

λ = specific air to fuel ratio

\dot{m}_f = fuel flow rate [kg/s]

H_i = fuel lower heating value [kJ/kg]

Dissipated power by exhaust gases

$$Q_{exh} = c_{exh} \dot{m}_{exh} (T_{exh,out} - T_{air,in}) \quad [kW] \quad (4.11)$$

where:

c_{exh} = exhaust gases specific heat capacity [kJ/kgK]

\dot{m}_{exh} = exhaust gases flow rate [kg/s]

$T_{exh,out}$ = exhaust gases temperature [K]

$T_{air,in}$ = air inlet temperature [K]

Dissipated power by lubricant oil

$$Q_{oil} = c_{oil}\dot{m}_{oil}\Delta T_{oil} \quad [kW] \quad (4.12)$$

If no measurements have been performed for the lubricant oil, it is computed with the empirical formula (3.4).

Dissipated power by convection and radiation

The dissipated thermal power by convection and radiation has been estimated as difference between the total thermal power introduced in the engine with fuel combustion and the total dissipated power already computed.

Turbocharger heat rejection

$$Q_{turbo} = c_w\dot{m}_{turbo}(T_4 - T_3) \quad [kW] \quad (4.13)$$

where:

c_w = coolant specific heat capacity [kJ/kgK]

\dot{m}_{turbo} = measured turbine coolant flow rate [kg/s]

T_3 = measured turbine inlet coolant temperature [K]

T_4 = measured turbine outlet coolant temperature [K]

The turbocharger coolant flow rate has been estimated as difference between the flow rate delivered by the pump and the flow rate going into the radiator:

$$\dot{m}_{turbo} = \dot{m}_1 - \dot{m}_2 \quad [kg/s] \quad (4.14)$$

Finally the computed heat rejection quantities have been compared with the simulated ones.

In particular, for the model validation, the comparison has been carried out for the radiator and turbocharger cooler.

For the latter, a calibration has been needed to match the heat rejection curves. In particular, the first step turbocharger cooler heat rejection value turns out to be higher with respect to the measured one. (Figure 4.11)

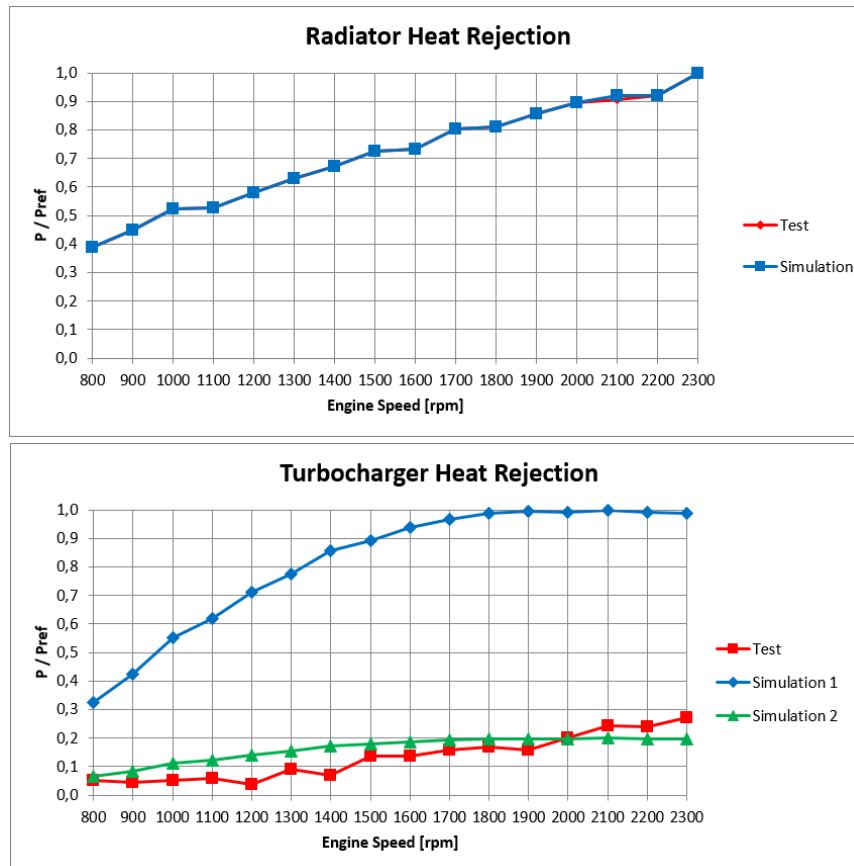


Figure 4.11: Radiator and turbocharger heat rejection

Chapter 5

Project results and model applications

The model turns out to be a reliable tool for the engine cooling system design and validation, being able to predict the system behavior at different working conditions and for different engine configurations and therefore, able to follow step by step the engine design process.

Having a calibrated model in line with the actual engine configuration, can be useful to test new technical solutions or proposals almost instantaneously and without spending time and money on a real prototype.

The big challenge is, in this case, to be able to make the model as much as possible close to the reality and always updated in the latest version, but anyway it turns out to be less demanding if compared with a real prototyping.

The project target has been achieved either in terms of simulation time or in results quality.

The capability of the model to obtain the same results of a tridimensional simulation in a short time is one of the most important goals of this kind of investigations.

The maximum error tolerance of 10% set as limit for the model validation, could be reduced to obtain even more precise results, but it was not the main request.

The need of creating a flexible tool has been guided by the willing not to just build a singular model for a specific engine, but to create a standardized methodology for the unidimensional modeling of different engines of the company.

In that regard, the proposed procedure for the automatic calibration of the engine water jacket, has been implemented also in other engine models and adapted to any calibration activity due to its flexibility, precision and quickness.

The test bench calibrated model has been then used for updating the vehicle configuration model, and test the engine behavior within the vehicle setup.

The trickiest phase of the project is related to the difficulty of collecting data from the customer side, and use the model for making considerations or previsions on the vehicle performances.

This is the reason why the calibration has been performed for the test bench model only, while the vehicle one has been presented in the most general way.

The latter, needs some information on installed components characteristics and, most importantly, on components control strategies, dependent on the customer vehicle application.

In the particular case of this thesis project, due to the lack of important data, has been decided to freeze the model and make it ready for future investigations.

5.1 Model applications

To conclude the thesis, in the following are going to be presented some model applications to understand the main reasons of performing this kind of investigations and the importance of virtual simulations in the design process.

The model can be applied either to test the vehicle side components fluid dynamic and thermal performances and find the best solution in the market for the specific application, or to make some previsions on the engine behavior in some particular conditions.

In particular, understanding the cooling system behavior at different ambient temperatures may be useful to prevent engine issues in countries with extreme environmental conditions.

Two interesting model applications are the cold start test and the ATD prevision. In both simulations, the main target is to change the air ambient temperature and monitor the coolant temperature to avoid critical conditions.

In case of the cold start, the ambient temperature is decreased in order to find when the coolant starts to freeze, in case of ATD prevision instead, the ambient temperature is increased in order to find the limit ambient condition for the engine derating. Both conditions must be avoided for preventing the engine integrity, so it is very important to study possible solutions in advance.



Figure 5.1: Example of extreme environmental conditions

The cooling system model can be used to run simulations and monitor the coolant temperature in all the circuit branches, suggesting new solutions to be applied in the real prototype.

Figure 5.2 shows some simulation results on the radiator inlet temperature variation with air flow speed and ambient temperature.

Results suggest to control the coolant temperature in case of either high ambient temperature, or low air flow speed.

A possible solution could be to programming the fan control strategy in order to prevent overheating in operation with critical ambient temperature, or in case of cold start operation, adding some extra components before starting the engine, to warm up the coolant and avoid freezing.

The main advantage of working with virtual simulations is to reduce the costs of the experimental activity.

Both cold start and ATD tests are performed in special test cells, where ambient temperature and other environmental parameters can be changed manually, to test the engine performances in critical conditions.

These tests require almost one day to be performed, due to the huge effort for the cell preparation and the complete execution under standardized procedures.

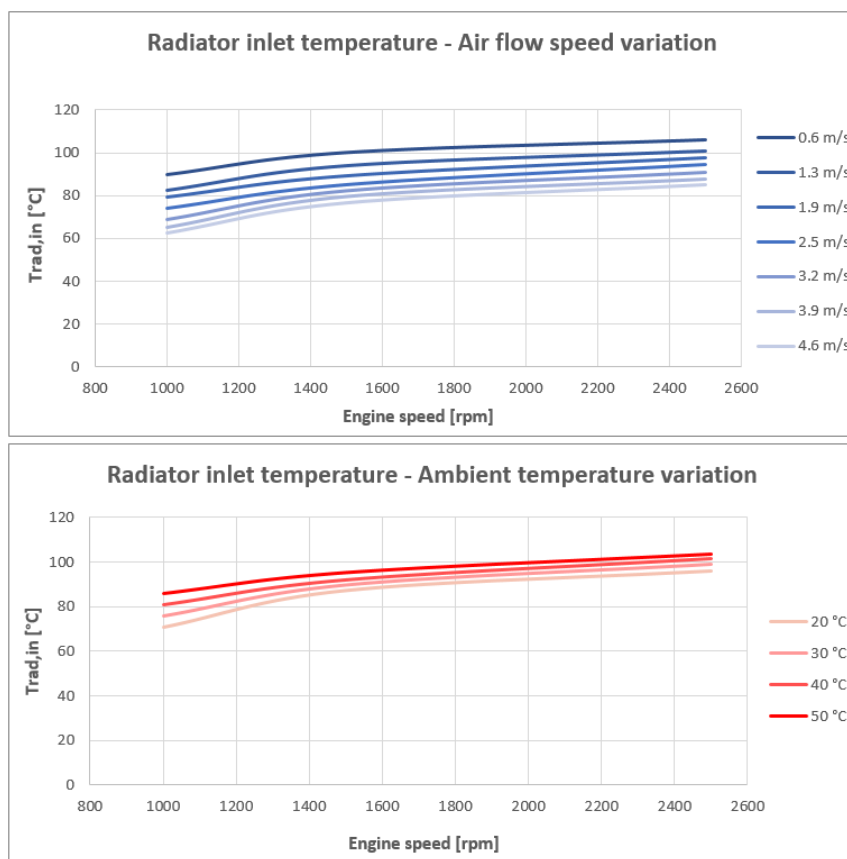


Figure 5.2: Air speed and ambient temperature variation effects on radiator inlet temperature

This is the reason why having a calibrated model able to make previsions on the real vehicle behavior can be useful to reduce the cost of prototyping and testing activities.

The big challenge is in this case, to have all the required information from the customer side, and tune the model with measured data on the real vehicle.

In that regard, a collaboration enhancement with customers during the engine development may be promoted by sharing the virtual models of the engine and the vehicle and run complete simulations with all the required data.

FPT Industrial is working in this way, improving the cooperation with customers to share existing models and provide all the data required for the calibration activity.

5.2 Conclusions

What comes out from this discussion is the important role of virtual simulations in the design and validation activities.

The possibility to make considerations on technical solutions and new proposals before running a real prototype on the test bench, improves the design efficiency, the product development and reduces time and costs of prototyping.

The continuous improvement of the used methodologies, and a strong collaboration with design engineers and testing cells, are the key factors for enhance the virtual models reliability.

Further project steps will be to improve the already existing models, either enhancing the collaboration with the testing facility, or extending the methodology also to other system engineers in order to let the models communicate each other and work in the most efficient way.

Moreover, a stronger collaboration with the customers, with the engine and vehicle models sharing, could help to calibrate complete vehicle models and built a synergy between companies.

Without hiding the huge problems of confidentiality, it would be a valid future step for improving the design activity and the final product goodness.

References

- [1] FPT Industrial-Powertrain Technologies, Online, Accessed on July 2018;
<http://www.fptindustrial.com/global/it>

- [2] GT-SUITE Gamma Technologies , Online, Accessed on July 2018;
<https://www.gtisoft.com/>

- [3] Politecnico di Torino, Ingegneria dell'Autoveicolo, "Applicazione sistema propulsore veicolo: Impianto di raffreddamento motore"

- [4] MAHLE Group , Online, Accessed on July 2018;
<https://www.mahle.com/>

- [5] GT-SUITE Gamma Technologies, Help Guide: PID Control

- [6] GT-SUITE Gamma Technologies, Help Guide: HX heat exchanger

- [7] AVL Test Systems, Online, Accessed on July 2018;
<https://www.avl.com/>

- [8] Online, Accessed on July 2018;
https://en.wikipedia.org/wiki/Resistance_thermometer

- [9] , Online, Accessed on July 2018;

- [10] Online, Accessed on July 2018;
https://en.wikipedia.org/wiki/Pressure_sensor

- [11] GE Digital Solutions, Online, Accessed on July 2018;
https://www.gemeasurement.com/sites/gemc.dev/files/unik_5000_series_datasheet_italiano.pdf

- [12] Online, Accessed on July 2018;
https://en.wikipedia.org/wiki/Flow_measurement

- [13] EUROMAG Electromagnetic Flowmeters, Online, Accessed on July 2018;
<http://www.euromag.com/en/products/electromagnetic-flowmeters/sensors/sensor-mut2200e1/>